Kinetic Investigation of the Base-Catalyzed Glycerolysis of Fatty Acid Methyl Esters

———

Kinetische Untersuchungen zur basisch katalysierten Glyzerinolyse von Fettsäuremethylestern

vorgelegt von
Diplom-Ingenieur Chemie
Tobias Kimmel
Berlin

Von der Fakultät II Mathematik und Naturwissenschaften
der Technischen Universität Berlin
zur Erlangung des akademischen Grades
Dr.-Ing.

genehmigte Dissertation

Promotionsausschuss

Vorsitzender: Prof. Dr. P. Hildebrandt
Berichter: Prof. Dr. R. Schomäcker
Berichter: Prof. Dr.-Ing. J. Starnick

Tag der wissenschaftlichen Aussprache: 5.11.2004

Berlin 2004

D 83

1 INTRODUCTION 3

2 BACKGROUND 5

2.1 Raw Materials and Monoglycerides 5
2.1.1 Origin and Uses of Glycerol and FAME 5
2.1.2 Production and Uses of Monoglycerides 8

2.2 Liquid-Liquid Reactions 11
2.2.1 Emulsions 11
2.2.1.1 Emulsion Type and Inversion 11
2.2.1.2 Drop Size and Distribution 12
2.2.2 Place of Reaction 14
2.2.3 Mass Transfer 15
2.2.3.1 Diffusion Coefficient Estimation 16
2.2.3.2 Mass Transfer Coefficient Estimation 17

2.3 Chemical Reaction 19
2.3.1 Base-Catalyzed Transesterification Reaction 19
2.3.2 Dimensionless Numbers 21

3 EXPERIMENTAL 23

3.1 Standard Reactor 23

3.2 Sampling 24

3.3 Standard Experiment 25

4 RESULTS I: ANALYTICS 26

4.1 Sample Withdrawal, Quenching and Silylation 28
4.1.1 Experimental 29
4.1.2 Results 30
4.1.2.1 Quenching Reaction by Dissolution 30
4.1.2.2 Preparation for GC 35
4.1.2.3 Sample Withdrawal 38
4.1.3 Conclusion 39

4.2 Gas Chromatography 41
4.2.1 Experimental 41
4.2.2 Results 42
4.2.2.1 Methanol Detection 43
4.2.2.2 Calibration 46
4.2.2.3 Analysis of Reaction Mixtures 48
4.2.3 Conclusion 49

4.3 Distribution of Catalyst Determined by AAS 50
4.3.1 Experimental 50
4.3.2 Results 52
4.3.3 Conclusion 54

4.4 Micro Photographic Drop Size Determination 56
4.4.1 Experimental 56
4.4.2 Results 58
4.4.2.1 Location of Endoscope 58
4.4.2.2 Drop Size during Reaction 61
4.4.2.3 Stirring Rate 63
4.4.3 Conclusion 67

5 RESULTS II: REACTION AND MODELING 68

5.1 Equilibrium Experiments in a Closed Autoclave 69
5.1.1 Influence of Molar Ratio of Reactants 70
5.1.2 Influence of Temperature 72

5.2 Kinetic Experiments 77
5.2.1 Influence of Stirring Rate 77
5.2.2 Influence of Phase Ratio 78
5.2.3 Influence of Temperature 79
5.2.4 Influence of Reduced Pressure 82

5.3 Concentrations and Selectivity 84
5.3.1 Methanol 84
5.3.2 Glycerol 88
5.3.3 Variation of Composition 93
5.3.4 Selectivity 95

5.4 Modeling 102
5.4.1 Model 1 106
5.4.2 Model 2 110
5.4.3 Equilibrium Constants and Pre-Equilibrium 112
5.4.4 Activation Energy 118

5.5 Mass Transfer 127

6 CONCLUSION 132

7 SYMBOLS AND ABBREVIATIONS 138

8 APPENDIX 143

8.1 Chemicals 143

8.2 Acid Number 145

8.3 Simulation: Kinetic Modeling of Methanolysis 146

8.4 Software Control of Image Recording 153

8.5 Impeller Design 175

9 LITERATURE 178

1 Introduction

The kinetics of the transesterification of fatty acid methyl ester with glycerol was under investigation. The products are mono- and diglycerides which are frequently used as emulsifiers in food, cosmetic and pharmaceutical industries. They are e.g. ubiquitous in ready-to-serve meals, part of margarine and sauces or dressings.

This reaction is closely related to the methanolysis of fats and oils which yield fatty acid methyl esters (FAME). They are increasingly used as a substitute for mineral oil based fuels. A second related reaction is the base-catalyzed glycerolysis of oils and fats which is the common method for the preparation of monoglycerides. It is likely that this method will be replaced in the future by enzymatic methods which promise a higher selectivity and a lower energy demand.

In this study monoglycerides are produced by the base-catalyzed glycerolysis of FAME with sodium methoxide as catalyst.

Eq. 1.1-1

The raw materials fatty acid methyl ester and glycerol form a two phase system. For the glycerolysis or methanolysis in liquid-liquid-systems no reliable kinetic data exists, because kinetic studies of multiphase systems are complex compared to homogeneous systems. The plot of conversion vs. time has a sigmoidal shape. This fact is observed frequently when liquid-liquid-systems are examined. In literature this is usually only qualitatively explained as a lag time or a problem with mass transfer. The sigmoidal shape is typical for either autocatalytic reactions or a change of reaction regime. The reaction to the products mono- and diglyceride is consecutive and preliminary experiments indicated that monoglyceride is obtained with a high selectivity and high yields as intermediate. Problems with the formulation of a kinetic model suggested the presence of a mass transfer limitation which was not taken into consideration. The limitation was thought to be caused by the size of the interfacial area between the two liquids. This was in accordance with the qualitative observation that the drops in the reactive emulsion became smaller with time which means that the size of the interfacial area increases. Small amounts of soap are formed as by-products which act as surfactant and the first product monoglyceride was thought to be surface active, too. As the concentration of the monoglyceride is increasing with time, it was likely that this concentration would control the drop size. Drop size could not be determined

at this time because the emulsion was coalescing very fast and standard methods like sampling and dilution or a direct photography through the reactor wall were not applicable.
Therefore the hypothesis of a mass transfer controlled reaction was formulated. For this purpose the reactive emulsion had to be characterized quantitatively by a set up that is able to record drop sizes. Sample handling and analysis are difficult for reactive systems at reduced pressures and high temperatures. The results of the preliminary investigation showed a high mass balance deficit that was not suited for kinetic modeling. Therefore this procedure had to be optimized. As the main aim was the production of monoglycerides, especially the conditions that affect selectivity had to be examined in detail. For further works a kinetic model had to be established.

2 Background

Monoglycerides can be obtained starting from different raw materials. Even the different routes to the raw materials like methanolysis and glycerolysis of fats and oils are closely related to the reaction under investigation. Processing and uses of raw materials are outlined. It is followed by a description of the uses of monoglycerides and how they can be obtained. The mechanism of the glycerolysis reaction is described in detail. When this reaction is carried out, a liquid-liquid emulsion is formed. It can be characterized by the determination of the type of emulsion and the size of the drops, which usually show a distribution. This information can be used together with the knowledge where the reaction is taking place for a first qualitative formulation of a kinetic model. For a quantitative modeling usually mass transfer over the phase boundaries has to be taken into consideration. Its magnitude can be estimated by the use of mass transfer coefficients that are dependent on the diffusion coefficients. For the quantitative modeling experiments at different conditions have to be compared, which can be done easily by using dimensionless numbers.

2.1 Raw Materials and Monoglycerides

In this study the glycerolysis reaction of fatty acid methyl esters is examined. This reaction shows from a kinetic point of view many similarities to the formation of the raw materials. When the results of the experiments are discussed in later chapters it is frequently referred to these reactions.

2.1.1 Origin and Uses of Glycerol and FAME

The reaction under investigation is the transesterification of fatty acid methyl esters (FAME) with glycerol forming monoglycerides and further undesired consecutive products.

$$\text{glycerol} + \text{FAME} \rightleftharpoons \text{monoglyceride} + \text{methanol} \rightleftharpoons \ldots \qquad \text{Eq. 2.1-1}$$

As this reaction is embedded in field of natural fats and their derivates, the way from the natural sources to the raw materials glycerol and fatty acid methyl esters is described first. In Fig. 2.1-1 this way is outlined. Additionally the way from fossil sources is included [1].

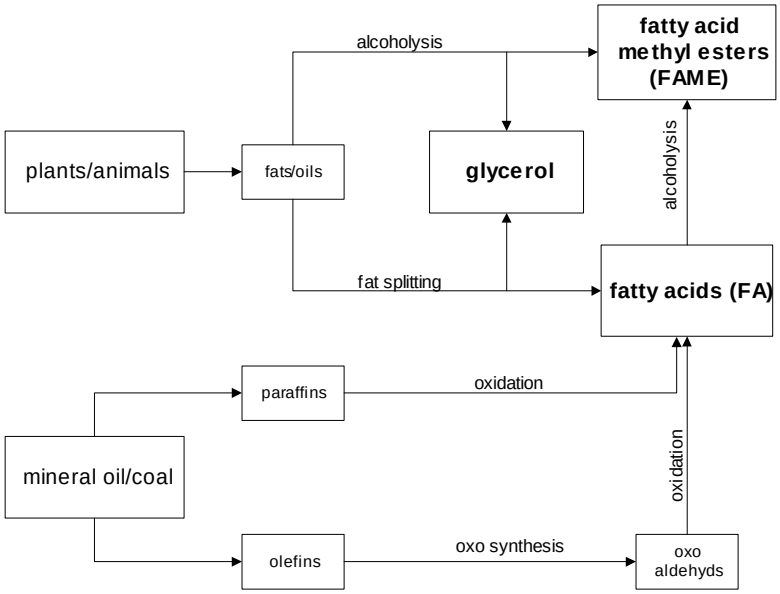

Fig. 2.1-1: Origin of the starting materials FAME and glycerol from natural and fossil sources.

The starting materials, fatty acid methyl ester and glycerol are usually derived from natural fats and oils. Natural sources are oil plants and animals. Distinguishing feature of fats and oils is the melting point; oils are liquid or semi-liquid at room temperature whereas fats are solid. The oil or fat molecule is formed by glycerol and three fatty acids (FA) which are either saturated or unsaturated.

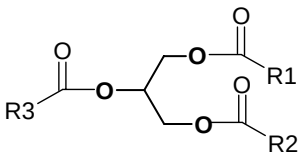

Fig. 2.1-2: Formula of oils and fats. The backbone of glycerol is bold. R1 to R3 are aliphatic groups which can be either saturated or unsaturated.

The FA contained in natural fats and oils consists of a spectrum of different FA that is characteristic of the original source. Individual FA are abbreviated by two numbers separated by a colon. The first number is the hydrocarbon number, the second the number of double bonds.

Most of the oils, i.e. palm, sun flower and peanut oil contain FA with a chain length of 18 C atoms. Examples are stearic 18:0, oleic 18:1 and linolic acid 18:2. Animal fats mainly contain

FA with 16 or 18 C atoms. Palmitic acid 16:0 is also found in palm oil as main component. Shorter FA like 14:0 and 12:0 are found in special fruits like in palm kern or coco nut. New cultivated species like Cuphea parsonsia contain up to 90 % fatty acids with 12 C atoms.

The glycerol and FA in oils and fats are usually separated by a reaction with a component with a hydroxyl function R'-OH. In the case of R'= H this process is called fat splitting by hydrolysis reaction. With R' = $CH_3(CH_2)_n$ with n starting at 0 it is an alcoholysis reaction.

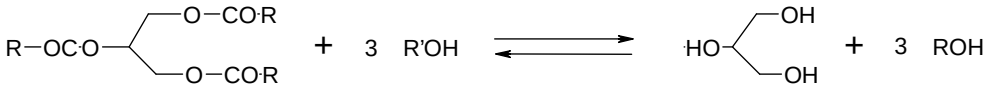

Eq. 2.1-2

Glycerol and FA or FA esters are separated by settling. Glycerol is used in pharmaceutical and cosmetic products, for food chemistry, as antifreeze agent, for the production of alkyd resigns, polyether and nitroglycerine [1]. The free FA can be converted to esters of alcohols or transformed to other derivates.

Fats contain 80 % of the heat content of diesel fuels but they show severe disadvantages when used in engines like oil deterioration and incomplete combustion. These problems and possible solutions are discussed in detail in[2]. The European Union aims to substitute mineral oil based fuels. In 2010 the proportion of natural fuels should exceed 5.75 %, in 2020 20 % [3]. To enhance the fuel properties and to reduce the viscosity fats are converted to fatty acid esters of short chain alcohols. Fatty acid methyl esters (FAME) are favored because of the low price of methanol and the easier processing. In this area research is done because new processes are expected to show less energy consumption compared to traditional processes [1] at temperatures of 240 °C and pressures of 9 MPa. One approach is the optimization of reaction conditions at low temperatures and atmospheric pressure with alkaline catalysts. Examples are found in literature for rapeseed oil[4], for soybean oil [5, 6] and for Pongamia Oil [7]. As acidic catalysis is much slower, this way only makes sense for special cases like used oil [3] which contains high fractions of free fatty acids that interfere with the use of alkaline catalysts.

Besides the use as diesel fuel substitute, FAME are intermediates for several products. They are used in cosmetics and detergents. Used as a raw material for the formation of fatty alcohols a broader spectrum of applications is available as additive for textile, paper and mineral oil as well as component in cosmetics or detergents [1].

In this study two different starting esters are used. One was 95 % pure methyl ester of palmitic acid (Henkel) and the second a mixture of methyl esters containing approx. 75 % of oleic acid (Lancaster). Palmitic acid is at least a minor constituent of nearly all natural oils and fats whereas oleic acid is one of the most common main components. Judged by the high content of oleic acid methyl ester in the "75 %" mixture shown in Table 2.1-1, it resembles methyl esters derived from oil plants with a high content of oleic acid esters like Pongamia pinnata, a tree cultivated in India or a new rape species. In literature [7] the composition of natural oil from Pongamia pinnata is reported, composition of rapeseed oil in literature [1].

Table 2.1-1: Analysis of fatty acid distribution in the starting materials and in natural oil plants, ME: fatty acid methyl ester.

	16:0–16:1	18:0–18:3	miscellaneous
≈ 95 % palmitic acid ME	92 %	3 %	5 %
≈ 75 % oleic acid ME	3 %	97 % (18:1 85 %)	<1 %
Pongamia pinnata oil	3.7–7.9 %	80 % (18:1 44.5–71.3 %)	15 %
rapeseed oil (new)	9 %	88 %	3 %
rapeseed oil (old)	2 %	38 %	60 %

As stated in Table 2.2-1 the oleic acid methyl ester in the "75 %" solution supplied from Lancaster has a much higher content of oleic acid of 85 % and an overall content of C18 of 97 %. Composition was determined by gas chromatography.

2.1.2 Production and Uses of Monoglycerides

Monoglycerides (MO) are partial glycerides of FA that contain only one fatty acid group either in α or β position. The α position is preferred. At low temperatures only 5–8 % and at high temperatures up to 30 % of the total monoglycerides formed consist of β-monoglycerides [7]. If two or three hydroxyl groups of glycerol are transesterified the products are subsequently called diglyceride (DI) and triglycerides (TRI). TRI itself are fats and oils. During storage MO shows interconversion between α- and β-MO.

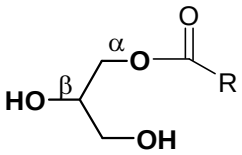

Fig. 2.1-3: Formula of α-monoglyceride. R-CO-O: fatty acid group.

MO is an intermediate formed during alcoholysis of fats and fat splitting, see Fig. 2.1-4. It is a minor component of fats and exists as natural intermediate of fat digestion and metabolism in vivo. Therefore glycerides of edible natural fats and oils are classified as "generally recognized as safe" (GRAS) [2].

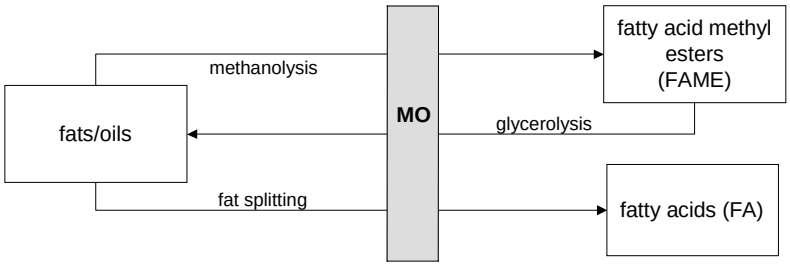

Fig. 2.1-4: Occurrence of monoglyceride (MO) as intermediate during the conversion of fats and oils which are triglycerides to fatty acid methyl esters and fatty acids.

In food industries they serve as emulsifying agent or control processing properties, e.g. they are ubiquitous in ready-to-serve meals, part of margarine and sauces or dressings. They are sold in two grades, either as mono-diglycerides or distilled monoglycerides. Mono-diglycerides contain nearly equal amounts of MO and diglycerides, whereas distilled MO are refined by molecular distillation. The content of monoglyceride in distilled MO is 82-95 %. A second area of application is cosmetic industries and pharmaceuticals. They are found in hair and skin products or toothpaste. Before 1995 the annual production in Europe was 28 kt mono-diglycerides and 42 kt of distilled MO [8].
The main route to obtain MO is the glycerolysis of oils and fats described in literature [9].

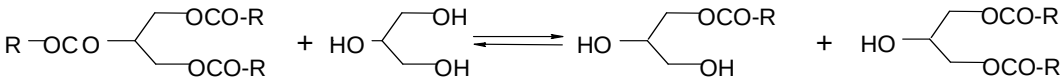

Eq. 2.1-3

Glycerol and fats are transesterified in a stirred tank reactor with a basic catalyst, preferably KOH or $Ca(OH)_2$. Temperature is about 250 °C to obtain a sufficient solubility of glycerol in the fat phase and a fast reaction. Nitrogen is used as inert gas to prevent oxidation and in the case of acidic catalysis formation of acrolein. After reaching equilibrium, the catalyst is neutralized with phosphoric acid and rapidly cooled to prevent reverse reaction.

$$Ca(OH)_2 + H_3PO_4 \longrightarrow CaHPO_4 + H_2O \qquad \text{Eq. 2.1-4}$$

Neutralization products are adsorbed with clays. The product is further purified by separating excess glycerol and washing with water. A survey of patents is given in a review [9], in literature[10] more recent patents are listed. A continuous glycerolysis process of soybean oil is described in literature [10, 11]. Reaction conditions in the pilot plant were 240 °C, 25 minutes reaction time, and a molar ratio of glycerol/oil of 5/2. Product composition was 56 % MO, 36 % DI and 8 % Triglyceride.

A second way to produce MO is the enzymatic synthesis which is currently under investigation. The use of lipase is reviewed in literature[12]. Advantages of enzymatic processes are energy savings because of milder reaction conditions and higher selectivities. It is expected that they will open a way to obtain distilled MO without the expensive step of molecular distillation. Yields of MO are reported in a range from 74–96 %. Raw materials are glycerol and FA or FA containing esters. A model compound is the MO of oleic acid, monoolein. Problems encountered are mainly the maximum conversion and the slow reaction rate. Conversion is controlled by the equilibrium of the reversible enzymatic reaction; temperature is restricted because of stability of the enzymes. High conversion can only be achieved by removing water in the case of glycerolysis, by continuously freezing out MO or by adsorption[13]. Repeatability is problematic because the complex interactions of various parameters like water content, temperature gradients, concentrations and co-solvents have to be controlled. Still reaction rate is not comparable to glycerolysis at high temperatures.

2.2 Liquid-Liquid Reactions

Liquid-liquid reactions usually involve the formation of an emulsion. It is characterized by the type of emulsion and the drop sizes of the dispersed phase. This physical information can only be used for a kinetic description if more information is available like the place of the chemical reaction, physical mass transfer rate of the reactants and parameters of the chemical reaction. Chemical reaction rate constants are determined in chapter 5.3. Physical mass transfer coefficient is the main transport parameter which can be estimated by an empirical correlation. Physical mass transfer rate and the rate of the chemical reaction are compared in chapter 5.4.

2.2.1 Emulsions

Emulsions are mixtures of two liquid phases. Mixing is performed usually by mechanical stirring. If the emulsion is thermodynamically stable it is called microemulsion with typical structural length scales of phase structures smaller than 100 nm [14]. The unstable case is called macroemulsion. It has to be stabilized either by constant mixing or the help of stabilizing agents.

When mixing is stopped, both phases start settling caused by density differences and gravity. When the dispersed phase fractions come closer they coalesce forming a continuous second layer. Metastable states often allow the existence of an emulsion for a long period of time, especially when the viscosity of the emulsion is high like in cosmetic products at room temperature.

2.2.1.1 Emulsion Type and Inversion

In this study a thermodynamically unstable macroemulsion of glycerol in an ester phase was examined. Size of glycerol drops was between 50 and 300 µm. Whether an emulsion of glycerol drops dispersed in a continuous ester phase is formed (glycerol/ME) or an emulsion of an ester in glycerol (ME/glycerol) is controlled by many parameters like geometry of the mixing unit, phase ratio φ, history of the dispersion and physical properties of the liquids like viscosity and surface tension. The upper limit of the volume fraction φ_{max} that can be dispersed in a continuous phase can be estimated empirically. As an example Equation 2.2-1 was derived for organic liquids in water stirred by an impeller at a rate of n. φ_{max} is dependent on system specific constants C and φ'.

$$\varphi_{\max} = \varphi' + \frac{C}{n^3} \qquad \text{Eq. 2.2-1}$$

An increase of the impeller rate n can lead to an inversion of the emulsion. If φ allows both kinds of emulsions usually two procedures allow to control which emulsion type is formed. First the position of the stirrer or the fill height can be controlled. In a baffled tank reactor the continuous phase is usually the phase in which the impeller is immersed when at rest [15]. Secondly, the continuous phase can be stirred first and then the phase is added that should be dispersed.
In the case of a reactive system, reaction can lead to inversion by changing the physical properties of the liquids and φ. In this study inversion of the glycerol/ME emulsion occurred occasionally when the catalyst solution was added. The solution caused foaming and surface tension was reduced. Normal dispersion could be recovered by stopping the stirring until phase separation showed that the impeller was immersed in the clear ME layer.

2.2.1.2 Drop Size and Distribution

A macroemulsion is characterized by the drop size of the dispersed phase. A selection procedure for a suitable method for drop size measurement is given in literature [16]. A comprehensive overview of methods for drop size determination is given in literature [17].
Three main groups of methods exist. The first group is photography which has the advantage of a direct drop size determination; this kind of method was used in this study. It is described in detail in chapter 4.4. The second group uses light for indirect measurements either by absorbance, scattering or reflection. Methods that use absorbance lose information about drop size distribution whereas the scattering methods usually require a prior knowledge or guess of the distribution. The last group consists of miscellaneous methods that are used less frequently like electronic probes. Scattering and absorbance are only applicable for small fractions of dispersed phase and if the optical properties of the emulsion do not change. For example the widely applied method of light extinction is used effectively at phase fractions up to 0.15. Around $\varphi = 0.3$ the intensity measured showed an attenuation of factor 1000 for a bubbly-flow [17]. For reactive conditions these methods are usually not suited because the refractive index difference of the liquids, color and fraction of the dispersed phase are usually affected by reaction.

Drop sizes are usually not uniform but show a distribution which can either be skewed or normal. Statistical functions can be used for the description of the drop sizes like a probability density function (*pdf*). Two frequently used functions are the Gaussian normal type and the lognormal type. In general those continuous statistical functions of a variate x allow describing and comparing different distribution by characteristic parameters like mean standard deviation *SD*, mean value μ and skewness. In Equation 2.2-2 an example for the *pdf* of the Gaussian normal type is given.

$$pdf(x) = \frac{1}{SD\sqrt{2\pi}} e^{\left[\frac{-(x-\mu)^2}{2SD^2}\right]} \qquad \text{Eq. 2.2-2}$$

The Gaussian normal *pdf* is symmetric around μ without skewness, while the log normal *pdf* is skewed. Several other functions are in use for special cases; a comprehensive and illustrative overview about the variety of statistical function is given in literature [18]. μ is defined as the 1st and the *SD* as the square root of the 2nd moment (*p*) about the origin.

$$\mu_{moment\ p} = \int_{-\infty}^{\infty} (x-\mu)^p\, pdf(x)dx \qquad \text{Eq. 2.2-3}$$

For practical purposes μ and *SD* can be calculated using the arithmetic mean as a guess for μ and calculating *SD* in respect of μ.

$$\mu = \frac{1}{n}\sum_{i=1}^{n} x_i \qquad \text{Eq. 2.2-4}$$

$$SD = \sqrt{\frac{\sum_{i=1}^{n}(\mu - x_i)^2}{n-1}} \qquad \text{Eq. 2.2-5}$$

For the analysis of a set of n measured values, e.g. drop sizes, data have to be divided into *i* classes x_i with a width of Δx and the frequency of each class has to be counted. Data are normalized by adjusting the sum of all frequencies to 1.

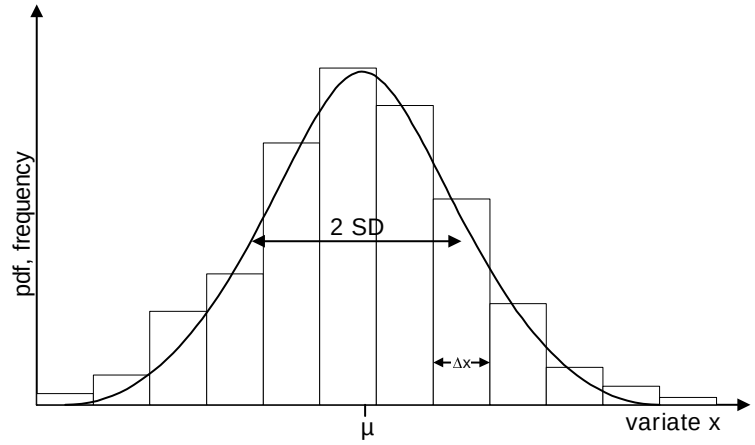

Fig. 2.2-1: Histogram of a variate *x*. The frequency of *x* in intervals of *Δx* is shown in a bar graph. A Gaussian normal *pdf* is overlaid. The mean *μ* and the standard deviation *SD* are marked.

The number of valid classes with a frequency different from 0 should not exceed the square root of n. The outline of the bar graph is called population distribution. It becomes smoother by using a bigger sample size n and a smaller interval Δx. The statistic parameters are obtained by fitting this population distribution to a *pdf* [19] as outlined in Fig. 2.2-1.

2.2.2 Place of Reaction

Even when an emulsion is present, in most cases the two phases can be regarded as quasi-continuous in the sense that the composition and physical state for the whole dispersed phase is the same at that point of time. For the continuous phase this is actually true in the case of vigorous mixing because this case resembles a dispersion of a solid in a stirred continuous phase. In the case of a dispersed phase this is not obvious as the drops are separate in space and time. Only if drops are broken and formed again in a fast dynamic process, exchange of material and physical properties is usually also fast, even in the dispersed phase. The use of local gradients or individual properties of each specific drop with respect to composition and physical properties is usually only required in special systems that show pronounced mass transfer limitations.

Where reaction mainly takes place depends on the solubility of the raw materials, catalyst and the reaction rate. In general in a liquid-liquid system, reaction can take place in each of the single phases or at the interface. E. g. in the case of a very limited solubility of catalyst in one of the liquid phases, reaction will take place predominantly in the phase that contains most of the catalyst. On the other hand if one of the starting materials is not soluble in this phase, reaction can also take place in the phase that contains less catalyst or at the interface where all components and catalyst meet. In general, reaction rates in each phase and the relative amount

of phase volumes have to be taken into consideration in order to evaluate the contribution of each phase to the overall reaction rate.
The simplest case is the reaction in one of the liquid phases without mass transfer restrictions. It is analogous to a homogeneous reaction. The second phase acts only as a reservoir which feeds one of the raw materials into the reacting phase. But this case is usually not to be expected in the case of liquid-liquid reactions. The main aim to perform a reaction at a specific quality level is a high space-time yield and a low power demand. Therefore reaction is usually carried out close to or under mass transfer limitations as reaction rate is maximized and time for mixing and amount of raw materials present in the reactor are minimized.

2.2.3 Mass Transfer

When two phases are present usually not all raw materials are soluble in one phase. Exceptions are e.g. emulsion polymerization in which the continuous phase is used to remove the heat of reaction. To obtain a reaction both raw materials have to meet. Therefore reaction involves crossing or at least approaching the interphase. A simple model that accounts for mass transfer in this region is the film model, Fig. 2.2-2.

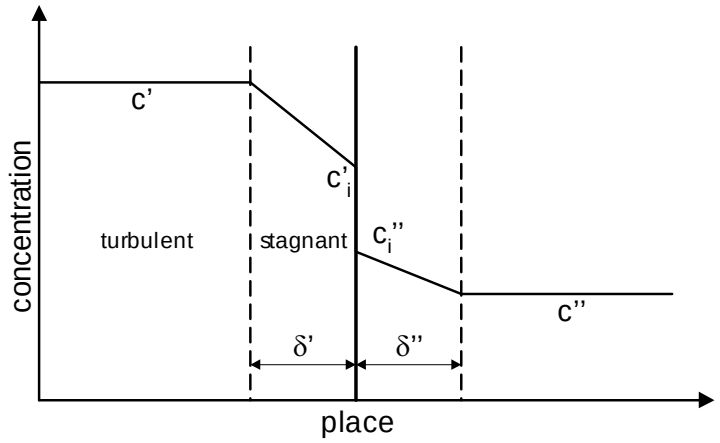

Fig. 2.2-2: Concentration (c) profile in the film model. The two stagnant films adjacent to the phase boundary (bold line) are separated from the turbulent bulk by a dashed line. The width of the stagnant film layers is δ, the inner concentration at the phase boundary has the subscript *i*.

In this model mass transfer is described with help of the mean bulk concentrations c' and c'' in the two phases. At the phase boundary a concentration jump is proposed between the concentration at the phase boundary c'_i and c''_i that depends on the equilibrium solubility of the component in each phase. Mass transfer is proportional to the linearly assumed concentration gradients in the film. The absolute value of mass transfer is determined by the

diffusion coefficient *D*, the thickness of the film δ and the surface of the interface. Those parameters are difficult to determine experimentally, especially the thickness of the film. Therefore *D* and δ are combined in a mass transfer coefficient $k_l' = D/\delta$.

For the estimation of mass transfer the individual transport properties of the transferred component glycerol, the diffusion coefficient, is needed first. Correlations for the mass transfer coefficient calculate the effect of mixing and liquid properties on the thickness of the stagnant layer at the interphase. Many correlations summarize simultaneously the influence of mixing in liquid-liquid systems on interfacial area and mass transfer coefficients. These correlations gain an overall mass transfer coefficient. In this study it is possible to determine the interfacial area experimentally. Therefore only correlations for the mass transfer coefficient at the ME layer are considered. As the glycerol film at the interphase only consists of the transferred species, in this phase mass transfer resistance is negligible.

2.2.3.1 Diffusion Coefficient Estimation

The diffusion coefficient D_{AB} of A (glycerol) in B (methyl ester) is calculated by the correlation of Wilke-Chang [20] in the unit of m²/s. As the original unit was cm²/s the factor 10^{-8} that is usually stated was replaced by 10^{-12} in Equation 2.2-6.

$$D_{AB}^{o} = \frac{7.4 \cdot 10^{-12} \left(\phi_B M_B\right)^{\frac{1}{2}} T}{\mu_B V_A^{0.6}} \qquad \text{Eq. 2.2-6}$$

In Equation 2.2-6 ϕ is an association factor that is for alcohols in organic liquids between 1.9 for methanol and 1.2 for propanol; no value for glycerol was available. The association factor for glycerol was chosen by a comparison of the ratio between the numbers of hydroxyl groups divided by the molecular weight. For glycerol this value is 0.033 compared to 0.031 for methanol or 0.022 for ethanol. Therefore the closest value for methanol with $\phi = 1.9$ was used. The values for the parameters in Equation 2.2-6 are given in the units that have to be used in the numerical equation. The molecular weight M_B of oleic acid methyl ester is 296.5 g/mol, the molar volume V_A at the normal boiling point of glycerol is 86.9 cm³/mol, viscosity μ_B is 0.8 mPas at 130 °C. Viscosity and molar volume were calculated from empirical correlations in literature [21].
The diffusion coefficient was calculated to be $D^{\circ}_{AB} = 6.08 \cdot 10^{-9}$ m²/s.

To validate this estimation the diffusion coefficient in m²/s was calculated using a second equation from Umesi-Danner which uses the radius of gyration R_i of both compounds which

was reported in [21]: R_A = 0.352 Å and R_B = 1.045 Å. This correlation is more recent but has the disadvantage that it does not account for the formation of associates.

$$D_{AB}^{o} = \frac{2.75 \cdot 10^{-12} T}{\mu_B} \left(\frac{R_B}{R_A^{\frac{2}{3}}} \right) \qquad \text{Eq. 2.2-7}$$

In this case D°_{AB} is $2.89 \cdot 10^{-9}$ m²/s. Both correlations yield coefficients in the range expected for diffusion in liquids of 10^{-9} to 10^{-10} m²/s. The difference of the two coefficients calculated indicates an uncertainty of the estimation of the diffusion coefficient that is higher than the usually stated precision of 20 % for Wilke-Chang and 16 % for Umesi-Danner. The difference of the calculated values is about factor 2. This difference is reduced to a factor of 1.5 when no association in Wilke-Chang is assumed. This indicates that the difference is mainly a result of association which was not considered by Umesi-Danner. Because the association factor was estimated too and no experimental data are available for comparison, the error is expected to be 50 %. For further calculations the value of Wilke-Chang of $6 \cdot 10^{-9}$ m²/s is used as diffusion coefficient of glycerol in oleic acid methyl ester.

2.2.3.2 Mass Transfer Coefficient Estimation

In literature it is common to express mass transfer by the use of the product of the mass transfer coefficient k'_l and the specific interfacial area *a*. But in this study the interfacial area *a* could be determined by the measurement of the drop sizes. Therefore only the mass transfer coefficient for the continuous phase k'_l was calculated according to an empirical formula for highly agitated systems in literature [20].

$$k'_l N_{Sc}^{\frac{2}{3}} = 0.13 \left[\frac{P_V \mu_c}{\rho_c^2} \right]^{\frac{1}{4}} \qquad \text{Eq. 2.2-8}$$

In this equation k'_l is dependent upon the power input per unit volume P_V which is generated by mixing and the fluid properties of the continuous phase, density ρ_c and viscosity μ_c. The diffusion coefficient *D* is part of the Schmidt Number N_{Sc}.

$$N_{Sc} \equiv \left(\frac{\mu}{\rho D} \right) \qquad \text{Eq. 2.2-9}$$

When N_{Sc} is introduced, Equation 2.2-8 is simplified.

$$k_l' = 0.13\left[\frac{P_V \mu_c}{\rho_c^2}\right]^{1/4}\left(\frac{D\rho}{\mu}\right)^{2/3} \qquad \text{Eq. 2.2-10}$$

Viscosity and density were calculated for pure ME of oleic ester from empirical correlations in literature [20]. For 130 °C viscosity is $7.8 \cdot 10^{-4}$ Pas, density is 874 kg/m³. Power input P_V per volume V was calculated for a six blade stirrer with baffles from the power number N_P at turbulent mixing, the impeller diameter $d = 0.033$ m and the stirring rate n according to literature [22].

$$P_V = \frac{N_P n^3 d^5 \rho}{V} \qquad \text{Eq. 2.2-11}$$

$N_P = 5$ was derived as a constant for the range of turbulent mixing from literature [23], this value is valid for a specific impeller geometry of a six-blade disc stirrer with a ratio of the height of the impeller blades to the diameter of the impeller of 1/5.

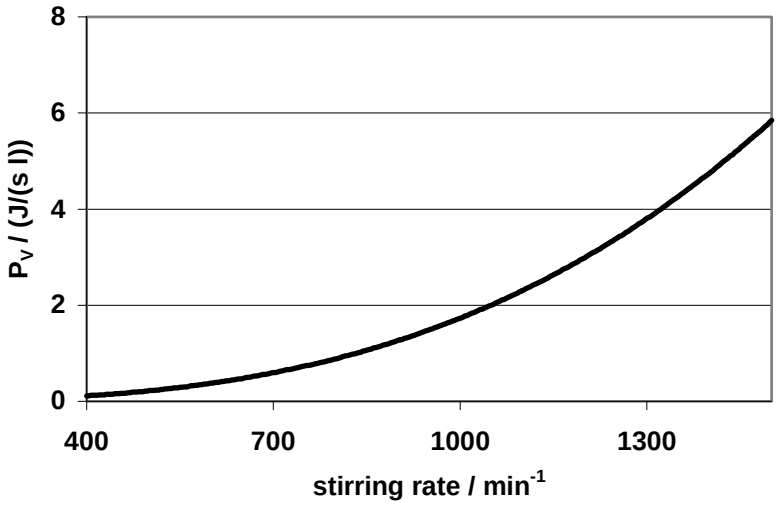

Fig. 2.2-3: Power input per unit volume P_V vs. stirring rate. Six blade stirrer with baffles, conditions at 130 °C: μ = 0.8 mPas, ρ = 0.91 kg/l, N_P = 5. *Re* is between $8.4 \cdot 10^3$ and $3.2 \cdot 10^4$.

At 500 rpm N_{Re} was calculated to be about 10^4. Turbulence is to be expected [20] for baffled tanks at $N_{Re} \geq 10^4$. Typical power inputs for mixing are 1 J/(s l), for reactions in liquid-liquid-systems they are usually higher. For 500 rpm P_V is 0.16 J/(s l).

2.3 Chemical Reaction

The mechanism of the reaction under investigation is the base-catalyzed glycerolysis of fatty acid methyl esters. The rates of this reaction will be determined in chapter 5 by the time dependency of the concentrations of all species. A standardized comparison of data and modeling will be done using dimensionless numbers.

2.3.1 Base-Catalyzed Transesterification Reaction

Transesterification describes the transformation of one ester into another through interchange of the alkoxy groups. When the original ester reacts with an alcohol, this process is called alcoholysis. In the case of methanol it is called methanolysis, with glycerol glycerolysis.
In this study transesterification reactions of carboxylic esters of methanol and glycerol are carried out. The general formulation is Equation 2.3-1.

$$\mathrm{RCOOR' + R''OH} \underset{\longleftarrow}{\overset{\text{catalyst}}{\longrightarrow}} \mathrm{RCOOR'' + R'OH} \qquad \text{Eq. 2.3-1}$$

Transesterification is an equilibrium reaction. The equilibrium constant K is defined in Equation 2.3-2 by the ratio of the concentrations c_i. K is reported to show only a negligible dependency on temperature.

$$K = \frac{c_{RCOOR''} c_{R'OH}}{c_{RCOOR'} c_{R''OH}} \qquad \text{Eq. 2.3-2}$$

K is also nearly independent of solvent and salt effects [24]. The replacement power of different primary and secondary alcohols was measured in equimolar mixtures of alcohols towards the formation of acetic acid esters at 200 °C. In this case one drop of water was used as catalyst. Values between 1.0 and 0.5 for the ratios $c_{RCOOR''}/c_{RCOOCH_3}$ of the esters relative to the ester of methanol are reported in literature [25]. This allows estimating the magnitude of K for transesterification reactions that should be about 1. For methanol usually the highest replacement values are reported. Therefore K for the reaction of the monoester of glycerol $RCOOR''$ and the ester of methanol $RCOOR'$ in Equation 2.3-3 should be about 1 because the replacing power is less, but in this case two primary hydroxyl groups are present in one molecule of glycerol.

Reaction is slow without catalyst. E.g. for the glycerolysis of fats uncatalysed reaction is usually negligible at temperatures below 200 °C. Reaction can be carried out either by acidic or basic catalysis. Base-catalyzed reaction is usually faster. The mechanism of the base-catalyzed alcoholysis includes the formation of a reactive alcoholate.

$$R''OH + \text{catalyst} \rightleftharpoons R''O^- + \text{catalyst-}H^+ \qquad \text{Eq. 2.3-3}$$

The alcoholate attacks the ester forming a tetrahedral intermediate which collapses and yields the transformed ester and the corresponding alcoholate as leaving group, see Fig. 2.3-1.

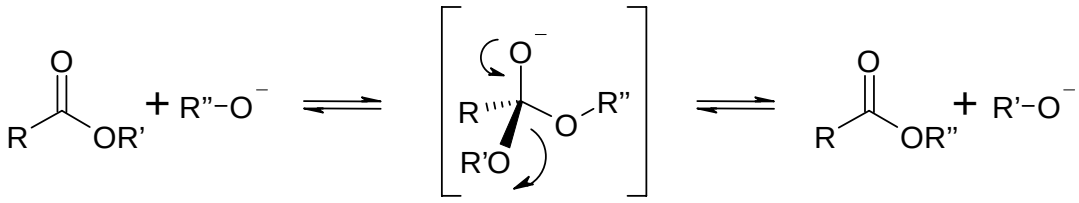

Fig. 2.3-1: Base-catalyzed alcoholysis reaction. The tetrahedral intermediate is enclosed in square brackets; arrows are showing the rearrangement of the ester carbonyl group with $R'O^-$ as leaving group.

This alcoholate is again in equilibrium with the alcoholate of the alcohol R″OH, see Equation 2.3-4, or with the catalyst, closing the cycle of the catalytic active species.

$$R'O^- + R''OH \rightleftharpoons R'OH + R''O^- \qquad \text{Eq. 2.3-4}$$

As alcohols are not easily deprotonated usually strong bases like the hydroxides of alkali or the even more basic alcoholates are used. Alcoholates like sodium methoxide are the most active catalysts but they require the absence of water. The hydroxides of sodium or potassium are cheaper but soaps are formed as undesired by-products, even at water free conditions [26]. The potassium hydroxide allows easy separation of the neutralization products with phosphoric acid [27]. Carbonates e.g. of calcium show slower reaction rates but no soap formation because traces of water are transformed to hydrogen carbonate [26].

2.3.2 Dimensionless Numbers

The course of a reaction can be described by dimensionless parameters in the range of [0,1] that reflect either the consumption or the formation of products. Conversion *X* is related to the consumption of a key component *k*. The criterion for the choice of the key component is usually that this component is stoichiometrically limiting the reaction, i.e. the initial molar amount n_{k0} would be totally consumed first.

$$X_k := 1 - \frac{n_k}{n_{k0}} \qquad \text{Eq. 2.3-5}$$

The yield *Y* is the molar ratio between the formed product *i* and the initial key component *k*. This ratio is multiplied by the absolute inverse ratio of the stoichiometric coefficients ν.

$$Y_i := \frac{n_i - n_{i0}}{n_{k0}} \frac{|\nu_k|}{|\nu_i|} \qquad \text{Eq. 2.3-6}$$

The integral selectivity *S* for a complex reaction is defined as ratio between the yield of component *i* divided by the conversion *X* of *k*.

$$S_{ik} = \frac{Y_i}{X_k} \qquad \text{Eq. 2.3-7}$$

In the case of the consecutive reaction given in Equation 2.3-8 with an excess of glycerol the key component *k* is ME.

$$\begin{aligned} &\text{ME + glycerol} \rightleftharpoons \text{MO + methanol} \\ &\text{ME + MO} \rightleftharpoons \text{DI + methanol} \\ &\text{ME + DI} \rightleftharpoons \text{TRI + methanol} \end{aligned} \qquad \text{Eq. 2.3-8}$$

If initially only the amount $n_{ME,0}$ is present and no other fatty acid containing components, balance equation during a chemical reaction for the fatty acid groups is Equation 2.3-9.

$$n_{ME,0} = n_{ME} + n_{MO} + 2n_{DI} + 3n_{TRI} \qquad \text{Eq. 2.3-9}$$

If the third step in Equation 2.3-8 is neglected, n_{TRI} is always 0. In this case the calculation of the selectivities for MO and DI can be simplified as shown in Equations 2.3-10 and 2.3-11.

$$S_{MO} = \frac{n_{MO}}{n_{MO} + 2n_{DI}} \qquad \text{Eq. 2.3-10}$$

$$S_{DI} = \frac{2n_{DI}}{n_{MO} + 2n_{DI}} \qquad \text{Eq. 2.3-11}$$

Selectivity cannot be calculated at initial conditions using Equations 2.3-10 or 2.3-11 because no products MO or DI are present. In this case selectivity is defined as $S_{MO,\,0} := 1$ for the purpose of computer aided calculations. This is asymptotically true, because MO is the first product in a consecutive reaction; $S_{DI,\,0} := 0$. The sum of all selectivities is 1.

3 Experimental

In this chapter only selected aspects of the experimental set-up for standard experiments are described that are not covered in chapter 4 or 5. The aim of this chapter is to ensure repeatability of the experimental procedure of standard experiments. Therefore details like choice of the syringe and addition of chemicals are discussed. The chemicals are listed in the appendix. The set-up for the autoclave experiments is given in chapter 5.1, for experiments with drop size recording in chapter 4.4.

3.1 Standard Reactor

Standard experiments were carried out in a double wall glass reactor (Wertheim LF 100) with an outlet at the bottom. The inner diameter is 0.1 m. It is equipped with four baffles and heated by a thermostat, heating medium is silicon oil with a low viscosity of 200 mPas. This set up allows visual inspection of the reactor content during reaction.

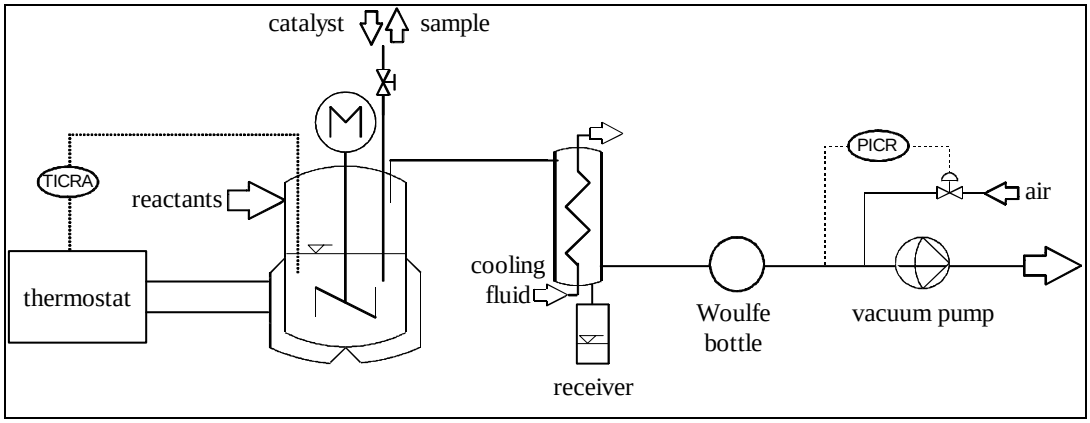

Fig. 3.1-1: Reactor with heating and cooling units, vacuum System and receiver for distillate.

Temperature was measured by a PT 100 sensor placed in the reactor; data were recorded by a data acquisition software. The steel impeller is a six blade disc stirrer which was available in two standard sizes; the first had a ratio between impeller diameter and inner reactor diameter of ⅓, the second of ½. Workshop drawings can be found in the appendix. Air tightness of the stirring unit was obtained by the use of a magnetic connection between the outer shaft of the stirrer motor and the inner shaft of the impeller. The lid was closed by a metal clamp, between

lid and reactor an o-ring was placed. The o-ring has to be replaced after reaction because it is irreversibly expanded by the ester. A distillation unit is attached to the lid consisting of a cooling unit that is held at 4 °C during operation by a thermostat with water as cooling fluid. The distillate methanol is collected in a cooled graduated double wall glass tube. Methanol was removed from the reactor in order to shift the equilibrium to higher conversions. This tube is connected to a diaphragm pump with controller (PC 2002 VARIO with Controller CVC 2000). When drop size had to be recorded, a microscopic endoscope is inserted into the reactor that is fixed by a Teflon coated rubber seal. The endoscopic system is described in detail in chapter 4.4.1.1, the used software in the appendix. It was cooled by compressed air at 2 bar. The compressed air from the endoscope was used to cool the electronic parts of the thermostat for the silicon oil. This thermostat was additionally cooled by two fans, one at the back and one in the front of the controller.

3.2 Sampling

Sample withdrawal procedure is described in detail in chapter 4.1.2.3.
If samples are withdrawn before the reaction comes to an end, it is usually not possible to turn of the stirrer. In this case samples are mixtures which start separating in the syringe. Only if the reaction is complete a phase separation in the reactor before sampling is possible. This was usually the case for the last samples in the kinetic runs and for the runs in the autoclave.
As samples are taken with preheated syringes at 130 to 160 °C the choice of the syringes is crucial. Up to five syringes were tested before operation to ensure that even one remains working till the end of the experiment.
The samples were usually taken with help of a glass syringe supplied by Fortuna. A better choice is the use of a Teflon tipped glass syringe produced by Hamilton. They both have disadvantages. The 10 ml Fortuna-model is not gas tight and may cause leakage during sampling at reduced pressure which leads to a darkening of the liquid in the reactor. When samples from separate layers have to be taken this is a major problem, because the air will mix the phases vigorously. The Hamilton-model is gasproof even if it falls to pieces because the Teflon becomes soft at elevated temperatures and is separated from the piston. The syringe will probably work when allowed to cool down to room temperature.
The second problem is the connection between syringe and needle. A Luer Lock system was used. The metal valves of the Luer lock system were not suited for long time operation because they are usually not gas tight at high temperatures. This is a result of a common problem with esters at high temperatures. They will wash away all kind of lubricants that may have been present initially; this tendency is supported by methanol in the gas phase of the reactor which is rinsing all cold parts after reaction is started. Because of this an air lock

consisting of a normal glass valve with a broad hole was used instead. The needle was inserted through a septum, the valve was opened and a 40 cm needle was immersed into the reactor and removed with the filled syringe. At the end of the experiment it is usually difficult to open or close the glass valves.

3.3 Standard Experiment

Either the methyl ester of palmitic acid or oleic acid is poured into the reactor. The reactor is continuously purged with nitrogen to prevent moisture entering the glycerol. Glycerol is poured into the reactor. Because it is very viscous at room temperature this lasts about 5 minutes. Both portions are determined by weighing the difference of the storage jar. At this point the impeller should be only immersed in the ester layer. This ensures that a glycerol in ester emulsion is formed. The nitrogen is stopped, the reactor nearly closed, mixing started and heated to the preset temperature. Then the vacuum is applied and it is tested for leakage. The reactor is allowed to regain atmospheric pressure and the catalyst is added as a solution of sodium methoxide in methanol. The needle must not be preheated or touch the surface of the liquids because this will lead to a blockage of syringe or needle. The needle is rinsed with 2 ml of methanol in a plastic syringe. After the needle is removed and the air lock is closed, the vacuum is applied step by step to prevent foaming. Additionally the thermostat for the condenser and the receiver of methanol is started beginning at room temperature; final temperature preset is 4 °C. After about 2 minutes the vacuum of 300 mbar is established. The valve at the Woulfe bottle is nearly closed still allowing small amounts of air to enter. If this is not done, pressure will decrease further because the vacuum controller is only able to reduce pressure. The point of time when pressure reached the preset value was regarded as start of the reaction at $t = 0$ minutes.

4 Analytics

Compared to homogeneous systems the analysis of samples of reactive liquid-liquid-systems is complex. Analysis comprises a procedure of phase separation and the verification that sampling conditions do not affect analysis results. Because of these special problems the analysis methods and procedures that were developed in this study are presented in an own section as part of the results.

The transesterification of vegetable oils to fatty acid methyl esters (FAME) is done at large scale because of its use as a substitute for petroleum-based diesel fuels. On the other hand the reverse reaction, the glycerolysis of fatty acid esters is investigated due to the high value added by producing monoglycerides and diglycerides for food, pharmaceutical and cosmetic industries. Another source of esters of short chain alcohols is the separation of fatty esters by the rectification of their esters.
The common methods for the production of monoglyceride include costly refinement steps, and are open for improvements of the process and the catalytic system. Different basic, acidic or enzymatic catalysts are currently tested in model system like the glycerolysis of FAME, vegetable oils or fatty acids.

Many methods for the analysis of glycerides and methyl esters have been developed. A comprehensive survey of commonly used methods like gas chromatography (GC) and high pressure liquid chromatography (HPLC) and alternatives is reviewed in literature [28]. Most articles are focusing on quality control of FAME used as biodiesel which are practically homogeneous and contain only small amounts of glycerides and glycerol.

In the initial state of the study the composition of each phase has to be monitored in order to identify the key components that determine reaction rate and mass transfer. In the case of a partial mutual solubility of both phases it is important to separate both phases without changing the composition. As the liquids are still reactive either the catalyst has to be removed or deactivated or phase separation has to be fast with respect to the change of composition. The samples were withdrawn at temperatures higher than 130 °C against subpressure and had to be homogenized for further analysis. For GC a silylation was necessary because of the high boiling points of glycerides. In literature, sample preparation for the related reaction of glycerolysis or methanolysis of oils and fats is usually carried out by quenching mixtures with water or neutralization at room temperature. In this case information about the individual composition of the phases is lost.

Each step can lead to errors that will show itself as errors of reproducibility or as deviation from the true composition. Optimization of the sampling procedure usually proceeds from conditions that are thought to be less favorable for quenching the reaction but which are easy to establish to more rigorous conditions. Usually optimization is stopped, when no dependency of composition on the improvement of the quenching conditions is observed. Examples for such parameters are amount of quenching solvent, cooling rate or pH in the case of neutralization. Nevertheless this does not grant that the determined composition is the true composition at the point of time when the sample was withdrawn from the reactor; truth is usually enclosed in a blind circle because any composition of the reactive mixture that is determined is itself dependent on the analysis procedure.

The analysis of reaction mixtures is difficult because of the simultaneous presence of low boiling components like methanol and high boiling components like glycerol and the glycerides in varying ratios. Only few articles are focussing on the analysis of reaction mixtures. A gel permeation chromatographic method is described in literature [29] separating glycerol and glycerides in one run. Samples were diluted with tetrahydrofuran, neutralized and filtered. Only three samples were analyzed. Content of ME was 64–87 %, triglyceride 1–16 %. Each sample prepared was injected 5 times. Minimum and maximum relative standard deviation of single components were reported to be between 0.3 % for methyl esters and 3.9 % for diglycerides. Most studies develop their own method but without an evaluation of accurancy or they use methods described in literature employed for biodiesel. Besides the more common GC and HPLC methods a thin layer chromatographic method is described in literature [30].

Analysis of reaction mixtures containing short chain alcohols by capillary gas chromatography (GC) does not allow using procedures that include a solvent change during sample preparation as proposed in literature [31]. A second problem is the solubility of the reaction mixture which contains oil soluble methyl esters, hydrophilic glycerol and the partial glycerides. Pyridine, 1,4-dioxane or phenols are described as solvents for reaction mixtures [32]. Additionally dimethylformamid (DMF) and hexane are described as solvents for FAME. For GC pyridine and dioxane are not ideal because they show broad peaks, making it difficult to separate low boiling components like methanol and the solvent on columns suited for high temperatures. In literature [33] a method for the quality control of FAME is described using DMF as solvent. Methanol and glycerides were simultaneously determined in a range of 0.02–0.49 % in FAME. DMF has a high boiling point compared to dioxane and pyridine

which allows separation of methanol, but it is not able to homogenize reaction mixtures with high contents of partial glycerides.

A reliable GC-procedure is described that allows homogenization of reaction mixtures and analysis of all components including short chain alcohols with dioxane as solvent within one run. This is achieved by using a prolonged initial period at room temperature for oven and inlet after a cool injection on column.

Catalyst concentration could not be determined by this method. The atomic absorption spectroscopy (AAS) was used for the determination of the catalyst sodium methoxide. As all components were nearly water free, sodium content of each phase is proportional to the amount of reactive alcoholates.
The emulsion is characterized physically by microphotography. The mean drop size it determined which is correlated to the size of the interfacial area. The set-up was adjusted to the conditions in the reactor. It was used the first time for a reactive system. Information about the correlation of power input and the interfacial area is of general interest for reaction engineering. When reaction is carried out at large scale, reaction conditions will usually be chosen near or at mass transfer limitation which is dependent on the interfacial area.

4.1 Sample Withdrawal, Quenching and Silylation

The three key steps in sampling are examined in detail: withdrawal of a sample, quenching the reaction and sample preparation for GC analysis. The reaction between vegetable fatty acid methyl esters (ME), in this case primarily from oleic acid, and glycerol yields mono- (MO) and diglycerides (DI), see Equation 4.1-1. Methanol is formed in both steps as couple product parallel to ME consumption.

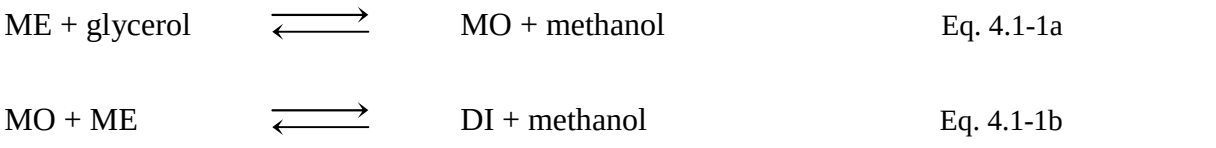

As ME is the limiting component of the reaction and methanol solubility at reaction conditions is constant and low, the methanol distilled during reaction is proportional to conversion. So this reaction has the advantage that conversion can be calculated by a second

approach independent of GC-analysis. Errors for the use of the condensate of methanol were that methanol was used as solvent for the catalyst, so at the beginning of the reaction methanol is present in the system which distills parallel to the methanol formed during reaction. Therefore methanol condensate was only regarded as qualitative guideline for conversion shape and magnitude.

4.1.1 Experimental

Reaction was carried out in the reactor described in Chapter 3. Quenching of the reaction was done using either pyridine 99.8 % (Fluka) or 99.5 % 1,4-dioxane stabilized with 25 mg/l 2,6-DI-tert.-butyl-4-methylphenol (Riedel-de-Haen). Catalyst is a 30 % solution of sodium methoxide in methanol (Fluka). As the catalyst is not soluble in dioxane or pyridine, the addition of catalyst to test solutions was done using a freshly prepared dispersion.
A technical grade mixture of FAME with approx. 75 % of oleic acid methyl ester was used as raw material purchased from Lancaster. Water content determined by Karl-Fischer titration was less than 0.01 %. Pure monoolein (MO) 99 % and diolein (DI) 99 % were purchased from Sigma, hexadecane 98 % and anhydrous glycerol 99.5 % from Fluka, N,O-Bis-(trimethylsilyl)trifluoroacetamide (BSTFA) 98 % from ABCR. Methanol 99.8 % was of HPLC-grade from Roth.

Dilutions were performed in 5 ml graduated glass flasks with a glass stopper, silylation in 1.2 ml auto sampler vials with screw caps and Teflon coated rubber discs.
Heating for silylation procedure was done in a thermostated metal block.
Analysis was done using gas chromatography. Instrumentation and capillary column type are identical to that employed in Chapter 4.2. The method used in this section was not optimized with respect to the duration of analysis: Temperature 40 °C, initial time 25 minutes, 1^{st} rate 15 °C/min up to 370 °C, final time 15 minutes, 2^{nd} rate -40 °C/min down to 50 °C, final time 7 minutes. Total running time was 77 minutes.

Conversion is calculated using the relative peak area ratios of the components that were determined by gas chromatography (GC). Additionally the amount of distilled methanol that was trapped in a cooled receiver was used to calculate conversion.

4.1.2 Results

First the quenching procedure will be described and motivated by problems encountered in preliminary studies. Because the chemicals used for quenching can affect analysis results, a comparison of different quenching chemicals is carried out. Only after these steps are completed the first step in the course of sampling, the sample withdrawal can be examined in detail.

4.1.2.1 Quenching Reaction by Dissolution

Starting point of the examination of sampling procedure was a comparison of two solvents that were used to quench the reaction mixture by dilution. Pyridine was used because it shows a higher solubility for glycerol at room temperature compared to dioxane. In Fig. 4.1-1 the conversion determined by GC is compared with the conversion trend calculated by the amount of distilled methanol.

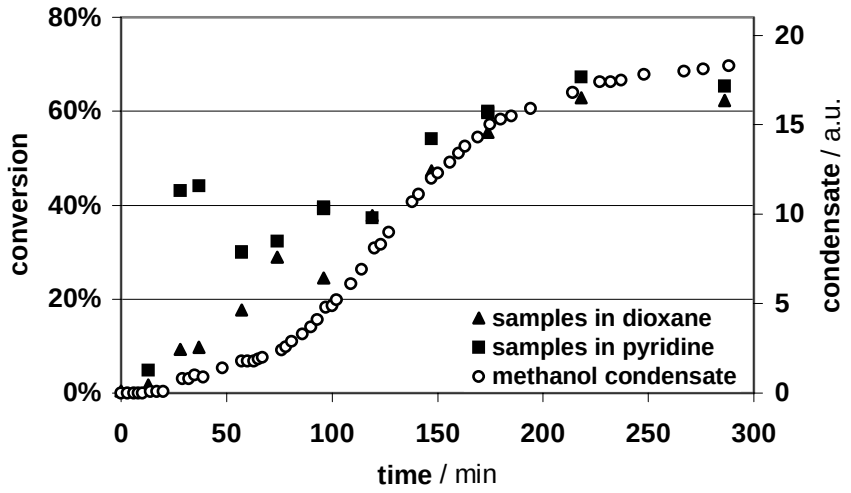

Fig. 4.1-1: Conversions determined in different quenching solvents. Samples in dioxane show the same conversion trend as the amount of condensate of the couple product methanol in arbitrary units (a.u.). Samples in pyridine show differences up to100 minutes, afterwards the same trend.

Samples dissolved in dioxane show the same conversion trend as expected by the condensed methanol. Samples dissolved in pyridine show much higher conversions in the first 100 minutes. After that both conversion plots converge. This indicates that the reaction still proceeds in pyridine. This was verified by injecting three samples quenched in pyridine two days later. A comparison is shown in Fig. 4.1-2.

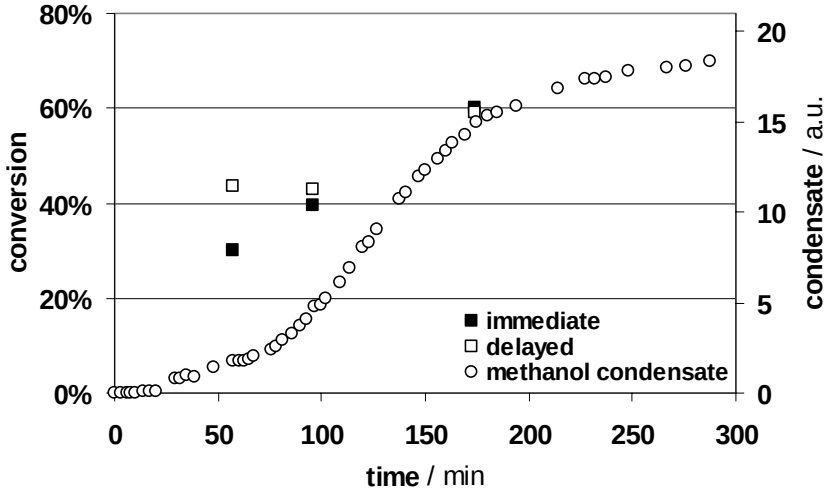

Fig. 4.1-2: Conversions for immediate and delayed sample preparation with pyridine. A delay of two days results in a contraction of conversions towards a medial conversion of approx. 50 %. Methanol condensate in arbitrary units (a.u.) is shown as guide for true conversion trend.

As all three conversions of the samples that were prepared after a delay of two days trend to a medial conversion, equilibrium conversion for pyridine is estimated to be in the area of 50 % ± 10 %. As the reaction rate is usually higher if composition is more different from equilibrium, this explains the high differences to the conversion trend of the methanol condensate for short reaction times. An additional factor is the glycerol amount in the samples. Phase separation is very slow at low conversion, so the amount of dispersed glycerol in the samples from the ME layer is usually higher. The excess of glycerol is solved immediately in the pyridine which will accelerate the formation of MO compared to samples with a lower content of glycerol. On the other hand the slow dissolution of glycerol in dioxane because of the low solubility could be one reason that conversions are similar compared to those derived from methanol condensate.

The comparison of dioxane and pyridine as solvents for quenching indicates a fundamental problem in determining the “true” composition of the reaction mixture. Even if preparation is fast and results are comparable with other data as it is the case for pyridine for high conversions, this is no proof that the true composition in the reaction mixture is figured out, especially for low conversions. Even for dioxane, determination of conversion should be tested in a way that is independent of a reactive system without knowledge about the true actual composition. Even if the right value of conversion is determined this does not verify

that selectivity will be determined correctly. In this case even selectivity converged for samples in pyridine and dioxane after 100 minutes.
Therefore “dummies” of quenched reaction mixture solutions were prepared from pure ME, MO, DI, glycerol and methanol, finally catalyst was added. Only if there was no reaction in this test system this would proof that reaction is stopped.

The central criterion for the solvent is complete solubility for the reaction mixtures, in this case a dilution of 1:60 was chosen for the sample-to-solvent-ratio at room temperature. Only pyridine and dioxane meet this specification. Pyridine has the best solvent properties. It shows the highest solubility for mixtures compared to other solvents; samples are quickly dissolved without residues. Solubility of single components at room temperature is for ME and glycerol better than 30 %. In dioxane mixtures of oleic acid glycerides are dissolved quickly, while glycerol containing samples should be stirred to speed up dissolution. Different experiments were carried out with pure palmitic acid methyl ester as raw material for glycerolysis. Samples with a high proportion of partial glycerides of palmitic acid are less soluble, leading to colloidal solutions, which are still usable for further processing of samples.
Other solvents may show a high solubility for ME and glycerol, but they will usually not be suited for samples containing high proportions of partial glycerides. Examples are dimethylformamide (DMF) used in literature [34] and tetrahydrofuran (THF). At 55 °C solubility of glycerol in THF containing 15 % methanol is better than 7 %, palmitic acid methyl ester quickly dissolves in THF up to 48 %. At room temperature DMF is able to solve samples at a low conversion of 20 %, but unable to solve higher contents of glycerides of oleic acid forming viscous precipitates.

Dummies are test solutions which resemble quenched samples of the reaction mixture at different conversion stages. The advantage is that the actual composition is known by directly mixing raw materials ME and glycerol with pure products monoolein (MO), diolein (DI), methanol and catalyst. Dilution of sample was approx. 1:60 by weight. Dioxane and pyridine were used as solvents which contained 0.4 % of hexadecane as internal standard.
4 ml of stock solution was prepared containing a mixture of ME, MO, DI and glycerol. 800 µl were transferred into three vials. All preparations were done parallel to prevent differences by handling procedure. 200 µl of a freshly prepared dispersion of the catalyst sodium methoxide was added to two of the vials. As the catalyst dispersion was prepared from a sodium methoxide solution in methanol this solution contained an excess of methanol. For this reason 200 µl of a methanol containing solution was added to the third vial without catalyst. For this procedure only small amounts of few mg of the expensive pure MO and DI were needed.

Table 4.1-1: Dummies prepared to test different conditions for quenching the reaction by dilution and neutralization. For comparison one preparation was done without catalyst. All compositions in percent refer to a relative composition of a hypothetical reactive sample. Catalyst content was 1.0 to 1.2 %.

No.	Solvent	Composition					Dilution	Reaction		
		ME	MO	DI	glycerol	methanol		with catalyst	neutralized	without
1	pyridine	68%	0%	0%	15%	3%	1 : 72	**yes**	**yes**	**no**
2	dioxane	69%	0%	0%	14%	2%	1 : 73	**no**	**no**	**no**
3		53%	0%	16%	9%	3%	1 : 65	**no**	**no**	**no**
4		0%	26%	0%	11%	3%	1 : 149	**no**	**no**	**no**
5	dioxane	50%	32%	9%	4%	2%	1 : 66	**-**	**warm: yes**	**no**
6		50%	32%	9%	4%	2%	1 : 66	**-**	**warm: yes**	**no**

A typical test vial contained a total of 16 mg of components that occur in reaction mixtures and 1 ml of solvent including 4 mg of internal standard. In vials with catalyst, the catalyst amount was 0.16 mg. One of the two catalysts containing vials was neutralized by adding one drop of acetic acid with a weight between 5 and 10 mg.
Last step was silylation with 200 µl of BSTFA and heating at 78 °C for three hours before the analysis by GC, the reaction [35] of a compound with a hydroxyl group, R-OH is shown in Equation 4.1-2.

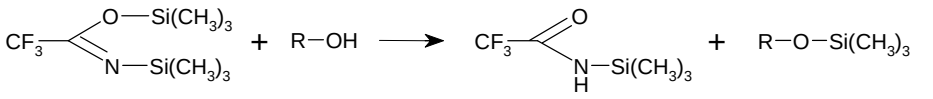

Eq. 4.1-2

Molar excess of acid to the basic catalyst was higher than 30. Acetic acid was selected because it is easily neutralized by the silylating agent and does not interfere with any other peaks in the GC because its retention time is within the solvent-peak.
To exclude problems with GC analysis by the formation of esters of acetic acid and glycerol, both were heated under reflux for 2 hours. Samples showed no additional products in the chromatograms. Only glycerol and the solvent-peak were detected.
Two more chemicals were tested for neutralization. Phosphoric acid is commonly used for neutralization in fat glycerolysis [36]. But in chromatograms its presence interfered with the glycerol peak showing overlapping. Trimethylchlorosilane (TMCS) was used for quenching, because it forms HCl during silylation. An additional advantage is acceleration of silylation with BSTFA. As the content of alcohols in samples is usually higher than the content of

catalyst the fast silylation of alcohols forms sufficient HCl to neutralize the catalyst. As TMCS forms salts with pyridine it was only used as 1 % solution in dioxane which was able to stop reaction.

Dummy 1 containing 73 % ME, 15 % glycerol and 3 % methanol was prepared, see Table 4.1-1. No products MO or DI were used. As expected the vial without catalyst showed no reaction. The vial with catalyst showed despite the high dilution of 1:60 a high conversion of approx. 50 %. To test if neutralization with acetic acid is able to stop reaction three more samples were prepared. All three samples were prepared with catalyst. The first was used as reference with reaction, the second was neutralized and the third was neutralized too, but heated at 78 °C for three hours and stored one day at room temperature before silylation. The third sample was prepared to see if the period before silylation has a strong effect on conversion. Chromatograms show that reaction in samples with catalyst cannot be stopped by adding acetic acid, even if the molar ratio of acetic acid to catalyst is 30:1. The third vial showed a higher conversion indicating that reaction occurs before silylation. But even in this case no DI was observed.

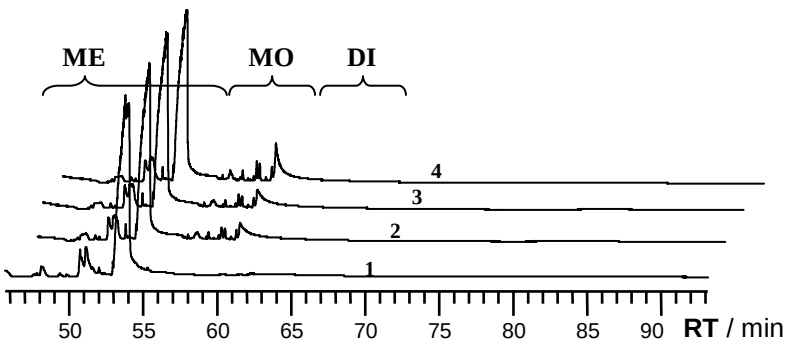

Fig. 4.1-3: Chromatogram of Dummy 1 with pyridine as solvent, zoomed area of ME, MO and DI. Area counts vs. retention time (*RT*). 1: without catalyst, only ME is present. 2: with catalyst. 3: with catalyst and acetic acid. 4: like 3, but heated before silylation. No formation of DI is observed.

As this behavior was not expected, this experiment was repeated with a sample from reaction that was dissolved in 1 % solution of acetic acid in pyridine. In this case catalyst would be immediately neutralized. Conversion was 10 % calculated from relative peak areas. Compared to samples prepared in dioxane with or without acetic acid, conversion was higher, but concentration of DI was not altered significantly.

It is concluded that reaction cannot be stopped in pyridine. Three reasons that the deactivation of the catalyst failed are imaginable. First it is likely that the neutralizing agent first reacts with the solvent itself, because pyridine is basic and known to forms salts with acids. Secondly, the formed neutralized product sodium acetate has catalytic properties in pyridine. Third, transesterification could be catalyzed acidic by the excess of acetic acid. The higher selectivity with pyridine cannot be explained this way, probably it is a result of a parallel reaction, the silylation.

Three dummies were prepared to check qualitatively if reaction occurs at low or high conversion levels and if a transesterification between products takes place. Data are summarized in Table 4.1-1. Dummy 2 in dioxane represents a conversion of 0 %, containing 69 % ME, 14 % glycerol and 2 % methanol. Dilution was 1:73. Without or with 1 % catalyst no product formation was observed. Dummy 3 represents a medial conversion, but only DI was contained as product. So the reverse reaction could be identified easier. Dilution was 1:65. Composition was 53 % ME, 11 % glycerol, 3 % methanol and 16 % DI. Dilution was 1:73. Without or with catalyst no formation of MO was observed. In a last test, Dummy 4, only MO was used as product. Composition was 26 % MO, 11 % glycerol, 3 % methanol. Dilution was 1:149. No forward or backward reaction took place with or without catalyst.
Therefore dioxane alone or with acetic acid is capable of quenching the reaction mixture.

As the catalyst sodium methoxide is corrosive for the coating of columns used in capillary gas chromatography, dioxane with acetic acid was chosen as quenching solvent. The acetic acid first neutralizes sodium methoxide and is itself neutralized by silylation.
To be sure that quantitative determination of the composition is not altered by the presence of a 1 % solution of acetic acid in dioxane, this solvent was evaluated in detail. Acetic acid could react with many of the components either by forming acetic acid esters of the alcohols glycerol and methanol, or it could act as acidic catalyst.

4.1.2.2 Preparation for GC

The first question was whether the choice of the quenching solvent 1 % acetic acid in dioxane changes composition determined by GC.
For this purpose Dummy 5 was prepared for a comparison of the influence of the presence of acetic acid (A) alone and catalyst (K) neutralized with A. Additionally one sample was heated before silylation for 10 minutes at 40 °C, simulating delayed sample preparation. Conversion

level was 50 %, dilution 1:66. Concentrations of the fatty acid derivates and glycerol do not change significantly with sample preparation, see Fig. 4.1-4.

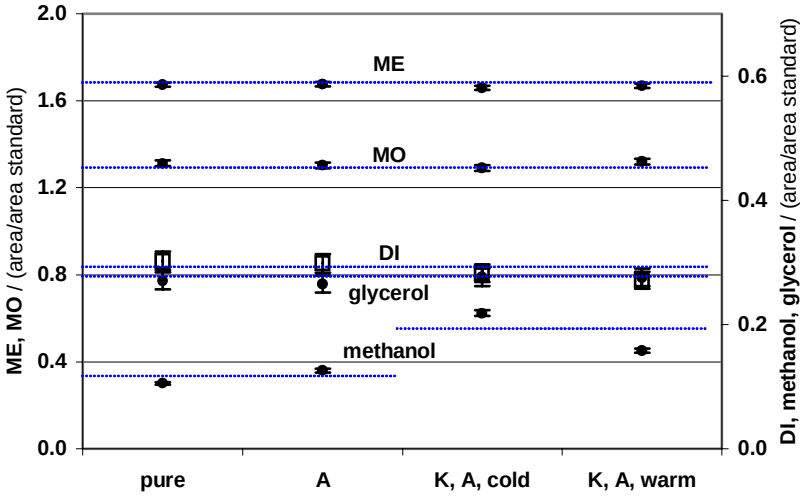

Fig. 4.1-4: Dummies to test the influence of acetic acid on composition of samples. Pure: solvent dioxane for comparison, A: with acetic acid, K: with catalyst, cold: normal preparation at room temperature, warm: sample heated before adding silylation agent, dotted lines: mean for two or four values

Only methanol concentration varies in a range of ± 35 %. Differences of methanol concentration levels with and without catalyst are a result of the methanol content in the catalyst itself. Neutralization of catalyst with acetic acid yields methanol, see Equation 4.1-3.

$$CH_3O^- Na^+ + CH_3COOH \longrightarrow CH_3COO^- Na^+ + CH_3OH \qquad \text{Eq. 4.1-3}$$

This contributes additionally 25 % methanol. If the methanol from the catalyst is subtracted, the methanol concentration of the neutralized warm sample “K, A, warm” is identical to that with acetic acid “A”. Because an effect of acetic acid should be more pronounced at higher temperatures, the unexpected higher methanol value for the sample at room temperature “K, A, cold” was not tried to be repeated. This difference between the concentrations of samples prepared with catalyst is likely to be caused by the use of unstable dispersion of catalyst in dioxane. The sample with delayed sample preparation “K, A, warm” shows an increase of MO, but a decrease of DI, so this preparation was repeated in a next Dummy.

Dummy 6 had the same composition as the previous one to see which step of sample preparation is critical: storage before silylation or silylation. One vial with neutralized catalyst was stored at 50 °C for 10 minutes before silylation. All samples were analyzed two times; first after the standard silylation period and second after an additional silylation period. For comparison one sample was prepared without catalyst. Conversion level was 50 %, dilution 1:66.

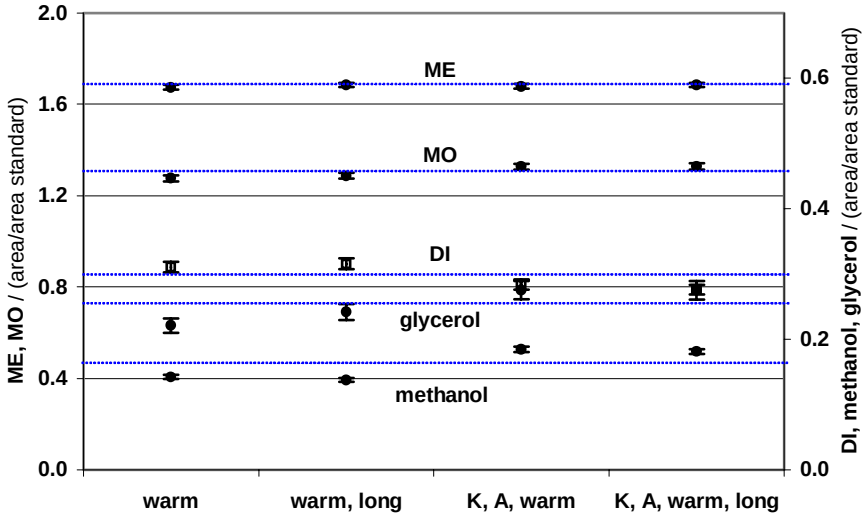

Fig. 4.1-5: Dummy 6, influence of storage temperature and silylation time on composition of samples. Warm: samples heated to 50 °C before silylation, long: additional time for silylation. K: with catalyst, A: with acetic acid, dotted lines: mean for two or four values.

ME content is not altered significantly. All other components show differences between preparations with and without catalyst which are very significant as differences are of a magnitude of five times mean standard deviation (*SD*). Relative differences are for glycerol 17 %, MO 4 % and DI -11 %. Differences in methanol content are mainly caused by the methanol content of catalyst. As samples were heated to 50 °C for 10 minutes, this indicates that storage of these solutions before silylation is critical. On the other hand if these differences are used for the calculation of the relative composition of fatty acid groups containing components, errors are less pronounced. In this case DI would decrease 1 % from 8.6 % to 7.6 % and MO would increase only by 0.3 % from 35.1 % to 35.4 %.

A prolonged silylation time has no effect on composition. Even the total sum of all areas shows no trend with silylation time. So no decomposition of silylated species is observed and silylation is maximal.

4.1.2.3 Sample Withdrawal

Samples were withdrawn from the stirred reactor by a 30 cm steel needle with an inner diameter of 2 mm with help of a glass syringe of 10 ml with luer lock connector. Reactor was at a reduced pressure of 300 mbar. Syringe and needle were preheated to reaction temperature of 130 °C to prevent a temperature decrease when the syringe is rinsed with products by three times filling it up and immediately emptying it. To prevent air from entering the reactor, the needle was first inserted through a septum which entered an air lock that could be evacuated separately. After evacuation, the connection of the air lock and the reactor was opened and the needle inserted into the emulsion. The syringe was rinsed three times with the emulsion in order to clean the dead volume in the needle of 2 ml.

Sample testing was done by varying the time between the last rinsing of the syringe and quenching in solvent. Usually it was waited till ME- and glycerol-layer separated. This time is usually dependent on conversion and temperature. If samples are taken faster, they usually contain a higher fraction of dispersed glycerol.

As conversions do not change fast near equilibrium, sampling was compared at medial reaction rates at low conversions. Samples were taken one by one, each time following the procedure outlined above. The first sample was quenched immediately, then waiting periods before quenching were 0.5 minutes and 2 minutes. A last sample of 4 ml was put into a glass and allowed to cool down without additional cooling for maximum delayed sample quenching at ∞ minutes.

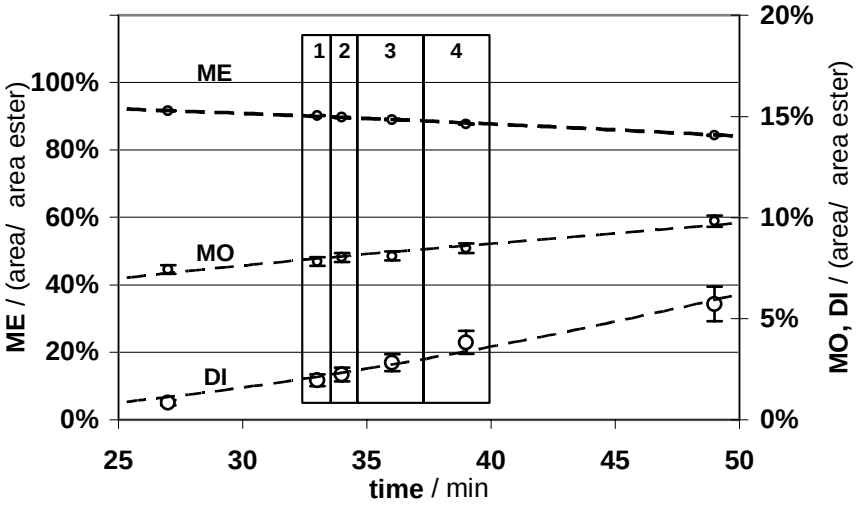

Fig. 4.1-6: Comparison of samples with delayed quenching, 1: immediate, 2: 0.5 minutes, 3: 2 minutes, 4: not quenched. For comparison the overall trend of conversion is shown (dashed line).

Samples show significant differences with a trend proportional to reaction time to higher conversions. As samples were taken at different times it is possible that this trend only reflects the overall conversion trend of the reaction and not the differences of the sampling procedure. Therefore data from different samples are compared with the overall conversion trend of the reaction in Fig. 4.1-6. If compared to the overall trend no significant change of composition is observed. For MO and DI a deviation from the overall trend is observed to a lower selectivity towards MO which is still not significant. This indicates that significant differences are to be expected at higher reaction rates. As this comparison was made at medial reaction rates at a low conversion, this would be the case for higher conversions in this run or generally at higher temperatures. As the trend is not very pronounced, phase separation in a preheated needle that lasts several minutes is possible without changing composition.

4.1.3 Conclusion

Reaction can be stopped by using dioxane with 1 % acetic acid as solvent, when samples are diluted 1:60. The quenched sample is homogeneous. Addition of acetic acid does not interfere with other peaks in chromatograms and does not change composition of test samples. Solutions are not stable even when neutralized and should be silylated as fast as possible. Delayed sample preparation or bad cooling will lead to approx. relative errors of 1 % for the composition of the fatty acid group containing components. Silylation time of 3 hours is

sufficient. Silylated samples are far more stable, not changing composition when additionally heated at 78 °C for three hours.
Samples quenched in pyridine still show reaction even if the catalyst is neutralized. Additionally they show a false high selectivity to MO. Problems with the use of pyridine are likely to be overlooked if sample composition is near equilibrium.
Transfer of fresh samples from the reactor with help of a preheated syringe to the quenching solvent is no critical step. So phase separation is possible in a preheated glass syringe prior to quenching without changing composition.

4.2 Gas Chromatography

After sample handling procedure was examined in detail, the method of gas chromatography (GC) had to be optimized. The aim was to analyze all components of the glycerolysis reaction in one run at a reasonable time. The method used in previous studies showed problems with the reproducibility of the methanol determination. This peak had to be separated from the solvent as a tangential peak. Therefore the results were dependent on the operator who examined the GC data. “Column bleeding” was a second problem. It is caused by degradation of components at high temperatures and a change of the flow rate due to the temperature of the oven. This effect is enhanced if active materials like the catalysts sodium methoxide are present on the column. In previous studies catalyst was neither neutralized nor removed prior to injection. The total time for the analysis of one sample was about 80 minutes.

4.2.1 Experimental

The same raw ME was used for calibration as for the glycerolysis. A technical grade mixture of FAME with approx. 75 % of oleic acid methyl ester was used as reference standard for methyl esters (ME) purchased from Lancaster. ME was chromatographically free of methanol and glycerides. Water content determined by Karl-Fischer titration was less than 0.01 %. Pure monoolein (MO) 99 % and diolein (DI) 99 % were purchased from Sigma, hexadecane 98 % and water free glycerol 99.5 % from Fluka, N,O-Bis(trimethylsilyl)trifluoroacetamide (BSTFA) 98 % from ABCR. Dilutions were performed in 5 ml graduated glass flasks with a glass stopper, silylation in 1.2 ml auto sampler vials with screw caps and Teflon faced rubber discs. Methanol 99.8 % and 1,4-dioxane 99.5 % stabilized with 25 mg/l 2,6-DI-tert.-butyl-4-methylphenol were of HPLC-grade from Roth.

The solvent dioxane contained as internal standard 0.383 % of hexadecane. Stock solutions containing ME, MO, DI, methanol and glycerol were used to prepare standard solutions. A standard solution contained a total of 1.5 % of glycerolysis components and 0.32 % of internal standard. The highest maximum relative weighting error for one component was calculated to be 0.82 % for DI. It is enhanced by the volatility of the solvent, gaining a combined maximum relative error of 0.92 % due to evaporation and handling of stock solutions during sample preparation.

After catalyst neutralization samples of glycerolysis were dissolved 1:60 in dioxane at room temperature. Usually 80 mg were dissolved in 5 ml of solvent containing the internal standard. In the case of high glycerol contents the solution was stirred with a Teflon coated magnetic

stir bar for several minutes. 1000 µl were transferred to a vial and mixed with 200 µl BSTFA, heating it at 78 °C in a metal block for 3 hours. The samples were allowed to cool down to room temperature and shaken before GC analysis to mix the condensate at the upper glass walls of the vial.

Analysis was performed by a Hewlett-Packard 5890 II gas chromatograph with a temperature controlled on-column-inlet, auto sampler and flame ionization detector. Carrier gas was N_2. Column was a DB5-HT column from J&W. A precolumn was used with a metal connector. Samples of 0.5 µl were automatically injected on column at an initial oven temperature of 35 °C. Inlet temperature was set automatically 3 °C above oven temperature. In the case of methanol detection initial temperature was held for 20 minutes. First rate is 2 °C/min for 6 minutes, second rate is 30 °C/min for 20.5 minutes to a level of 355 °C that was held for 10 minutes. Cooling was done at a rate of 40 °C/min. Operating condition was without split. Run time incl. cooling down without methanol detection was 37 minutes, with methanol detection 54 minutes.

4.2.2 Results

A typical CGC chromatogram without detection of methanol is shown in Fig. 4.2-1. Glycerol and the regions of ME, MO- and DI-peaks can be detected with good resolution. The sample is from a reaction mixture at a low pressure of 450 mbar and 130 °C. Triglycerides were not detected in these runs, but can be resolved without problems at a retention time (*RT)* of 20–25 minutes as shown in literature [37]. In this procedure no solvent change for silylation is necessary and *RT* of the components ME, MO and DI are similar to those reported in literature.

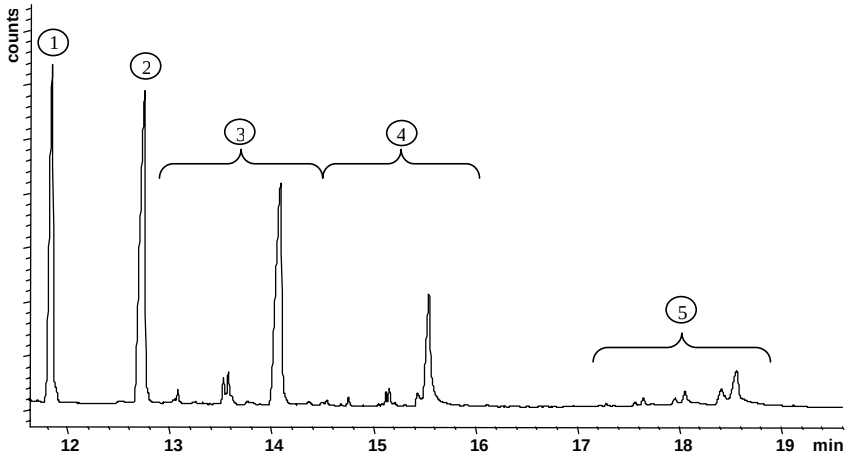

Fig. 4.2-1: CGC chromatogram of a reaction mixture without detection of methanol. Section of glycerol and glycerides, 1: glycerol, 2: internal standard hexadecane, 3: ME, 4: MO, 5: DI.

4.2.2.1 Methanol Detection

The main problem to determine methanol is the broad solvent peak. To separate methanol the initial temperature of the column was held at 35 °C for several minutes (waiting period *WP*) before starting the temperature program. This temperature can easily be reached even during the summer period without a cryogenic unit. A slow or faster temperature ramp at the beginning (2–30 °C/min) or a higher initial temperature at the beginning showed no advantages to separate methanol.

Retention times are generally longer with a longer low temperature period, but the separation of peaks of the low boiling components is enhanced. So this is an optimization problem. *WP* was varied from 2 to 25 minutes and the separation *S* determined. *S* is defined as the distance between the *RT* of the small methanol peak and the rising edge of the solvent peak at the same height as the half-peak height of methanol, shown in Fig. 4.2-2.

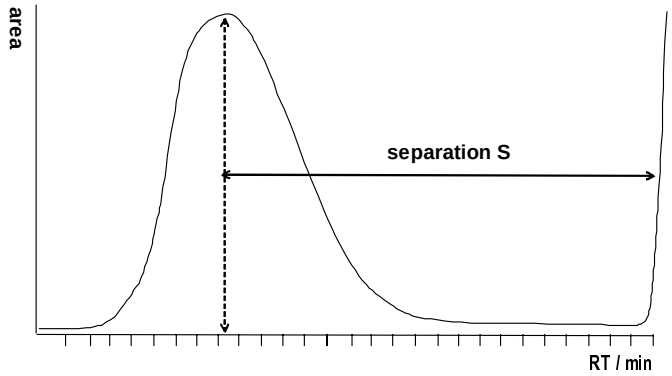

Fig. 4.2-2: Sketch of the definition of the separation *S*: distance in minutes between the retention time of methanol and the rising edge of the solvent peak at the ½ height of the methanol peak.

S is not defined as difference between the retention times of methanol and the solvent, because the solvent peak is much broader and usually only a small amount of methanol is present in the mixture due to the preparation procedure. So differences in *RT* do not reflect separability.

The *RT* of the internal standard as a high boiling component is simply the initial *RT* time with a *WP* of 0 minutes which was 16 minutes plus the *WP*. Separation of methanol shows a linear trend directly proportional to *WP* with a correlation of $R = 0.98$. The factor of the linear trend is 1:10, meaning that 1 more minute of *WP* will enhance separation only by 0.1 minute.

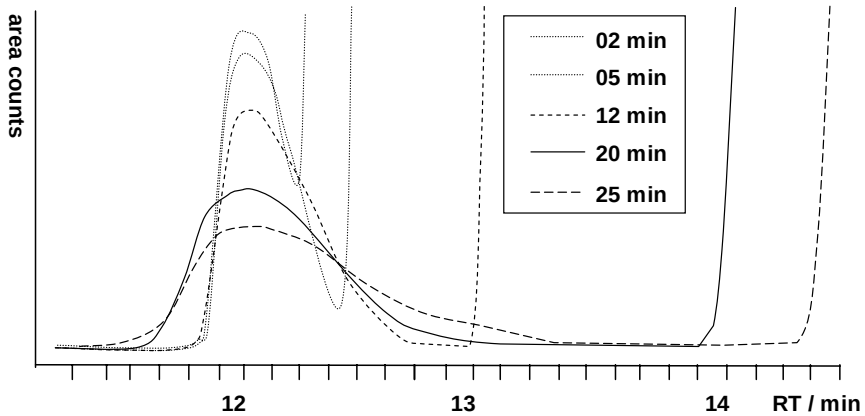

Fig. 4.2-3: Separation of methanol from the solvent peak for different initial waiting periods (*WP*). The retention time of all methanol peaks was adjusted to 12 minutes for comparison.

A convenient separation of methanol and solvent was found at a *WP* of 20 minutes. The same sample used in Fig. 4.2-1 was analyzed with a *WP* of 20 minutes, see Fig. 4.2-4.

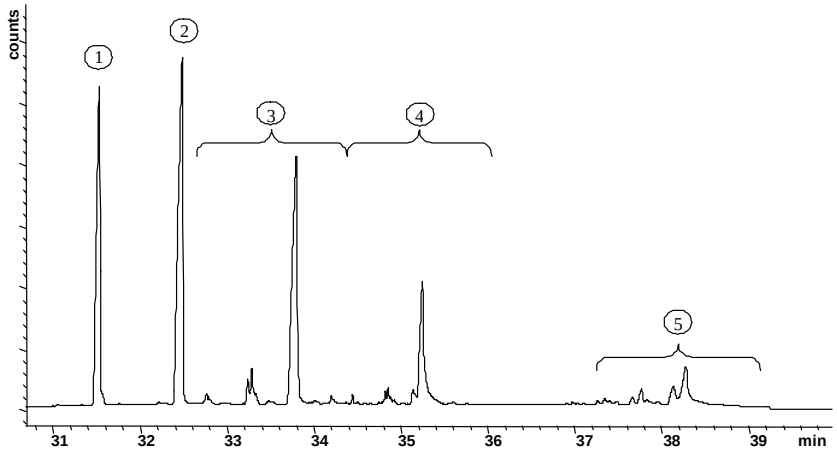

Fig. 4.2-4: CGC chromatogram of a reaction mixture with methanol detection, section of glycerol and glycerides, 1: glycerol, 2: internal standard hexadecane, 3: ME, 4: MO, 5: DI, waiting period (*WP*) of 20 minutes before oven and inlet temperature is raised.

The section of the glycerides and glycerol was not altered by this procedure. No additional tailing, drift of relative *RT* or change in peak area was observed.

RT of short chain alcohols with a *WP* of 20 minutes followed by a rate of 5 °C/min are for methanol 22.5, ethyl alcohol 23.7 and for isopropyl alcohol 24.3 minutes. Separation *S* of methanol and ethyl alcohol are 2.6 and 2.2 minutes. Isopropyl alcohol is still not separable from the solvent at this *WP*.
The simultaneous determination of a mixture of short chain alcohols is not possible with a practical value of *WP* because of overlapping. Therefore the use of a second internal standard before the solvent peak is not possible. But even without a second internal standard the used auto sampling allows a reliable quantification as shown in the calibration.
Only by adjusting *WP* it is possible to separate single short chain alcohols or similar single low boiling components, as they appear in transesterification reactions of fatty acid esters of short chain alcohols or the production of “biodiesel”. A second advantage is that the same GC-program only with different *WP* can be applied to analyze reaction mixtures containing different short chain alcohols.

The concentration of the alcohols methanol and glycerol varied between 0.9 to 4.9 % referring to the composition of a 80 mg sample from a typical reaction mixture that was dissolved in 5 ml of dioxane; DI content was 2 to 31 %, MO 5 to 69 % and ME 9 to 94 %. Each standard was injected three times, injection sequence was randomized. The average relative standard deviation (*SD*) of all injections was between 0.4 % for ME and 2.6 % for DI. The maximum relative *SD* found for one component at one composition was 4.0 % for DI. No injection was rejected for calibration.

4.2.2.2 Calibration

Calibration was done with a *WP* of 20 minutes, see Fig. 4.2-5. The plot of methanol shows a linear correlation with $R = 0.997$ when the axis intercept is set to 0. Due to impurities of the used ME in this region the correlation could be improved to $R = 0.999$ by using a small axis intercept of 0.007.

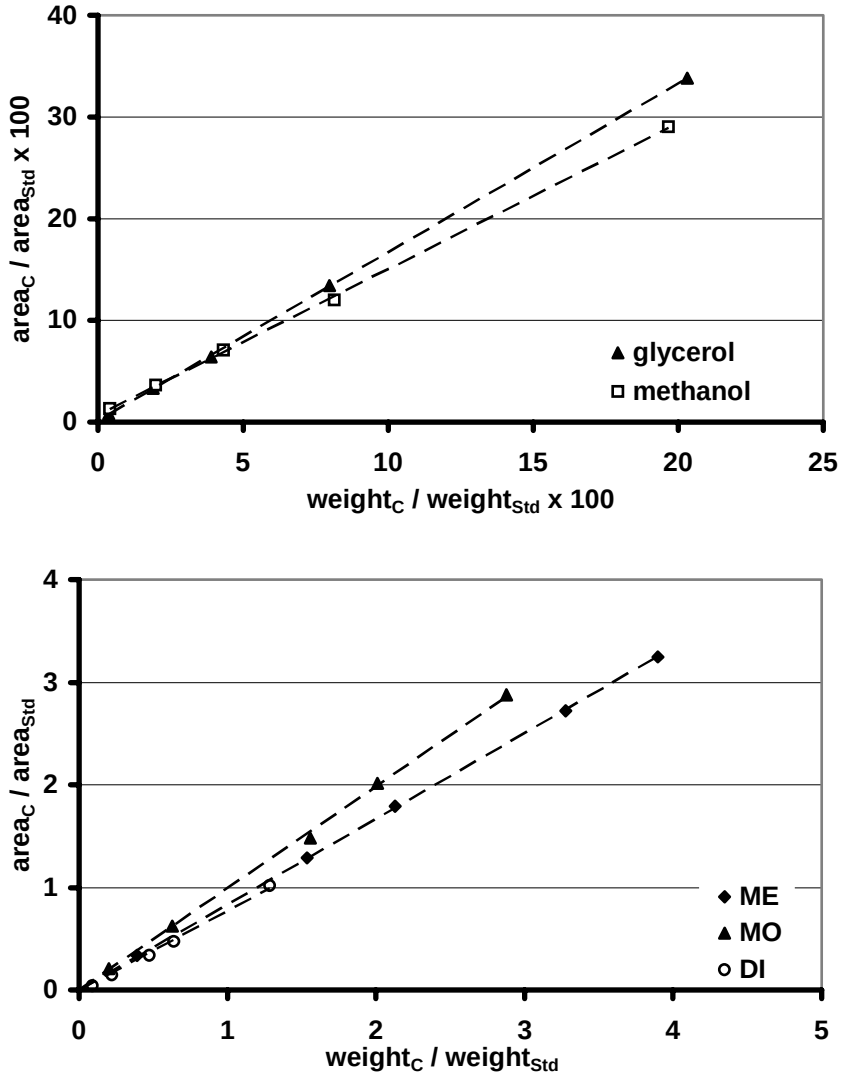

Fig. 4.2-5: Calibration of area of components (*C*) divided by area of internal standard (*Std*) vs. weight fraction. Upper plot: Calibration for methanol and glycerol. Lower plot: Calibration for ME, MO and DI. Dashed lines are linear regressions with an axis intercept of 0, except for methanol with an intercept of 0.007.

Calibrations of Glycerol, ME, MO and DI were fitted with an axis intercept of 0. The correlations are better than $R = 0.998$ except for DI with $R = 0.994$.

4.2.2.3 Analysis of Reaction Mixtures

The reaction between glycerol and ME was used as a test for the GC-method. Hot samples were added to dioxane containing the internal standard and 1 % acetic acid, dilution was approx. 1:20. Sample amount was weighted as difference after addition of 0.1 to 0.3 µl. Samples were further diluted to 1:60 and silylated as stated above. Calibration factors for pure MO and DO were applied for the product spectra of monoglycerides and diglycerides. Data are given in Table 4.2-1.

Table 4.2-1: Composition of reaction samples. Reaction conditions: methyl ester of oleic acid (ME), 500 rpm, 300 mbar, initial ME-glycerol-ratio 0.72, 0.79 % catalyst. Products are monoglycerides (MO) and diglyceride (DI). Mean standard deviation (*SD*) is given absolute and relative for all components. Conversion is 0 to 63 %.

Time / min	ME		MO		DI		Methanol		Glycerol		Sum
	abs. SD	rel. SD	abs. SD	rel. SD	abs. SD	rel. SD	abs. SD	rel. SD	abs. SD	rel. SD	
12	**80.48%**		**4.89%**		**0.00%**		**0.24%**		**18.84%**		**104.5%**
	0.22%	0.28%	0.22%	4.50%	-	-	0.005%	2.24%	0.02%	0.10%	
23	**65.37%**		**6.50%**		**1.50%**		**0.33%**		**21.72%**		**95.4%**
	0.09%	0.14%	0.22%	3.41%	0.01%	0.80%	0.006%	1.88%	0.01%	0.06%	
36	**61.56%**		**9.47%**		**6.33%**		**0.31%**		**16.52%**		**94.2%**
	0.13%	0.21%	0.24%	2.57%	0.43%	6.72%	0.005%	1.50%	0.01%	0.08%	
45	**64.09%**		**14.38%**		**14.59%**		**0.24%**		**5.94%**		**99.3%**
	0.13%	0.20%	0.29%	2.01%	0.65%	4.47%	0.002%	0.75%	0.02%	0.29%	
66	**39.42%**		**21.24%**		**30.83%**		**0.29%**		**6.74%**		**98.5%**
	0.05%	0.12%	0.33%	1.55%	0.67%	2.18%	0.006%	2.04%	0.02%	0.26%	
85	**28.63%**		**22.55%**		**33.34%**		**0.25%**		**11.67%**		**96.4%**
	0.16%	0.57%	0.61%	2.71%	0.65%	1.94%	0.003%	1.09%	0.03%	0.27%	
108	**26.57%**		**24.13%**		**35.71%**		**0.23%**		**10.81%**		**97.5%**
	0.12%	0.44%	0.22%	0.93%	0.56%	1.56%	0.007%	3.21%	0.04%	0.40%	
142	**25.50%**		**26.21%**		**36.84%**		**0.21%**		**8.37%**		**97.1%**
	0.18%	0.72%	0.21%	0.80%	0.24%	0.64%	0.006%	3.11%	0.02%	0.21%	
175	**24.52%**		**25.33%**		**34.38%**		**0.22%**		**12.07%**		**96.5%**
	0.12%	0.48%	0.40%	1.57%	0.17%	0.48%	0.003%	1.29%	0.02%	0.18%	

SD of sample injections and of mass balance shows no trend. Maximum deviation of mass balance observed was 5.8 %. Main source of error is expected to be sampling procedure and weighting back the samples because of evaporation of solvent during addition of the hot

sample. This would explain why most of the samples show a loss of material, average mass balance is 97.7 %. Another source of error is determination by GC. Because of simultaneous high concentrations of all components base line is higher. Precision could be increased by subtracting a chromatogram of a sample containing only solvent. No sample preparation was rejected for analysis.

4.2.3 Conclusion

GC method was optimized with respect to total time, resolution of glycerides and detection of methanol. The total analysis time is 54 minutes compared to an initially used method that needed 80 minutes with a lower resolution of methanol. Without methanol detection the same method can be used to determine only glycerides and glycerol. Methanol as well as ethanol can be detected as single low boiling components. The separability of low boiling components can be estimated using the proposed rule of thumb. Separability is enhanced only by a factor of 1:10 with respect to a prolonged initial time of the oven program. The combination of the sample handling procedure described in chapter 4.1 and optimized GC method was proven to be effective. When all samples of one experiment of glycerolysis reaction were analyzed, mass balance deficit was below 6 %. Maximum relative *SD* of the reproducibility for a single component was smaller than 5 %.

4.3 Distribution of Catalyst Determined by AAS

Starting point of this experiment is the question if the S-shaped form of the conversion curve could be caused by an increase of catalyst concentration in the methyl ester layer during reaction. As the reaction takes place mainly in the methyl ester layer this would lead to an acceleration of reaction rate and thus transform the ordinary hyperbolic plot of a second order reaction to an S-shaped form. The change of concentration that would cause this behavior can be estimated by assuming that reaction rate is proportional to catalyst concentration. In order to explain the S-shaped form, the change of solubility should be in the order of the change from the initial to the maximum conversion rate, a factor of approx. 3.
Catalyst concentration is expected to be higher in the glycerol layer because sodium methoxide is known to be sparingly soluble in alcohols different from methanol. Distribution coefficient and its dependency on composition are not known.

At high conversions the properties of the methyl ester phase changes drastically. As two hydroxyl groups are present in the main product monoglyceride and one in the consecutive product diglyceride, properties become more similar to those of glycerol. It is also possible that sodium transfers as salt of the glycerides. As glycerides are known to act as emulsifiers or conditioners catalyst may be transferred physically solved in glycerol to the methyl layer in a solvation sheath of the glycerides or in micellar state. A transfer of sodium as soap due to continuous reactive saponification is not expected, because raw materials are nearly water free.

4.3.1 Experimental

Analysis was done by a two beam atomic absorption spectrophotometer 2380 from Perkin-Elmer. Beam is chopped to compensate changes in light source intensity from a hollow cathode lamp of sodium in neon. A mixture of 0.5 l/min acetylene and 15.5 l/min air was used during measurement of samples in organic solvent. Because concentration was high, absorption at the doublet 330.2/330.3 nm with a characteristic concentration of 2 mg/l was chosen; monochromator was set to 330.2 nm with a slit of 0.7 nm.

Different solvents were tested that were able to dissolve the glycerol as well as the methyl ester layer. To prevent errors caused by sodium extracted from glass, all preparations after the withdrawal of the sample from reactor were done with polypropylene materials or for short contact time with polyethylene. As single solvents toluene, methanol, isopropyl alcohol and ethanol were tested for the ability to solve sodium soaps and sodium acetate. Maximum solubility for the samples of methyl ester and glycerol was found for a mixture of

ethanol with isopropyl alcohol with a ratio of 5:4 by weight. It is able to dissolve up to 20 % of glycerol or methyl ester layer from experiments either with palmitic acid or oleic acid esters. Solubility is only sufficient at a temperature of 45 °C, so all solutions were kept in a water bath during measurement and preparation at 50 °C.

To minimize ionization of sodium in the acetylene flame, an equivalent of 1000 mg/l of cesium was added to the solvent as 1.444g/l acetate. This solution was used as matrix reference.
Four to five standard solutions of 0.5 l were prepared by directly mixing sodium acetate with solvent. Standard concentrations are 0.009 to 0.046 %. Complete dissolution is difficult to observe due to the use of opaque polypropylene flasks. In order to subtract sodium from other sources, the absorption of matrix is determined in every run. Additionally samples from the pure raw materials ME and glycerol without catalyst were analyzed.
The instrument showed a linear drift of 0.03 to 0.09 % absorbance/min for low and high standard concentrations. Drift was compensated by fitting all data of each standard solution from up to 6 calibrations in one session to a linear time dependent equation. Calibration was repeated every ½ hour during one session. Data between two calibrations were analyzed with respect to the mean calibration values in this time period.

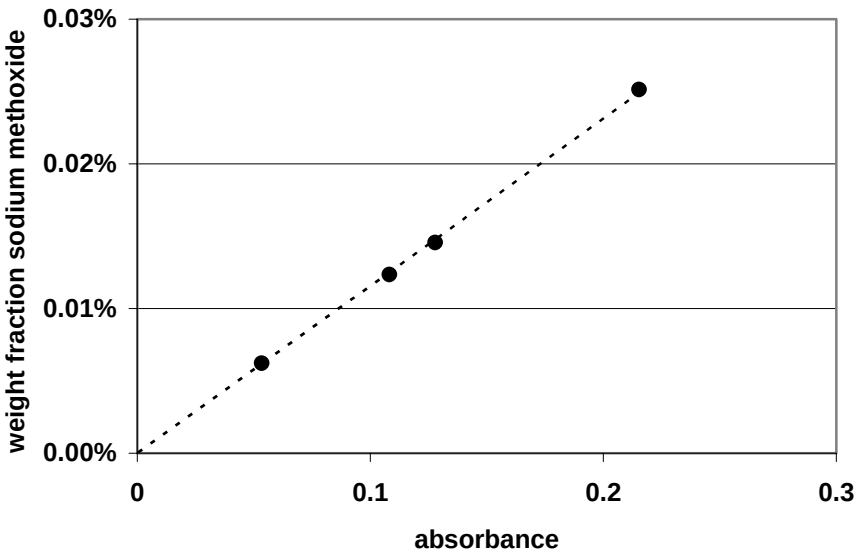

Fig. 4.3-1: Calibration of standard solutions containing sodium acetate. Amount calculated as equivalent to sodium methoxide, dashed line: linear trend.

All trends were fitted by a linear equation. Calibrations using these fitted values show a high correlation better than $R = 0.993$. In Fig. 4.3-1 an example of the used calibrations is shown with an axis intercept of 0 and a slope of 0.012 % sodium methoxide/absorbance. The average relative mean standard deviation for three values measured in sequence for all standard solutions was 1.6 %. The maximum and minimum relative standard deviation was 4.0 and 0.6 %.

Samples from the reactor are withdrawn with help of a 10 ml glass syringe with a metal valve and a steel needle; syringe, valve and needle were connected by the Luer Lock system. All parts are preheated to 130 °C. The syringe was three times filled with reactor mass and emptied back into the reactor to rinse out remainders from previous samples. Samples were taken through a septum at a reduced pressure of 300 mbar. The valve was closed, the needle removed and the syringe was inserted to a metal block that was thermostated at 130 °C. After phase separation that needed approx. 5–30 minutes, samples of 4 ml of each phase were transferred into polypropylene flask. Samples were diluted to 1 % with a 5:4 ethanol:isopropyl alcohol mixture containing cesium acetate. Each sample was measured three times. Measurements were repeated twice after new calibrations. After each measurement a cleaning solvent was used till absorbance was zero again.

4.3.2 Results

An experiment was conducted at a temperature of 130 °C and a pressure of 300 mbar. Catalyst concentration was 0.80 % relative to the total mass of reactants. Initial molar ratio of oleic acid methyl ester and glycerol was 3:4. Total mass was 356 g.
The sodium methoxide is expected to be solved mainly in the glycerol layer. This was verified by testing the solubility in the pure phases. Pure glycerol dissolves 2 % sodium methoxide at 130 °C. Pure methyl ester forms a brown slurry. Even one drop of a sodium methoxide solution in methanol is not soluble in 5 ml of pure methyl ester at room temperature.

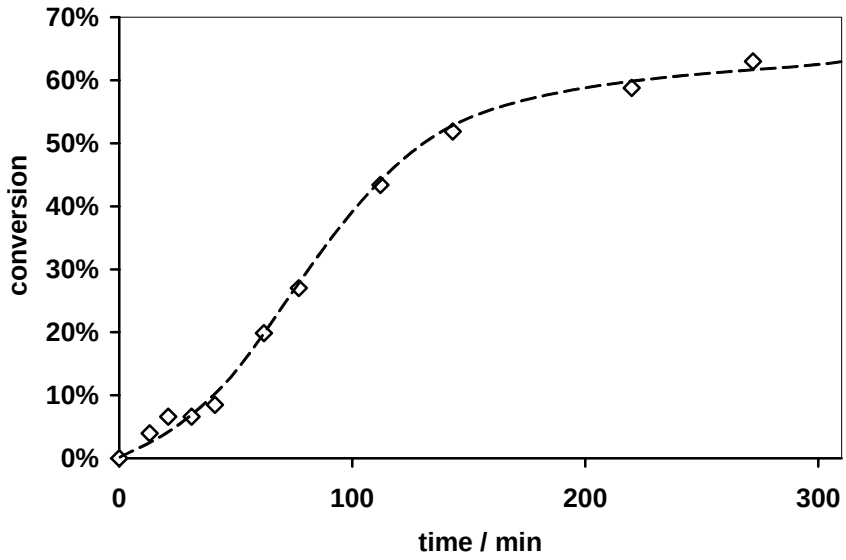

Fig. 4.3-2: Conversion plot of the experiment in which the sodium content was determined. Dashed line: overall trend. Reaction conditions: 130 °C, 300 mbar, 0.8 % catalyst, initial molar ration between oleic acid methyl ester and glycerol 0.75.

Reaction was monitored qualitatively by methanol distillate which is proportional to conversion. Maximum conversion after 3 hours is known from several different experiments to be approx. 63 % by GC.

In Fig. 4.3-2, the first two points at 13 and 21 minutes show a higher conversion as the S-shaped trend curve. This is possibly a result of the time needed for the separation of the sample in the syringe which was at the beginning a longer period in which reaction still proceeds, see chapter 4.1.2.3. Results of atomic absorption spectroscopy (AAS) analysis are shown in Fig. 4.3-3. No change in sodium content of the glycerol layer or methyl ester layer is observed.

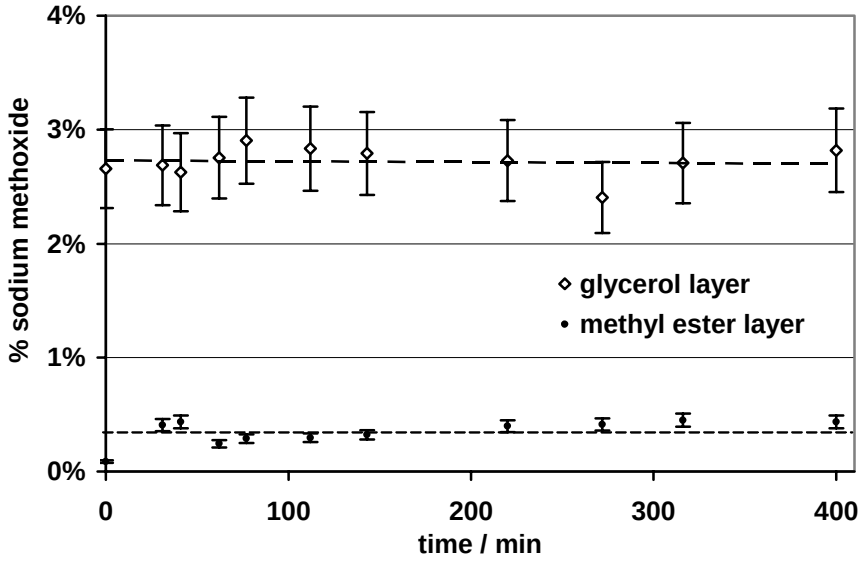

Fig. 4.3-3: Sodium distribution between glycerol and methyl ester layer during a reaction**.** Reaction conditions: 130 °C, 300 mbar, 0.8 % catalyst, initial molar ratio between oleic acid methyl ester and glycerol 0.75. Dashed line: mean.

The mean content of the catalyst in the glycerol layer is (2.72 ± 0.13) %, in the methyl ester layer (0.34 ± 0.11) %. For the calculation of mass balance, masses of glycerol and methyl ester layer were calculated according to conversion. The total sum of sodium methoxide was (3.0 ± 0.4) g. Standard deviation of mass balance is much higher than that of the reproducibility of AAS. As mass balance reflects deviation from the true concentrations, the relative standard deviation of mass balance is shown in Fig. 4.3-3 as error bars. Initial addition of catalyst by weight was 2.8 g. The difference is within standard deviation. Additional sodium may come from the glass walls of the reactor. Tests to solve higher contents of sodium methoxide in glycerol showed that glass walls are etched at 130 °C, remaining milky in dry state.

4.3.3 Conclusion

No change of sodium distribution was observed. As expected, the proportion was higher in the glycerol layer. Monitoring of sodium for a reaction at 130 °C with 0.80 % catalyst sodium methoxide showed a constant content in glycerol layer of 2.72 %, in methyl ester layer of 0.34 %. Ratio between both is 8:1 for glycerol and methyl ester. Transfer of catalyst from the

glycerol to the methyl ester layer during reaction as reason for the S-shaped conversion curve can be excluded.

4.4 Micro Photographic Drop Size Determination

Drop size distributions are usually measured in non-reactive systems and the continuous phase is in most cases water [38, 39, 40]. Only few examples for reactive systems are found in literature. One example is given in literature [41]. Samples were taken continuously by branching off a small liquid stream from the reactor in which polymerization of vinyl chloride took place. Drop sizes were determined by a microscope. Continuous phase was an aqueous solution.

In reference [42, 43] drop size was determined by a chemical method for a system similar to the nitration of aromatic hydrocarbons in a water based nitration acid and the aromatic phase. But reaction itself was carried out in a vessel without monitoring drop sizes during reaction.

4.4.1 Experimental

For drop size measurements by micro photography a modification of a medical endoscope was used as described in literature [43]. The outer shell is an air-cooled high-grade steel tube with a glass window which can be inserted directly into the reactor, see Fig. 4.4-1.

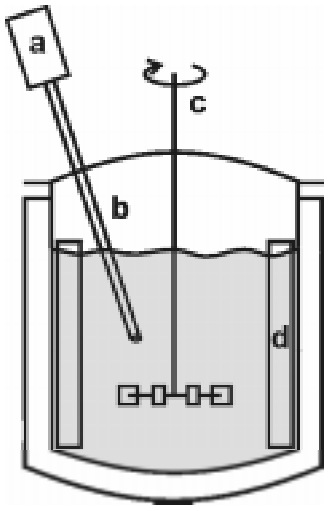

Fig. 4.4-1: Endoscope system in a double wall glass reactor: (a) CCD-camera, (b) endoscope, (c) stirrer, (d) baffles.

The magnification system consists of an additionally covered rod lens system with variable focal length, allowing measurements of drops in the range of 10 to 1000 µm. The light source is a flashlight (Drelloskop 250, Drello) with a half-intensity width of 5 µs.

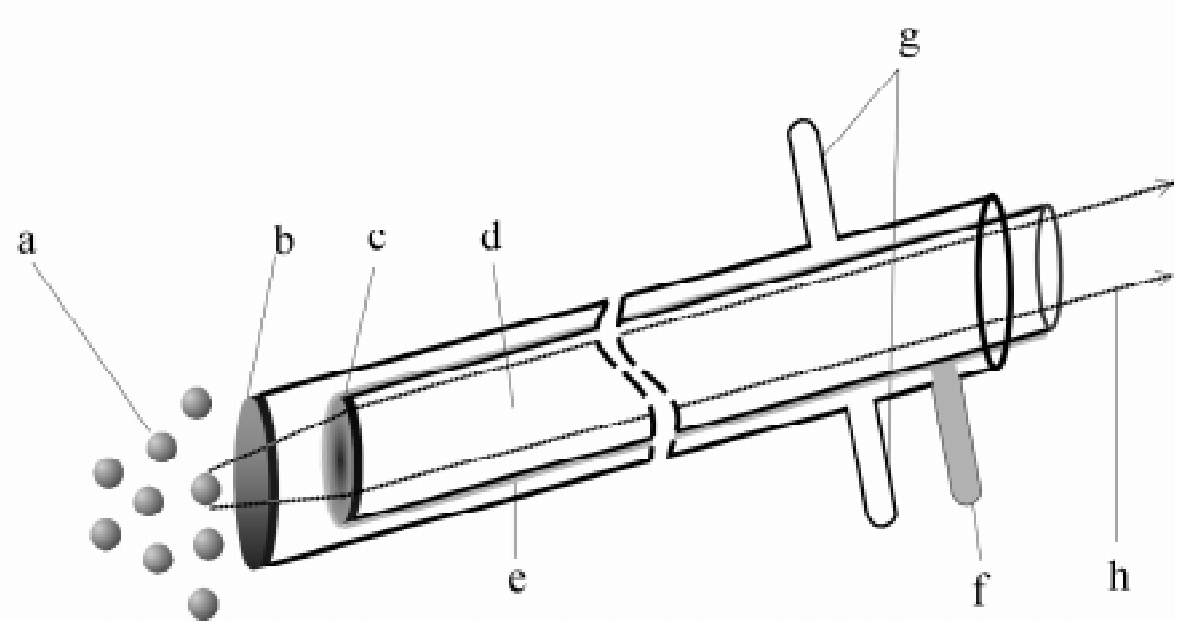

Fig. 4.4-2: Micro photographic endoscope, a: drops, b and c: glass windows, d: rod lens, e: glass fibers, f: connector for light source, g: cooling medium in and out, h: way of light.

The CCD-Camera is non-interlaced (CV M10 BX, JAI). Synchronization of camera and flashlight was done by software written in Visual Basic, see appendix. The light is conducted by a glass fibre system integrated in the tube. For the evaluation of the mean diameter 200 drop images are usually sufficient. The size of the drop diameter is determined manually. Photographs of drops are shown in Fig. 4.4-3.

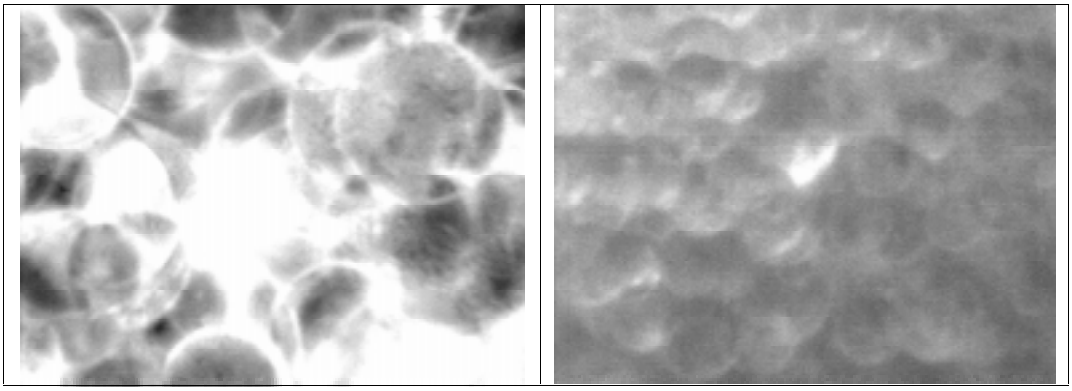

Fig. 4.4-3: Drop images. Left: drops without catalyst between 200 and 300 µm. Right: drops at reactive conditions between 50 and 100 µm, less contrast caused by darkening of the solution. Both images show overlapping of drops.

On the left, drops in the non reactive system are shown with a diameter of approx. 200 µm. Contour of drops has a high contrast. In the right image contrast is less pronounced in a reactive system. The main reason is a coloring of the glycerol phase during reaction. Distinction of phase boundaries depends on the refractive index difference which is at the beginning is small. Refractive index difference at reaction temperature could not be determined because devices are usually not suited for measurements above 100 °C. At room temperature, refractive index difference Δn^{d}_{20} for oleic acid methyl ester and glycerol is 0.0220, for palmitic acid methyl ester 0.0028. Compared to a common liquid-liquid system without reaction like toluene-water with Δn^{d}_{20} = 0.178 this difference is small. So only small changes of the refractive index by contaminants or reaction products like methanol with a lower value of n^{d}_{20} can affect contrast of phase boundaries. A second effect is mass transfer during reaction which additionally changes composition at the boundaries.

4.4.2 Results

4.4.2.1 Location of Endoscope

For one run without reaction, drop size was determined at four different locations in the reactor as shown in Fig. 4.4-4.

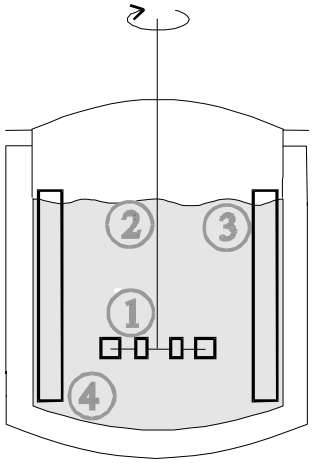

Fig. 4.4-4: Drop size determination at four different locations.

Flow induced by the stirrer forms two circulation flow systems, one above and one below the plane of the stirring disc. Flow starts radial from the plane of the stirring disc to the walls where it is divided into one streaming up and one streaming down, circulating back to the center of the stirrer. The loop going up will follow the glass wall upwards and pass location 3 and 2 on its way back to the stirrer. If there is significant settling of larger drops on this path or a high coalescence tendency, a decrease of drop size between position 3 and 4 should be observed. Density difference between glycerol and methyl ester is very pronounced which accelerates phase separation and requires a high minimum power input for gaining full dispersion. If dispersion is not well developed, this will lead to bigger drops at the lowest point 4. Standard position for the runs with reaction was position 3 due to the geometric design. Results for the drop diameters are shown in Fig. 4.4-5.

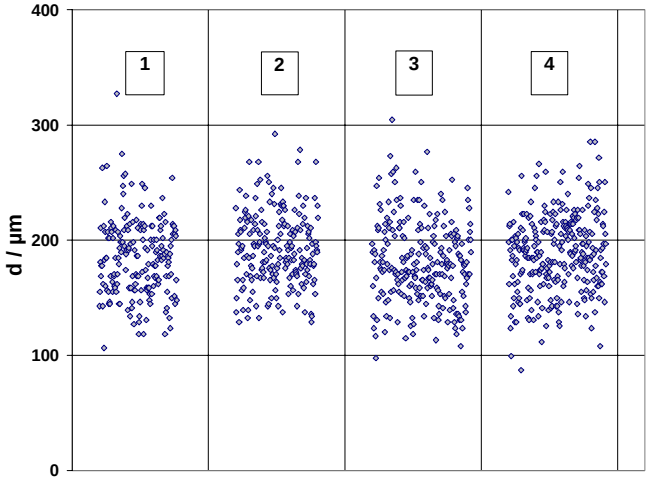

Fig. 4.4-5: Drop sizes determined at different positions 1–4 in the reactor. Dispersion of glycerol in oleic acid methyl ester without reaction. $\phi = 0.3$, $T = 130$ °C, 545 rpm. Numbers of the positions are according to Fig. 4.4-4.

Statistical data and Sauter mean diameter d_{32} are given in Table 4.4-1. For the calculation of d_{32} a Gaussian distribution was assumed. Drop sizes show only small differences at different positions of the reactor.

Table 4.4-1: Drop sizes determined at different positions in the reactor. d_{32}: Sauter mean diameter, $<d>$: average diameter, *SD*: standard mean deviation, *n*: number of drops. The number of the position is according to Fig. 4.4-4.

Position		d_{32} /µm	$<d>$ /µm	*SD* /µm	*n*
1	central	195	184	32	134
2	top, central	203	193	32	143
3	top, lateral	200	185	38	122
4	bottom	206	196	33	130

Maximum relative deviation of d_{32} from a mean value for all positions is 3 %. Measurement errors of 10 % are reported for a similar set up in reference [44]. It is concluded that Sauter mean diameter is not dependent on the place of the endoscope in the reactor.

4.4.2.2 Drop Size during Reaction

Drop sizes were recorded for a run at 130 °C. Before adding the catalyst drop sizes are determined, then catalyst is added and reaction started. Maximum conversion was 63 %. Range "a" in Fig. 4.4-6 shows the drop size before starting reaction which is much higher than in the following sections b and c. Decrease of drop size is very fast and can be observed only by the naked eye because after adding the catalyst, image recording is not possible for a period of 10 to 30 minutes. The reason is the low contrast caused by the addition of the catalyst solution. The catalyst is solved in methanol which evaporates and flows back from the reactor walls that are not heated. Therefore the emulsion contains in this period high fractions of gas and methanol.

Drop size decrease will be linked mainly to a change in surface tension because temperature is kept constant and density changes only slowly. The products mono- and diglyceride are used as emulsifiers and conditioners in food and cosmetic industries. Therefore a change in surface tension can be expected. But when the emulsion is neutralized with phosphoric acid in excess after reaching equilibrium, initial surface tension seems to be instantly restored as drops become much larger again. Neutralization affects ionic strength and pH. But the main effect that leads to a decrease of drop size is believed to be soap formation directly after adding the catalyst. The use and efficiency of soaps as emulsifiers for the glycerolysis of fatty acids and their methyl esters was studied in literature [45]. Even small amounts of emulsifiers have strong effects on the surface tension. Neutralization with a strong acid will instantly transform the sodium salts of the fatty acids back to fatty acids which have no pronounced effect on surface tension.

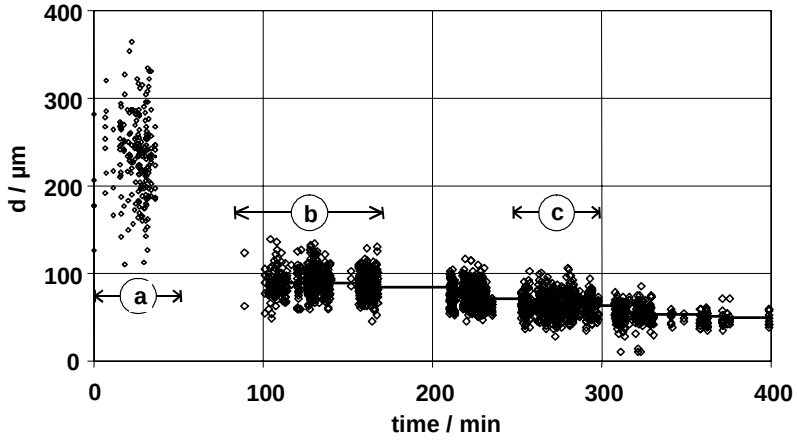

Fig. 4.4-6: Drop sizes in a reactive system. Range (a) is without reaction, before adding catalyst at 40 minutes. Ranges (b) and (c) are at reactive conditions 130 °C, 300 mbar, 545 rpm, 1 % catalyst, initial $\phi = 0.3$. Solid line: mean value.

In Fig. 4.4-7 a histogram of the drop sizes arranged in groups according to Fig. 4.4-6 is plotted and compared to a Gaussian distribution function (GD). The GD is a non normalized probability density function (*pdf*) of Gaussian type according to Equation 2.2-2 that was fitted to frequency data using a constant factor. Number of drop sizes evaluated were 200 (a), 600 (b) and 700 (c). This means that the use of a GD is justified and even a small number of drops of 200 is sufficient for the evaluation of the mean diameter and *SD*.

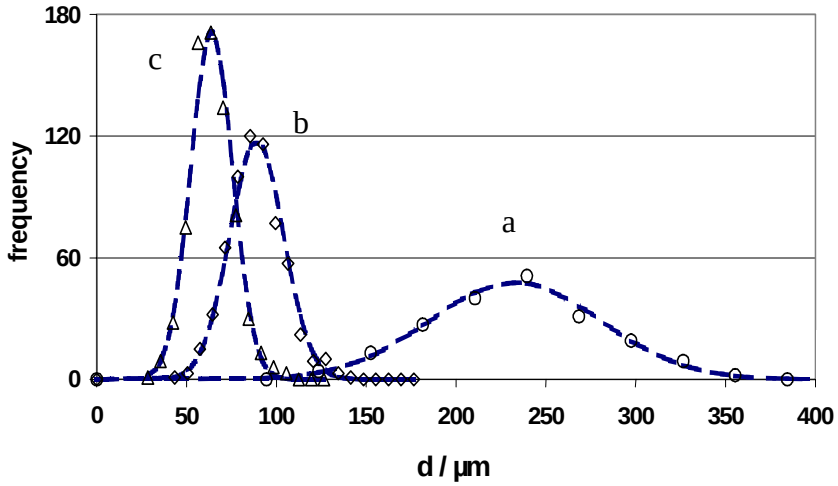

Fig. 4.4-7: Comparison of the frequency of grouped drop size data with a Gaussian distribution function (GD). Dashed line: GD, (a): without reaction, (b) and (c) with reaction.

4.4.2.3 Influence of Stirring Rate

Results for the Sauter mean diameter d_{32} without and with reaction are compared in Fig. 4.4-8. The trend of the Sauter mean diameter d_{32} is usually correlated in literature by Equation 4.4-1, in which d_{32} is proportional to a system specific constant C and the Weber number We to the power of –0.6, see literature [46].

$$d_{32} = CWe^{-0,6} \qquad \text{Eq. 4.4-1}$$

We reflects influences of geometry of the reactor D, stirring rate N, density of continuous phase ρ_C and surface tension σ.

$$We = D^3 N^2 \rho_C / \sigma \qquad \text{Eq. 4.4-2}$$

Using Equation 4.4-2 the relative change of the Sauter mean diameter can be calculated according to Equation 4.4-3 by raising the ratio between the stirring rates to the power of 1.2. This is only valid, if the system specific constant C does not change.

$$\frac{d'_{32}}{d''_{32}} = \left(\frac{N''}{N'}\right)^{1,2} \qquad \text{Eq. 4.4-3}$$

For a non reactive system in equilibrium no change of C is to be expected, but a reactive system will change composition and phase fraction according to conversion. Therefore only drop sizes determined at the same conversion should be compared. The period for taking photos used for one value of d_{32} was less than 3 minutes.
For an estimation of the trend of d_{32}, data were fitted to a similar correlation in which the exponent E is a free parameter, see Equation 4.4-4.

$$d'_{32} = d''_{32}\left(\frac{N''}{N'}\right)^{E} \qquad \text{Eq. 4.4-4}$$

Data obtained in five runs at an initial phase fraction between 0.22 and 0.30 at 130 °C are compared with the predictions by Equation 4.4-4 in Fig. 4.4-8. The trends for three different exponents E (dotted lines) start at the lowest stirring rates of 450 rpm predicting relative changes of d_{32}.

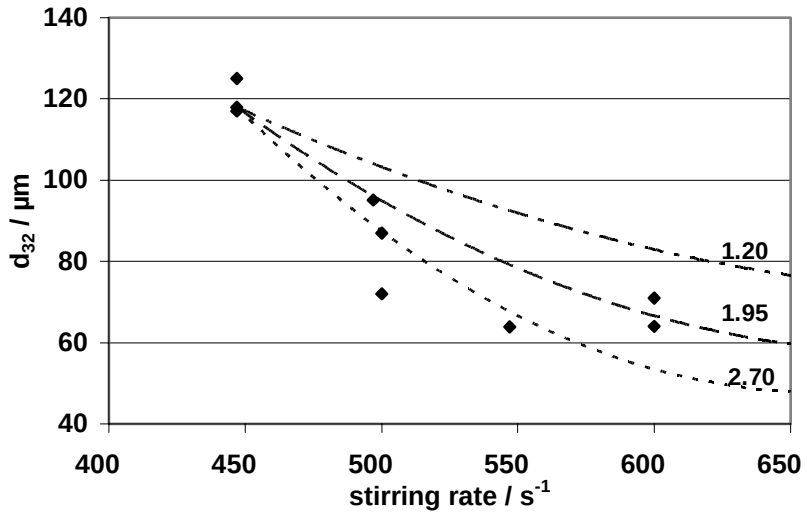

Fig. 4.4-8: Sauter mean diameter d_{32} vs. stirring rate and predictions of Equation 4.4-4. Data from five experiments with reaction at 130 °C, initial phase fraction between 0.22 and 0.30. Data are compared to trends based on Equation 4.4-4 with an exponent E of 1.20, 1.95 and 2.70. All trends start at the minimum stirring rate.

The trend of drop sizes with reaction shows a strong dependency on the stirring rate. It is even more pronounced than the usually cited correlation with an exponent of 1.2. The best fit is obtained with an exponent between 1.95 and 2.7. As drop sizes were recorded at different

conversion levels, the different drop sizes at one stirring rate usually cover the range that was observed for medial to high conversions.

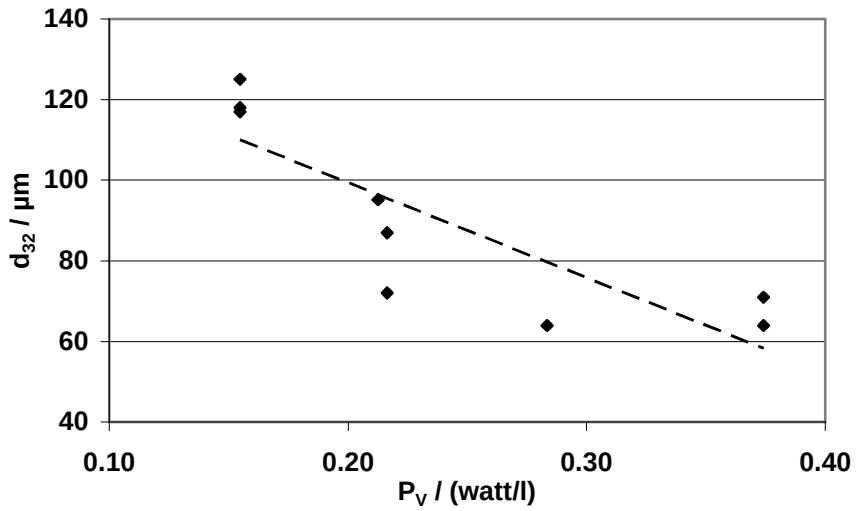

Fig. 4.4-9: Sauter mean diameter d_{32} vs. power input per liter P_V. Data according to Fig. 4.4-8, dashed line: linear trend.

For comparison with raw data from other experiments a plot of d_{32} vs. P_V is shown in Fig. 4.4-9. The power input per liter P_V was calculated according to Equation 2.2-11. In Fig. 4.4-10 drop sizes are shown for three runs before catalyst was added.

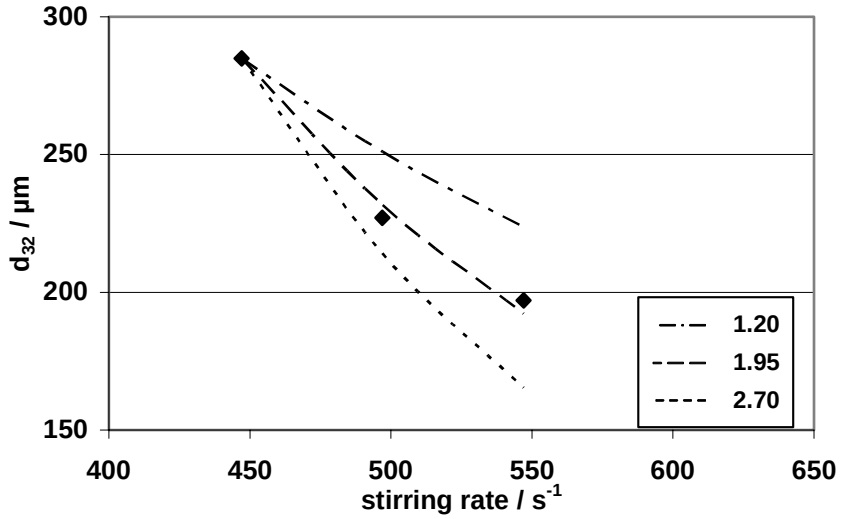

Fig. 4.4-10: Sauter mean diameter d_{32} vs. stirring rate without catalyst and predictions of Equation 4.4-4. Data from three experiments before reaction is started at 130 °C and an initial phase fraction between 0.22 and 0.30. Data are compared to trends based on Equation 4.4-4 with an exponent E of 1.20, 1.95 and 2.70. All trends start at the minimum stirring rate.

In Fig. 4.4-10 a gap of drop sizes of more than 100 µm is observed compared to Fig. 4.4-8 with reaction at a stirring rate of 500 rpm. The reasons for this gap were discussed in the previous chapter. A similar trend of d_{32} with stirring rate without reaction is observed in Fig. 4.4-10. The best fit is obtained with E = 1.95.

The usually stated exponent of 1.2 is a consequence of Kolmogorov´s theory of homogeneous isotropic turbulence in which the maximum drops size is predicted [47]. From that value d_{32} is calculated. In this theory drop formation is controlled by drop breakage.
A decision which process, coalescence or breakage is responsible for the deviation from the exponent of 1.2 is difficult, because even for dispersions dominated by coalescence which should deviate from Equation 4.4-3 exponents of 1.2 were reported [48]. In literature [49] two exponents smaller than 1.2 are reported, an exponent of 0.72 for a system with a high fraction of dispersed phase of ϕ = 0.5 and an exponent of 0.75 for a system with pronounced coalescence. In literature [50] a dependency of exponent and ϕ was reported. The exponent decreased from 1.2 to 0.65 when ϕ was increased from 0.1 to 0.6. These results were obtained by using a strongly coalescing as well as a non-coalescing system. In literature [51] higher exponents are reported for a system containing tri-n-octylphosphine oxide (TOPO) which is surface active and works as a coalescence inhibitor. The exponent increased from 1.2 to 1.8

when the concentration of TOPO was increased from 0 to 5 mmol/l. The reasons for deviations from Kolmogorov´s theory are still under investigation, especially in the most complex case of a reactive system in which all relevant parameters change that affect drop size, like composition, surface tension, phase fraction and inter phase mass transfer.

4.4.3 Conclusion

The micro photographic set-up allows recording drop sizes with or without reaction at 130 to 160 °C, pressures down to 300 mbar and a high initial volume fraction of dispersed phase of 0.3. The drop sizes are independent of the location of the endoscope in the reactor. A total of 200 to 300 drops is sufficient to determine the mean drop size. Drop size distribution is of normal Gaussian type before and after addition of the catalyst. After addition of the catalyst, drop size decrease in one step from 300–200 to 150–50 µm. Drop sizes decrease continuously during reaction. Reaction does not interfere with the assumption of a Gaussian normal distribution. The influence of stirring rate on the mean drop size is more pronounced than predicted by the theory of Kolmogorov. An exponent of 1.95 gives the best fit in a similar correlation in Equation 4.4-4 that is higher than the exponent predicted by Kolmogorov of 1.2. This exponent was compared to the range of exponents that is reported in literature.

5 Reaction and Modeling

A set of experiments with respect to temperature and phase ratio was carried out in an autoclave. These experiments do not yield directly kinetic data, but describe equilibrium conditions that can be used for a kinetic modeling.

Standard experiments for the determination of reaction rates were carried out in the stirred tank reactor described in chapter 3. The first part of the experiments was conducted without the use of the complex sampling and analysis procedure described in chapter 4.1 and 4.2. The influence of different reaction conditions like stirring rate, temperature and phase ratio was examined. The effects are compared with respect to the conversion. Conversion was determined by GC with respect to the concentration of the fatty acid methyl ester as well as by the amount of distillate of the co-product methanol. Additionally the apparent activation energy is estimated.

Effects of reaction conditions on the total set of concentrations are discussed in chapter 5.3. First the concentration measurement of the alcohols methanol and glycerol is discussed. The determination of those concentrations is dependent on the degree of completeness of phase separation and equilibrium conditions. The reaction under investigation without solvent did not allow changing the initial concentration separately because the possibilities to change composition are limited. The effect of pressure and temperature is discussed by means of the selectivity and conversion. The influence of temperature is discussed in respect of literature that covers a temperature range from 30 to 240 °C.

Modeling is done using experiments at different pressures and temperatures. Two models are employed. Additionally a pre-equilibrium of the alcoholates is formulated and discussed with respect to the equilibrium constants. Finally the activation energy is determined and compared to reports in literature.

Using this model, the occurrence of mass transfer is estimated using results from the estimation of transport properties in chapter 2.2.2.3.

5.1 Equilibrium Studies in a Closed Autoclave

These experiments were not conducted in the standard glass reactor described in chapter 3 but in an autoclave which was made of steel. The lid is closed by six screws, maximal pressure was 4 bar. It was stirred by a magnetic stir bar and heated by a metal jacket (not shown). The reactor is shown in Fig. 5.1-1.

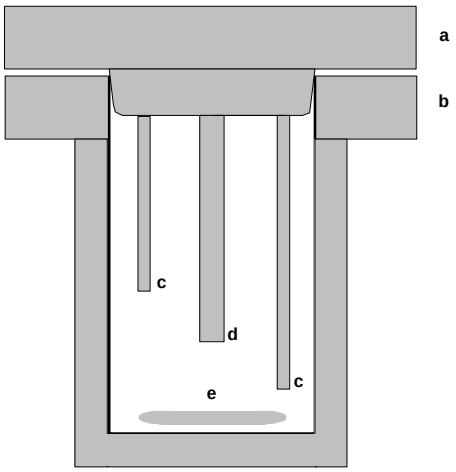

Fig. 5.1-1: Steel autoclave, a: lid with three inner tubes, b: bulk reactor, c: sampling tubes which are immersed in liquid during reaction, d: tube that is closed at the bottom for temperature measurement, e: magnetic stir bar. The lid contained an additional tube for pressure control (not shown).

Temperature was measured by a thermoelectric couple that was inserted into the closed central tube in the lid. Samples were withdrawn from two tubes immersed into the liquid in the reactor at different levels.

The catalyst 95 % sodium methoxide (Fluka) was added as solid matter. The reactor was filled with the 75 % oleic acid methyl ester (Lancaster) and 99.8 % glycerol (Fluka) which formed a two phase system. Afterwards the reactor was flooded with 3 bar nitrogen at room temperature to check leak tightness. After a period of 1 hour without change of pressure, the reactor was slowly allowed to regain atmospheric pressure, closed and heated with a thermostat to the desired temperature ± 5 °C. Samples were taken after 48 hours. The stirrer was turned off for 30 minutes and samples from each separate layer were taken. Samples were immediately cooled by a water cooling system attached to the sampling tubes.

At this time no calibration standards for mono- or diglyceride were available. Therefore concentration measurements have to be regarded only as indicator for qualitative trends. As the system was closed, the final methanol content is proportional to the conversion. The methanol content is on a higher level compared to reactions at atmospheric or reduced pressure that were carried out in a different reactor. The final difference of vapor pressure to atmospheric pressure was between 1 and 3 bar.

Establishment of equilibrium was verified by taking pure samples from each phase after different times in steps of 24 hours. After 48 hours no change of composition could be observed when pressure maintained constant. Pressure increase was finished within one day.
The effect of different conditions is only discussed with respect to the concentrations measured in the ME layer. In the glycerol layer no products were detected except methanol.

5.1.1 Influence of Molar Ratio of Reactants

The effect of the initial molar ratio (*MR*) between glycerol and ME was determined in four runs. *MR* was changed from 2:1 to 4:1. When *MR* is increased, the absolute content of ME in the autoclave is reduced because the total volume of the two liquids was held constant. The results in Fig. 5.1-2 show an increase of conversion with an increasing *MR*.

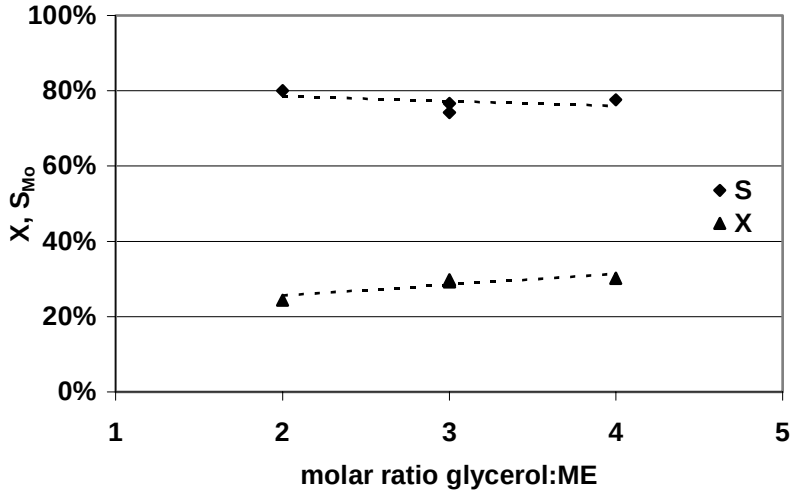

Fig. 5.1-2: Equilibrium conversion X and selectivity towards monoglyceride S_{MO} vs. initial molar ratio between glycerol and oleic acid methyl ester (ME). Experiments in an autoclave at 150 °C, 0.5 % catalyst.

This is in accord with the law of mass action because methanol is a co-product. Even at the same levels of conversion a lower *MR* will lead to the formation of more methanol. As the system is closed the increasing partial pressure of methanol will limit the maximum conversion because solubility at a given temperature is proportional to pressure according to Henry's law. Therefore a decision whether the initial molar ratio has an influence on the equilibrium can only be drawn when the influence of methanol pressure is taken into account. Therefore the measured methanol concentration in the ME layer was used to correct the conversion. For this purpose a simplified equilibrium constant K for the ME layer is formulated.

$$K = \frac{c_{product} c_{methanol}}{c_{ME} c_{glycerol}} \qquad \text{Eq. 5.1-1}$$

The products MO and DI are regarded as one product component $c_{product}$ because selectivity change is small and ME could be measured with a higher precision than the compounds MO and DI. The concentration of product is calculated using the component mass balance of the fatty acid groups which are initially present only as ME with a concentration of $c_{ME,0}$.

$$c_{product} = c_{ME,0} - c_{ME} \qquad \text{Eq. 5.1-2}$$

The mean K of (2.22 ± 0.23) was calculated from four experiments. Conversions for all four experiments can be recalculated using only the concentration for glycerol and methanol and K.

$$X = 1 - \frac{c_{methanol}}{c_{methanol} + Kc_{glycerol}} \qquad \text{Eq. 5.1-3}$$

The result is shown in Fig. 5.1-3. The trend is reduced by 40 % compared to the data in Fig. 5.1-2 without correction of the influence of methanol. The experiment at a ratio of 3 shows an absolute error of reproducibility of 4 % conversion.

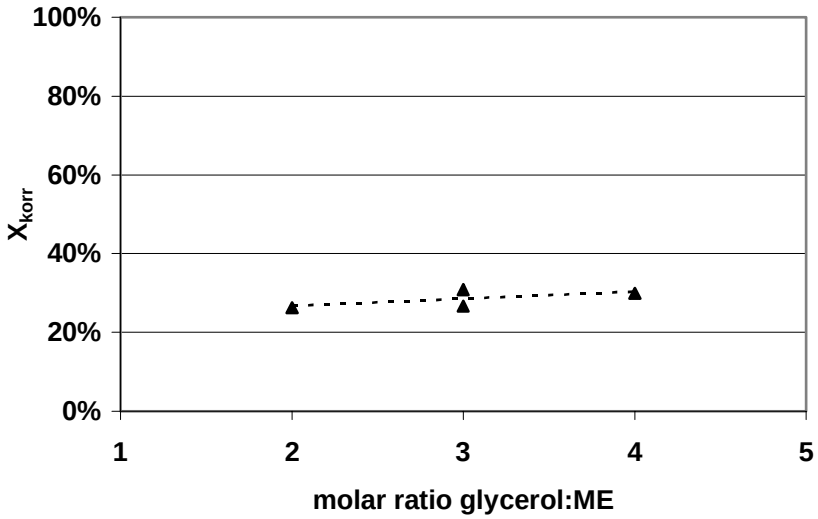

Fig. 5.1-3: Corrected equilibrium conversion X_{korr} vs. initial molar ratio between glycerol and oleic acid methyl ester (ME). Experiments in an autoclave at 150 °C, 0.5 % catalyst.

Therefore the difference of conversions of the recalculated values is regarded as non significant. The mean conversion is $X = (0.28 \pm 0.02)$.

5.1.2 Influence of Temperature

Experiments were carried out at different temperatures between 110 and 150 °C. Equilibrium conversions are shown in Fig. 5.1-4, selectivity towards MO in Fig. 5.1-5.

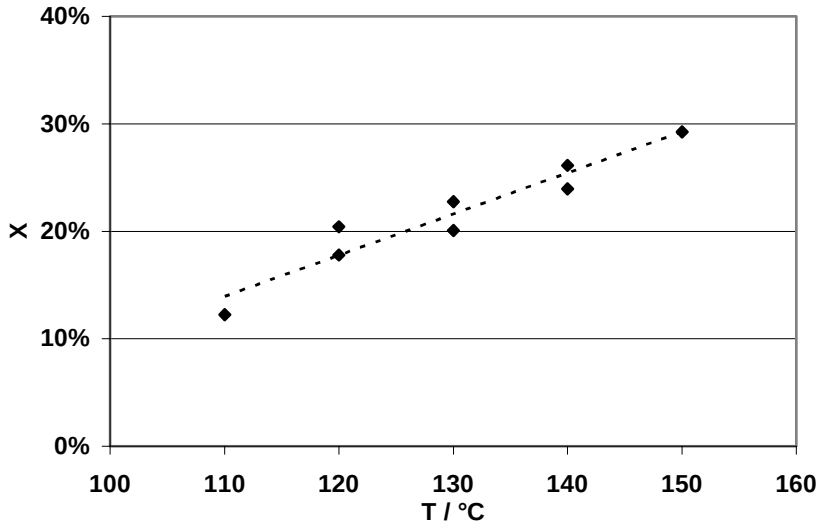

Fig. 5.1-4: Equilibrium conversion *X* vs. temperature in an autoclave. Initial molar ratio between glycerol and oleic acid methyl ester 3:1, 0.5 % catalyst.

Conversion increases with temperature. This is in accordance with the expected decrease of the solubility of the co-product methanol. It leads to an increase of the concentration of the associated products MO and DI according to the law of mass action. The selectivity towards MO shows no distinct trend, see Fig. 5.1-5.

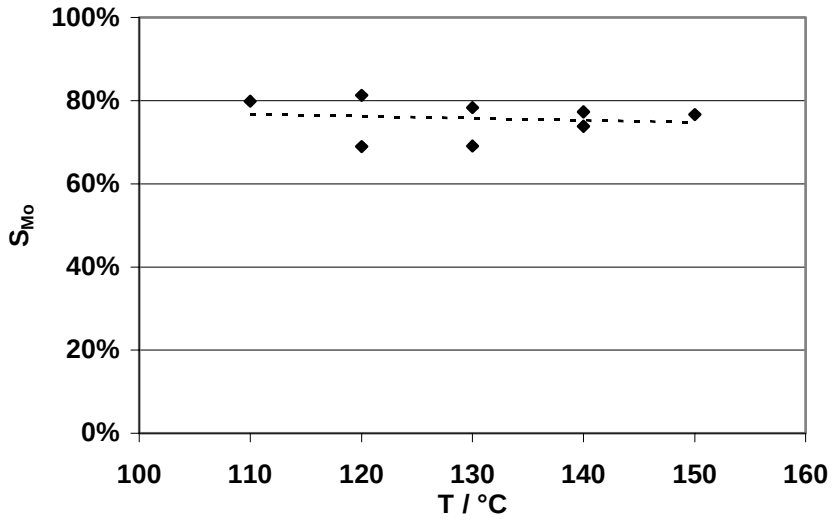

Fig. 5.1-5: Selectivity towards monoglyceride (S_{MO}) vs. temperature in an autoclave. Initial molar ration between glycerol and oleic acid methyl ester 3:1, 0.5 % catalyst.

The experimental error of the determination of selectivity is high compared to the range of selectivity observed that was between 69 and 81 %. Therefore a significant trend of selectivity could not be found in the range between 110 and 150 °C. The mean selectivity is (75 ± 6) %. It has to be stated that the absolute value of selectivity obtained in autoclave experiments could not be verified because no standards for MO and DI were available at this time.
A closer examination of the data shows a decrease of selectivity with conversion, see Fig. 5.1-6.

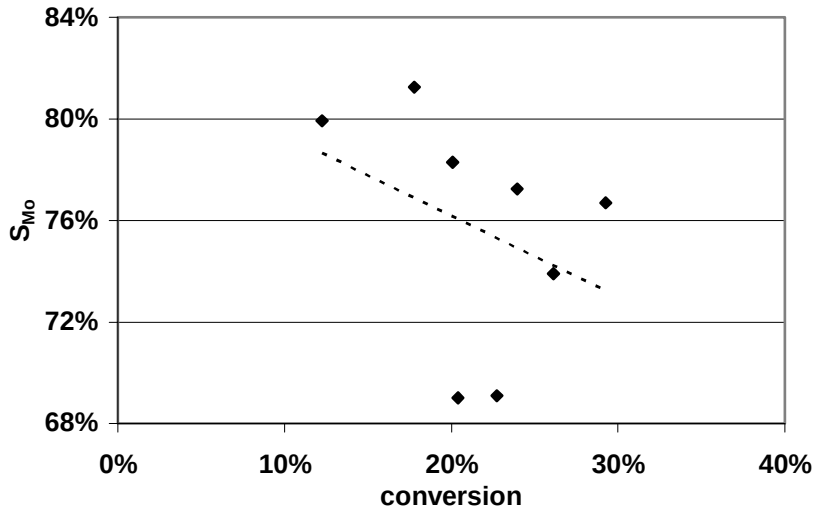

Fig. 5.1-6: Selectivity towards monoglyceride (S_{MO}) vs. conversion for different temperatures in an autoclave. Initial molar ratio between glycerol and oleic acid methyl ester 3:1, 110–150 °C, 0.5 % catalyst.

These data are difficult to interpret because of data scattering. If a linear trend is stated, two of the values below 71 % selectivity have to be regarded as outliers.

This trend is in accordance with observations that were obtained in a later stage of this study, when accuracy of concentration measurements was enhanced. In these runs selectivity is decreasing exponentially with conversion, particularly in the range of low conversions smaller than 25 % the dependency of selectivity on conversion is very pronounced.

Vapor pressure and methanol content in the ME layer show an opposite trend, see Fig. 5.1-7. Both trends are linear with respect to temperature.

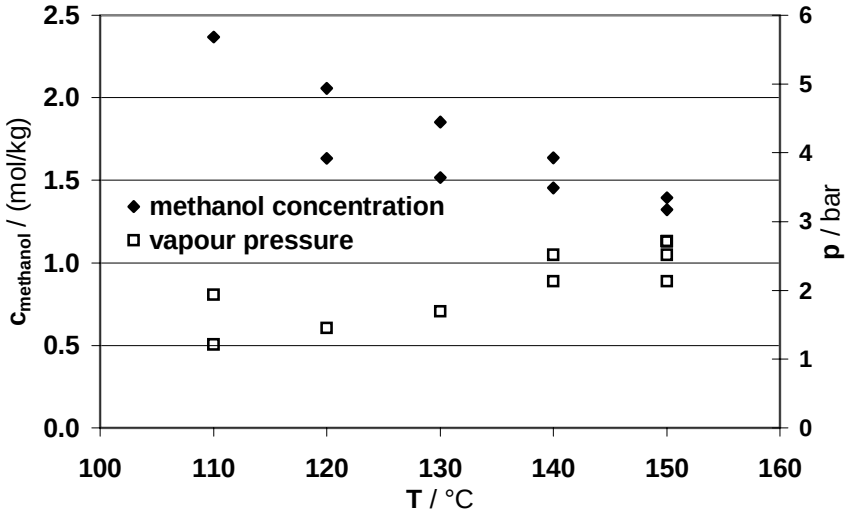

Fig. 5.1-7: Final methanol concentration $c_{methanol}$ and vapour pressure p vs. temperature T in autoclave experiments. Initial molar ratio between glycerol and oleic acid methyl ester 3:1, 0.5 % catalyst.

This indicates that the methanol content is controlled by temperature leading to a decrease of methanol with temperature. The excess methanol released by the reaction is in the gas phase indicated by the increase of vapour pressure.

5.2 Kinetic Experiments

5.2.1 Influence of Stirring Rate

First experiments showed a weak dependency of conversion on stirring rate. When the study started, stirring rate could be varied only within a small range. At lower rates dispersion was not fully established and at higher rates image recording was not possible. As the range between 450 rpm and 550 rpm was very small, it was tried to verify the influence of the stirring rate with an improved micro photo graphic set up. The ratio of stirrer to reactor diameter was changed from 0.33 to 0.50 because this set up showed less vortex formation. Image recording was possible up to 900 rpm. Results are shown in Fig. 5.2-1.

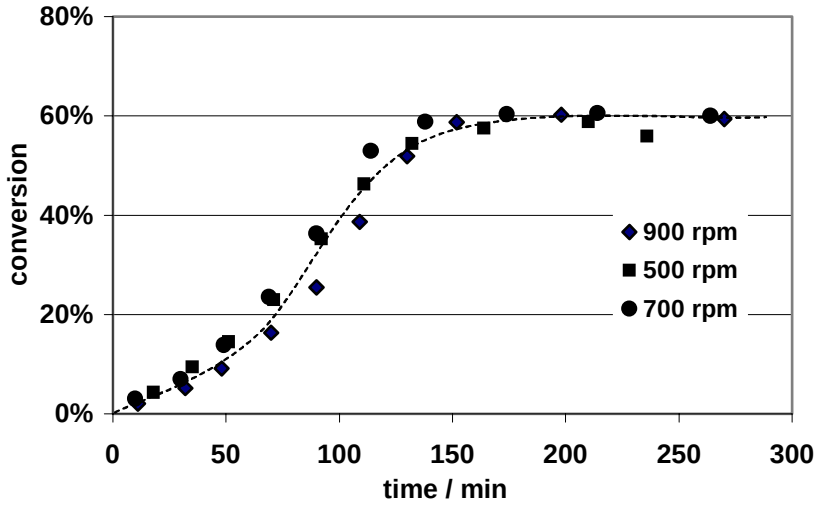

Fig. 5.2-1: Conversion determined by GC at different stirring rates. Legend: rpm: revolutions per minute, dashed line: overall trend, conversion determined by gas chromatography (GC). 130 °C, 300 mbar, initial ME-glycerol-ratio 0.74, 0.78 % catalyst.

No increase of reaction rate with stirring speed can be observed. Contrary to all expectations the run with the slowest reaction rate is the run with the highest stirring rate at 900 rpm, the highest rate is observed at 700 rpm. As differences are small, these results of GC analysis are verified by comparing the amounts of distilled methanol which give an independent measurement of conversion. Distillate curves are compared in Fig. 5.2-2. The maximum levels of methanol differ because methanol could not be condensed completely.

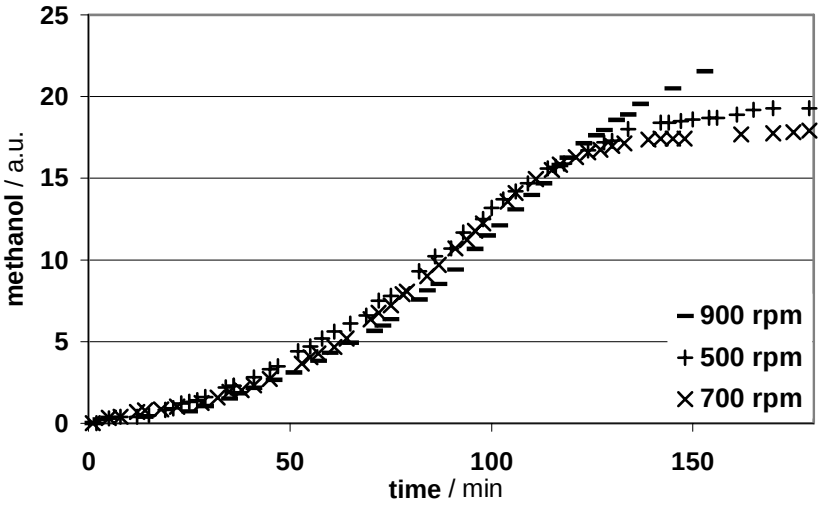

Fig. 5.2-2: Conversion determined from the amount of distillate at different stirring rates. Distillate of the couple product methanol in arbitrary units (a.u.), 130 °C, 300 mbar, initial ME-glycerol-ratio 0.74, 0.78 % catalyst.

Similar to Fig. 5.2-1 no difference between the runs can be observed up to 120 minutes, especially the maximum reaction rate between 50 and 100 minutes is the same for all three runs.

Therefore it is concluded that stirring rate has no effect on reaction rate at stirring rates higher than 500 rpm. Differences of the measurements at different stirring rates are regarded as experimental error of reproducibility of GC analysis combined with errors due to sample handling. Error of reproducibility for maximum reaction rate was determined by a linear regression between 60 and 135 minutes from GC data. Maximum reaction rate is (0.0059 ± 0.0006) conversion per minute; the relative error is 10 %.

5.2.2 Influence of Phase Ratio

To see effects of phase fraction, the ratio of glycerol to ME was reduced by approx. 50 %. To prevent unintended changes of the reaction systems other than phase fraction, glycerol was removed after starting reaction similar to the sampling procedure. Glycerol fraction was not changed by initial composition because this could lead to a different catalyst content in the ME layer or occurrence of undissolved catalyst. Precaution was advisable because glycerol layer usually takes up most of the catalyst. If equilibrium of phase distribution is reached before changing phase fraction, catalyst concentration in both phases should be unaffected. This experiment was repeated. In run (1) 44 % and in (2) 52 % of the initially added glycerol

was removed after 44 and 39 minutes. Stirrer was turned off during removal of glycerol. It was removed using the sampling syringe within 10 minutes. If reaction would take place in the glycerol layer this should lead to a decrease of reaction rate of approx. 50 %. The same trend should be observed if reaction occurs at the liquid-liquid-interface or a strong mass transfer limitation is present.

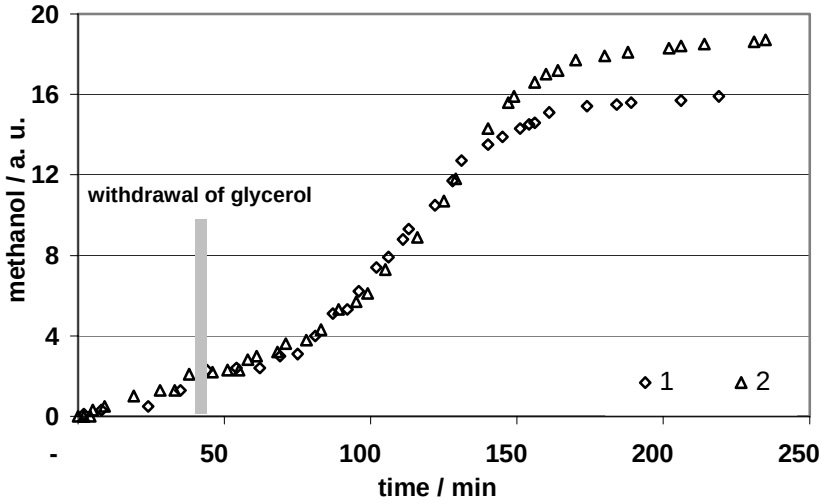

Fig. 5.2-3: Comparison of distillate for two runs with glycerol removal. Oleic acid methyl ester (ME), 130 °C, 300 mbar, initial ME-glycerol-ratio 0.73, 0.83 % catalyst, 500 rpm.

In Fig. 5.2-3 we see that the two experiments are reproducible and show no reduction of reaction rate up to 130 minutes. The maximum reaction rate for the two runs is 0.0053 conversion/min. Compared to (0.0059 ± 0.0006) conversion/min that was obtained in the previous experiments with the double glycerol content no significant change in maximum reaction rate is observed.

5.2.3 Influence of Temperature

Four runs with palmitic acid methyl ester were performed. Maximum conversion was determined by GC analysis; the shape of conversion was obtained from methanol distillate.

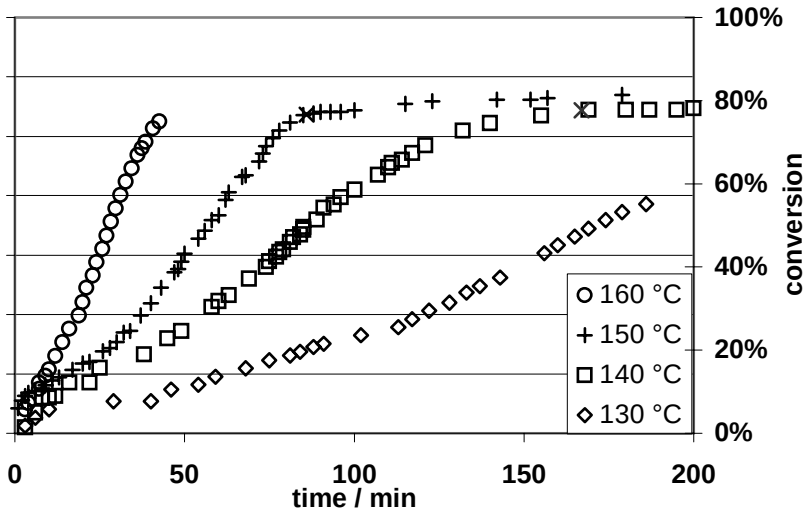

Fig. 5.2-4: Conversion at different temperatures for palmitic acid methyl ester (ME); 300 mbar, initial ME-glycerol-ratio 0.46, 0.80 % catalyst, 500 rpm.

Temperature has a very strong effect on reaction rate, as seen in Fig. 5.2-4. Maximum reaction rate increases from 0.0043 to 0.0225 conversion/min. Sigmoidal shape of conversion curve remains even for higher temperatures.

Inverse Dispersion

A change of dispersion state was observed in the runs at 140 and 160 °C. The initial glycerol-in-ester emulsion was inverted to an ester-in-glycerol emulsion after addition of the catalyst solution, which caused foaming because of the evaporation of methanol. Establishment of inversion was tested by diluting 1 ml of the emulsion either in glycerol or in methyl ester. GC analysis of the final products showed for the runs with inverse emulsion a higher content of glycerol in the methyl ester layer than in the runs with normal dispersion. Glycerol as continuous phase has a higher viscosity. This leads to a delayed phase separation during sample preparation. Average glycerol contents for normal dispersion is (6 ± 4) %, for inverse dispersion (26 ± 1) %. As seen in Fig. 5.2-4 inversion has no pronounced effect on reaction rate. All conversion plots show qualitatively the same increase of reaction rate per 10 °C indicated by the same increase of angle between x-axis and curve. Effects should be shown by different angels that indicate a transition between normal to inverse emulsions in the plots at 130/140 or 150/160 °C. Or shape of the conversion plot should show more resemblance between 130/150 and 140/160 °C. But shape or angle show no alternating forms or magnitude.

Two complete runs at 130 and 140 °C were performed with oleic acid methyl ester. After the run at 140 °C was completed it was additionally waited for equilibrium at 150 °C and 160 °C.

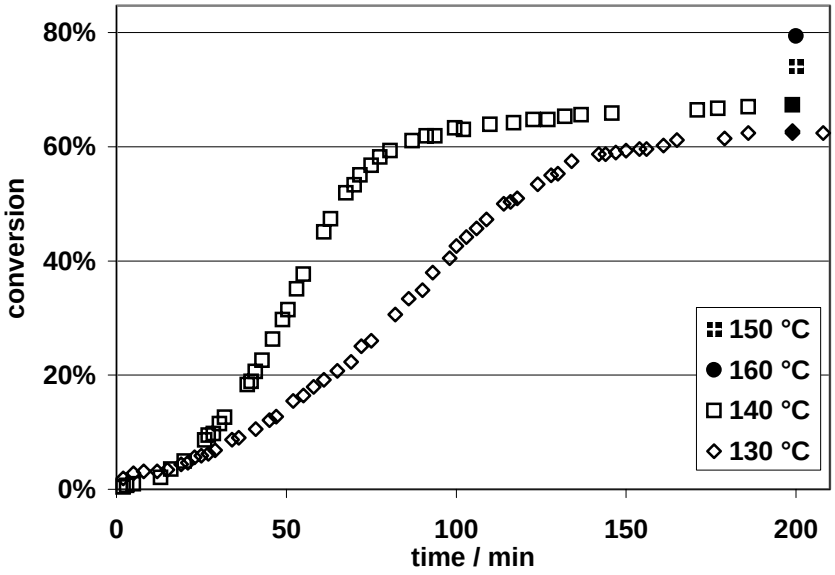

Fig. 5.2-5: Conversion at different temperatures for oleic acid methyl ester (ME). Conversion for two runs at 130 and 140 °C and two more equilibrium conversions at 150 and 160 °C. Full symbols: determined by GC analysis, shape of conversion plot from methanol distillate. Methyl ester of oleic acid, 500 rpm, 300 mbar, initial ME-glycerol-ratio 0.72, 0.79 % catalyst.

Establishment of equilibrium was monitored by taking sample in intervals of 30 minutes. The two conversion plots and two additional maximum conversions are shown in Fig. 5.2-5.
Reaction rate is higher compared to the runs with palmitic acid. Maximum reaction rate at 130 and 140 °C are 0.0062 and 0.0123 conversion/min. Even the increase of the maximum rate with temperature is higher. Reaction rate is enhanced by a factor of 2.0 per 10 °C. With palmitic acid as methyl ester, increase is slightly less pronounced with an average increase by a factor of 1.8 per 10 °C.

5.2.4 Influence of Reduced Pressure

Three runs at 1012, 450 and 300 mbar with oleic acid as ME were performed. After the first run was finished, pressure was further reduced and waited for equilibrium at 600 and 300 mbar. Establishment of equilibrium was monitored by taking samples in intervals of 30 minutes. The three conversion plots and the additional points for equilibrium conversion are shown in Fig. 5.2-6.

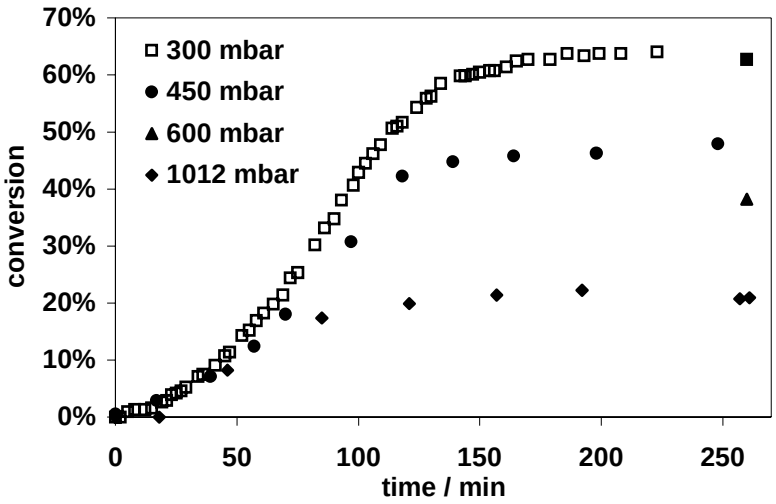

Fig. 5.2-6: Conversion plots and equilibrium conversions at different pressures. Full symbols: determined by GC analysis. Open symbols: shape of conversion plot from methanol distillate. Methyl ester of oleic acid (ME), 500 rpm, 130 °C, initial ratio between ME and glycerol 0.44, 1.09 % catalyst.

As transesterification is an equilibrium reaction, the removal of the product methanol by evaporation at lower pressures changes reaction conditions drastically: equilibrium proportion of the products remaining in solution MO and DI is increased as well as reaction rate is accelerated. At 1012 mbar maximum reaction rate is 0.0028 conversion/min, it is about ½ of that at 300 mbar.

Comparison of methanol distillate and GC data for the run at atmospheric pressure show that the evaporation of the methanol added with the catalyst solution is much slower than at reduced pressure. Distillate curve shows an additional S-shaped region with a turning point at 30 minutes.

5.3 Phase Compositions and Selectivity

In this chapter data are presented and discussed that will be used in the following section for modeling.

Methanol and glycerol concentrations are treated in separate chapters because they could not be determined by GC without correction or only at special sampling conditions. Subsequently the effect of the operating conditions on the composition and the limitations of the variation of composition are summarized. Finally selectivity is discussed with respect to pressure as well as with respect to temperature.

5.3.1 Methanol

Methanol content in samples was determined by GC analysis. Objective was the methanol content in the pure ME layer. Because of a slower phase separation at levels of low conversion, usually no complete phase separation is achieved at a conversion below 20 %. As methanol solubility in glycerol is higher than in ME layer, dispersed glycerol will lead to an overestimation of methanol in the ME layer and in some cases even to a false trend of methanol content.

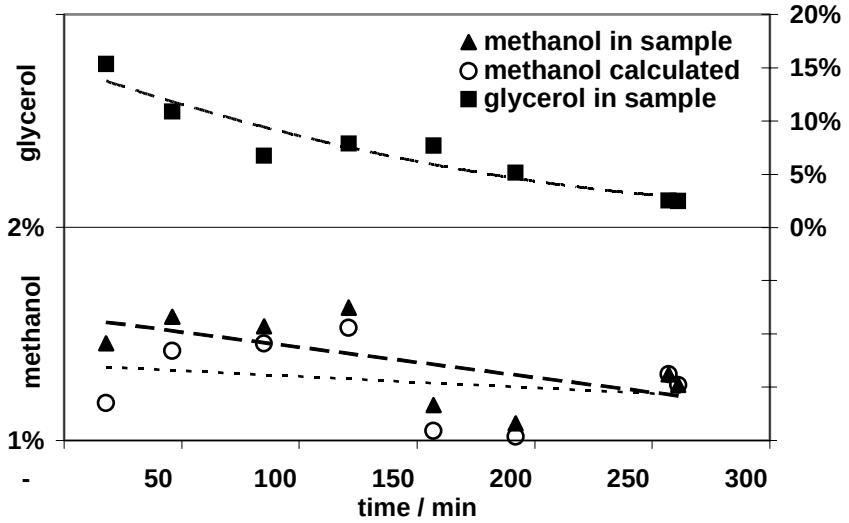

Fig. 5.3-1: Glycerol and methanol content in samples of the ME-layer. Methanol content in pure ME-layer (o) was calculated by subtracting methanol from disperse glycerol in the samples. Lines are trends for GC data (dashed) and for the corrected methanol content (doted). Reaction conditions: 1012 mbar, 130 °C, 500 rpm, 1.09 % catalyst, initial molar ratio ME/glycerol 0.44.

As an example the interpretation of one run at atmospheric pressure of 1012 mbar is discussed that showed the smallest maximum conversion obtained in all runs. In Fig. 5.3-1 the glycerol and methanol contents in the samples from the ME layer are shown. In the upper part of Fig. 5.3-1 a decrease of glycerol content from 15 to 2 % can be observed.
Methanol content in the glycerol layer was determined separately from pure samples of glycerol at 18 and 261 minutes. Partial phase separation to obtain pure samples of glycerol layer is fast, ester content was less than 0.5 %. Methanol content was 3.33 and 3.21 %. Therefore methanol content in the glycerol layer $w^{Gly}{}_m$ is regarded as constant at a level of 3.25 %.
As an upper limit of the glycerol solubility in the ME layer, the maximum solubility of glycerol was determined which is expected at the maximum conversion. An experimental value was obtained by a complete phase separation after reaching equilibrium at 261 minutes. Glycerol content $w^{ME}{}_g$ in the clear ME layer was 2.48 %. For the calculation of the corrected methanol content in the ME layer $w^{ME}{}_m$, the difference between glycerol content in the raw sample and maximum solubility of glycerol in the ME layer was regarded as disperse glycerol. Sample amount of the ME-layer was corrected for the glycerol and methanol that result from the disperse glycerol which was subtracted; formula is given in Equation 5.3-1. w_i is the mass fraction of component i (m: methanol, g: glycerol). The fraction w is calculated with respect to the mass of the raw sample withdrawn from the reactor (without superscript), or either to the mass of the ME layer or the glycerol layer (superscript *ME* or *Gly*).

$$w_m^{ME} = \frac{w_m w_g^{ME} - w_m + w_m w_m^{Gly} + w_m^{Gly} w_g - w_m^{Gly} w_g^{ME}}{w_m^{Gly} + w_g - 1} \qquad \text{Eq. 5.3-1}$$

Results for methanol are shown in the lower part of Fig. 5.3-1. The linear trend (dashed line) for the methanol fraction without correction shows an absolute decrease of 0.15 % per 100 minutes. This trend is reduced about ⅓ by the correction with Equation 5.3-1 to a value of 0.06 % per 100 minutes (dotted line). As this trend is smaller than the scattering of the methanol content, methanol concentration is regarded as constant throughout the run at a level of (1.3 ± 0.2) %. This average is identical to the value obtained when a complete phase separation at the end of the reaction was achieved, in this case methanol content was (1.3 ± 0.1) %. Analogous results were obtained for a run at 300 mbar and 140 °C.
This allows a simplified collection of methanol data. Concentration measurements of methanol for a whole run can be reduced to one measurement after a complete phase separation of the final products at reaction conditions.

Results for different temperatures with oleic acid methyl ester are shown in Fig. 5.3-2. In this graph the methanol concentration in both phases is shown. As it is assumed that the methanol content is in equilibrium between the liquid phases, the content of methanol in the glycerol layer can be used to decide if the measurement in the methyl ester layer is plausible or not.

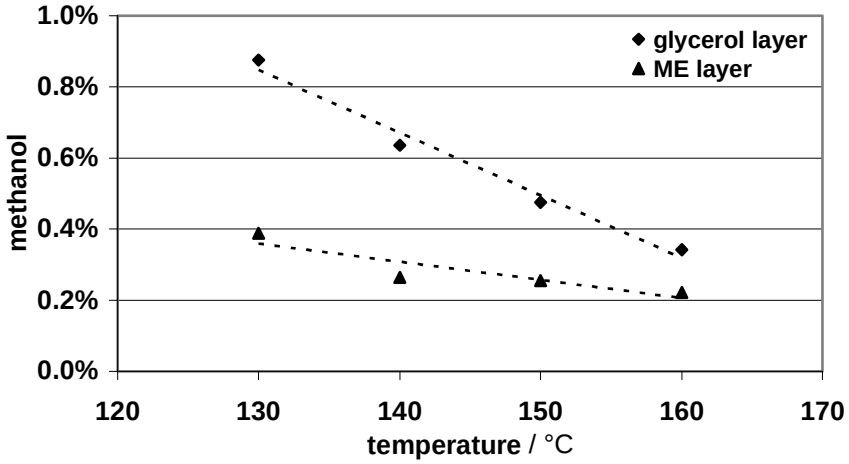

Fig. 5.3-2: Methanol content in the ME and glycerol layer at different temperatures. Dotted lines: linear trend. Reaction conditions: Methyl ester of oleic acid, 500 rpm, 300 mbar, initial ME-glycerol-ratio 0.72, 0.79 % catalyst.

Both trends of the methanol content are linear with respect to temperature. The correlation coefficient for the glycerol layer is $R > 0.98$. The correlation coefficient for the ME layer is smaller, $R > 0.78$. The lower correlation of the methanol content in the ME layer is explained by the more difficult sampling because this layer is reactive whereas in the glycerol layer no methanol can be consumed or produced by reaction. Therefore it is concluded that the decrease of the mass fraction of methanol $w_{methanol}$ is linear with respect to temperature ϑ.

$$w_{methanol} = -0.0000510\,\vartheta + 0.0102240 \qquad \text{Eq. 5.3-2}$$

From the temperature dependency of the mole fraction solubility x of a gas at a constant gas pressure, the enthalpy of solution $\Delta_s H$ can be calculated [52]. For this purpose the temperature dependency is fitted to a correlation like Equation 5.3-3. A and B are constant parameters, T is the absolute temperature and R is the gas constant.

$$\ln(x) = A + \frac{B}{T} \qquad \text{Eq. 5.3-3}$$

$\Delta_s H$ can be calculated using the parameter B from $\Delta_s H = -RB$ with R being the gas constant. E.g. in the case of a solution of oxygen in water [53], $\Delta_s H$ shows a very strong dependency on temperature which results in a change of its sign. Therefore application of this data is restricted to the temperature range in which the value was measured. $\Delta_s H$ is given as an additional measure of the temperature dependency, but this value is not used for the calculation of the solubility of methanol, instead the explicit empirical correlations like Equation 5.3-2 were used for simulation purposes. For a solution of methanol in ME, $\Delta_s H$ was calculated to be -25 kJ/mol.

The partition coefficient of methanol at a pressure of 300 mbar between the glycerol and the ME layer is decreasing with temperature. The slope of the decrease is 0.0027/°C, the mean partition coefficient for the temperature range between 130 and 160 °C is 2.0 with a relative *SD* of 0.2. The dependency of the mass fraction of methanol upon pressure p in mbar is shown in Fig. 5.3-3.

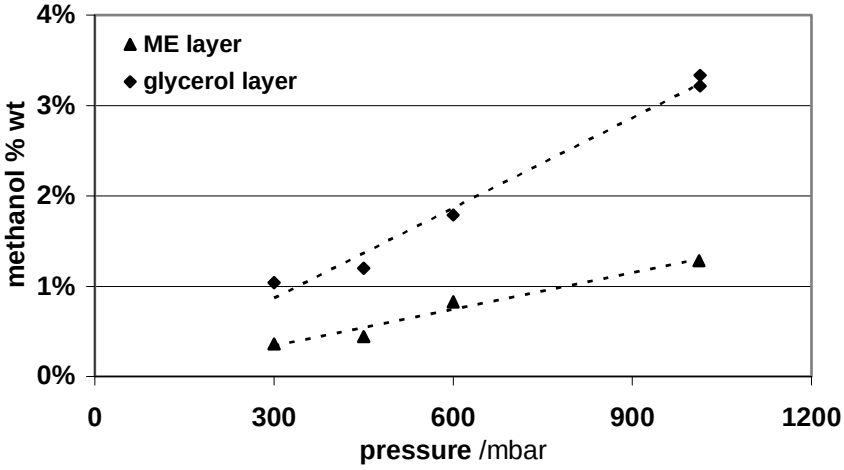

Fig. 5.3-3: Methanol content in the ME and glycerol layer at different pressures. Dotted lines: linear trend. Reaction conditions: Methyl ester of oleic acid (ME), 500 rpm, 130 °C, initial ratio between ME and glycerol 0.44, 1.09 % catalyst.

In this case the linear correlation coefficient for both plots is higher than $R = 0.97$. The dependency of the weight fraction of methanol $w_{methanol}$ in the ME layer from the pressure is given as a linear correlation in Equation 5.3-4. It will be used for the simulation.

$$w_{methanol} = 0.0000135p - 0.0007279 \qquad \text{Eq. 5.3-4}$$

From the pressure dependency of the methanol solubility, the Henry coefficient H can be calculated. This coefficient can be defined according to Equation 5.3-5 as the limit of the ratio between the partial pressure of methanol p and the mole fraction solubility x of methanol in the ME layer [54] for $x \rightarrow 0$. For the calculation it was assumed that the gas phase consists of pure methanol.

$$H = \lim_{x \to 0} \left(\frac{p}{x} \right) \qquad \text{Eq. 5.3-5}$$

The value of H was calculated to be 1.05 MPa for 130 °C in the ME layer.

5.3.2 Glycerol

For kinetic investigations it is important to know the glycerol content in the ME layer. Samples withdrawn from the reactor during reaction are emulsions. Samples are allowed to settle some minutes before they are quenched, but the ME layer still contains varying amounts of dispersed glycerol. Without reaction the solubility of glycerol in ME can easily be obtained because the time for phase separation is not critical. The weight fraction of glycerol $w_{glycerol}$ in palmitic acid methyl ester without reaction increases with temperature ϑ.

$$w_{glycerol} = 0.000083\vartheta - 0.00623 \qquad \text{Eq. 5.3-6}$$

The trend shown in Fig. 5.3-4 is linear with a correlation of $R = 0.994$. This correlation will be used for the calculation of the initial glycerol content in the ME layer during reaction.
Theoretically it is possible to calculate the amount of dispersed glycerol in samples withdrawn during reaction similar to the approach in Equation 5.3-1, because the equilibrium concentration of methanol is different in both layers. Due to the high scattering of 15 % for the methanol content in the samples and the small difference of solubility in both phases this is not possible.

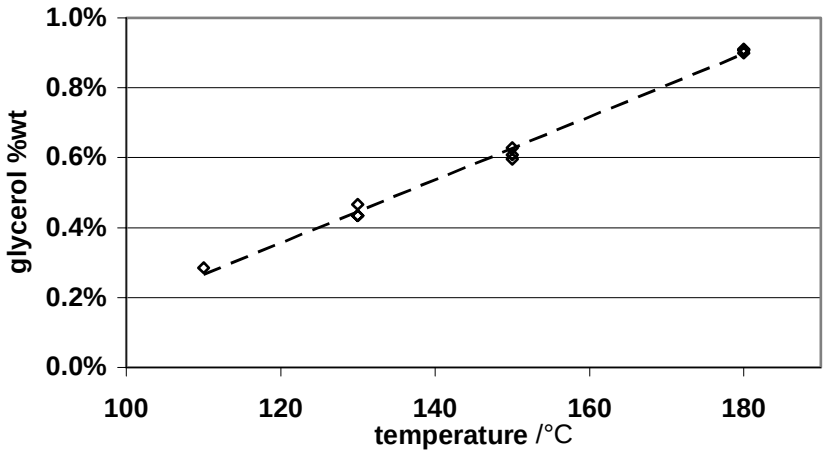

Fig. 5.3-4: Glycerol content in palmitic acid methyl ester without reaction at 110 to 180 °C. Linear trend as dashed line.

Examination of data from preliminary investigations shows that the glycerol content in the ME layer is likely to increase linearly with conversion. Conversion is determined with respect to the consumption of ME determined by GC. Experimental values are shown in Fig. 5.3-5. The increase of solubility of glycerol in the ME layer is a result of the formation of products that contain one or two hydroxyl groups like DI and MO which are more similar to glycerol than the initially present ME and which accumulate in the ME layer. A second influence on the solubility is the temperature. Data in this Figure were obtained by the measurement before analysis and sampling procedure were optimized according to chapters 4.1 and 4.2. Therefore the results in Fig. 5.3-5 will only be discussed qualitatively. Results from several experiments are shown because the values for the glycerol content show a high scattering.

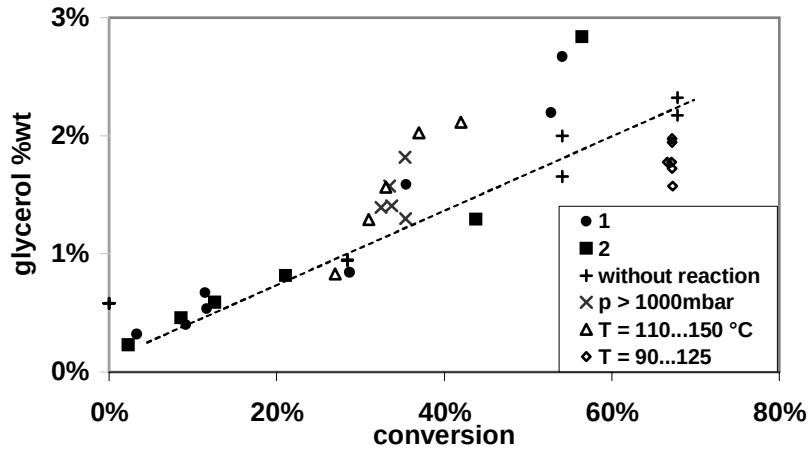

Fig. 5.3-5: Glycerol content in samples vs. conversion. Dashed line, linear trend; • and o, runs (1) and (2) at 130 °C and 300 bar; x and Δ, equilibrium composition for higher pressures at 130 °C and for different temperatures; ◊, non reactive mixtures at lower temperatures.

Glycerol content of samples for two runs (1) and (2) at 300 mbar and 130 °C are shown. Glycerol content increases with conversion. Additional data are given for mixtures at equilibrium. Higher pressures (x), lead to a smaller equilibrium conversion of 30–40 % because of a higher methanol content. Higher temperatures (Δ) lead to an increase of glycerol content. At lower temperatures (◊) neutralized reaction mixtures at high conversions of approx. 70 % show that the glycerol content decreases with decreasing temperature.

All data support the hypothesis of a linear trend for the glycerol content of the ME layer with respect to conversion at a fixed temperature. For different temperatures different levels are expected. In this case the trend throughout one reaction can be modeled by the starting point at a conversion of 0 to the maximum conversion. Therefore glycerol measurements can be reduced to measurements at equilibrium without reaction and the determination of the equilibrium composition of the ME layer after reaction is complete that can be accessed directly by a complete phase separation.

For this reason the glycerol content in the ME layer was measured after reaching equilibrium for different pressures using the optimized analysis and sampling procedure.

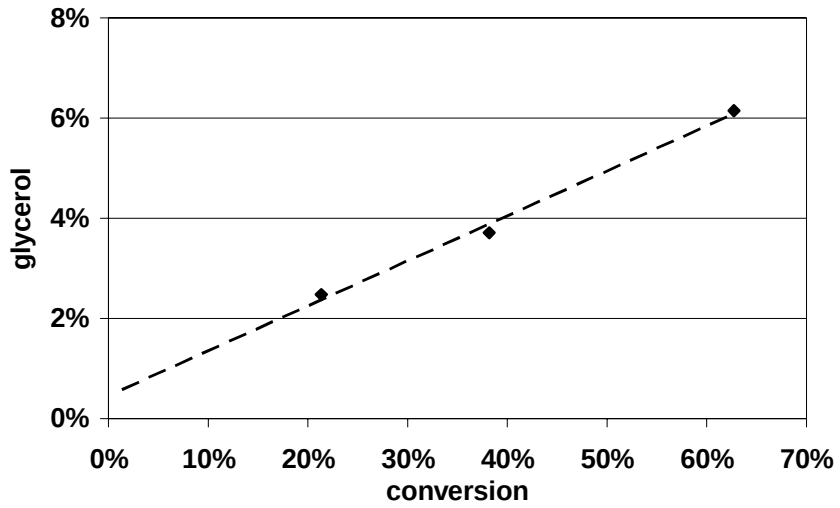

Fig. 5.3-6: Glycerol content determined by phase separation in ME layer after reaction was complete. Condition changed due to different pressures between 1012 and 300 mbar; 500 rpm, 130 °C, initial oleic acid methyl ester-glycerol-ratio 0.44, 1.09 % catalyst, linear trend as dashed line.

As expected the trend shown in Fig. 5.3-6 is linear with respect to conversion X with a correlation of $R = 0.994$.

$$w_{glycerol} = 0.0898X + 0.0045 \qquad \text{Eq. 5.3-7}$$

The glycerol content at a conversion of 0 in this trend $w_{glycerol,0} = 0.0045$ is identical to the value obtained from measurements without reaction for palmitic acid methyl ester. This behavior will be used for kinetic modeling because it allows interpolating the glycerol content of the ME layer with respect to conversion.
Temperature enhances the solubility as shown in Fig. 5.3-4. Data of the glycerol content at equilibrium after runs at 130 to 160 °C are shown in Fig. 5.3-7.

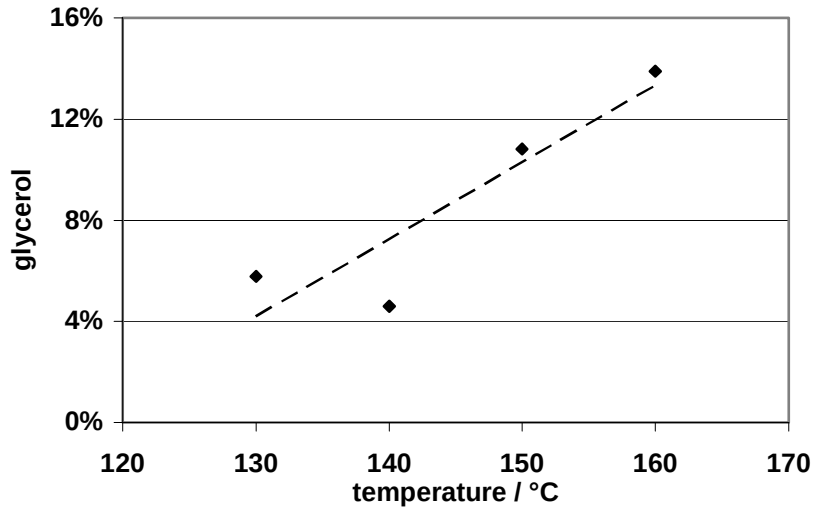

Fig. 5.3-7: Glycerol content in ME layer at equilibrium determined by phase separation. Methyl ester of **oleic acid**, 500 rpm, 300 mbar, initial ME-glycerol-ratio 0.72, 0.79 % catalyst.

A linear trend has a correlation of $R = 0.822$, see Equation 5.3-8. This correlation will be used for the interpolation of the glycerol content of the ME layer at different temperatures. In Fig. 5.3-7 the value at 130 °C shows unexpectedly a higher glycerol content than the run at 140 °C.

$$w_{glycerol} = 0.0031\,\vartheta - 0.3548 \qquad \text{Eq. 5.3-8}$$

A comparison of all samples showed that samples at 130 °C taken before equilibrium contain a very high fraction of glycerol of 15-16 % which usually indicates inversion of the emulsion. This makes it difficult to obtain a complete phase separation. Similar problems occurred when the maximum conversion of runs with palmitic acid methyl ester were determined as shown in Fig. 5.3-8. In these cases phase inversion was clearly noticed by an increase of sample viscosity.

Glycerol content shows different levels with and without inversion. With inversion the content is higher (26.0 ± 0.9) %; without inversion the content is similar to the former runs with oleic acid methyl ester of (6 ± 4) %.

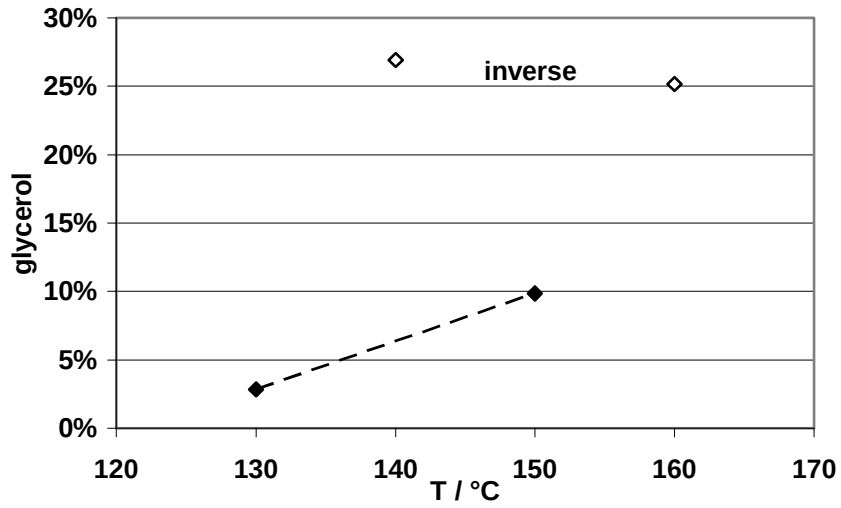

Fig. 5.3-8: Final glycerol content in ME layers with (◊) or without (♦) inversion. Trend without inversion as dashed line, Reaction of methyl ester of **palmitic acid** with glycerol, 500 rpm, 300 mbar, initial ME-glycerol-ratio 0.46, 0.80 % catalyst.

No complete phase separation was obtained in the runs with palmitic acid methyl ester. The samples without inversion show a similar trend to that observed in the runs with esters of oleic acid.

$$w_{glycerol} = 0.0035\,\vartheta - 0.4274. \qquad \text{Eq. 5.3-9}$$

Glycerol content in the ME layer can be measured accurately only at equilibrium conditions. Precautions should be taken to avoid phase inversion that leads to drastically higher fraction of glycerol. Glycerol content within one run at one temperature is proportional to conversion, starting at the equilibrium content without reaction. Glycerol fraction increases linearly as temperature is increased.

5.3.3 Variation of Composition

A typical plot of concentrations vs. time at 140 °C is shown in Fig. 5.3-9. The plot of ME has a sigmoidal shape which is equivalent to the S-shaped conversion curve that was shown in the previous chapters. According with the assumption of a consecutive reaction, the second product DI is formed with a lower initial reaction rate than the first product MO.

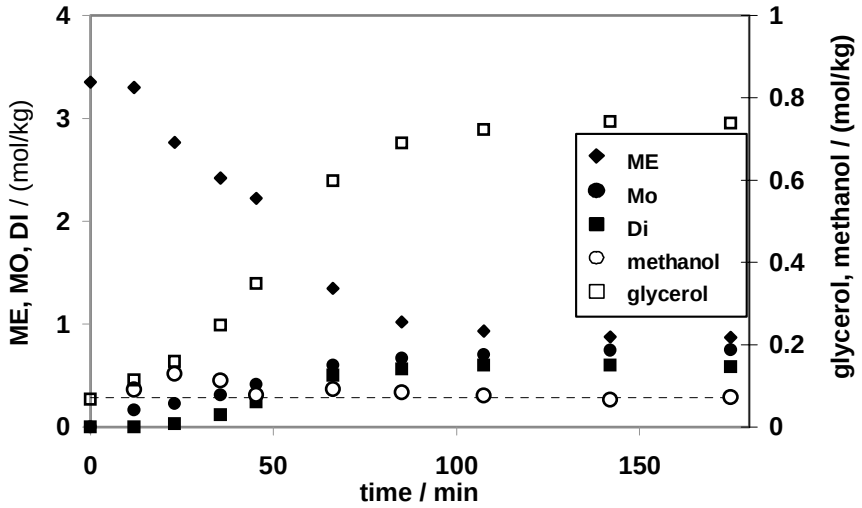

Fig. 5.3-9: Typical plot of all concentrations. Full symbols: ME, MO and DI, open symbols: alcohols methanol and glycerol. Values for glycerol were calculated according to Equation 5.3-7 and 5.3-8, the constant methanol content indicated by a dashed line was calculated according to Equation 5.3-1. Methyl ester of oleic acid, 500 rpm, 140 °C, initial ME-glycerol-ratio 0.73, 0.79 % catalyst.

The reaction system does not offer many degrees of freedom. The concentration of ME at the beginning of the reaction is fixed by the raw material ME. Mono and DI are too expensive to be used as raw materials.

Only one study [55] reported the used of monoglycerides as raw materials. Methanolysis of 4 g of MO from Pongamia oil was carried out with potassium hydroxide as catalyst. Molar ratio was 10:1 for methanol:MO. Temperatures were 30, 45, 55 and 60 °C. The rate of MO formation was modeled as second order with respect to the concentrations c_i according to Equation 5.3-10. $k_{\rightarrow}$ and $k_{\leftarrow}$ are the reaction rate constants.

$$\frac{dc_{Mo}}{dt} = -k_{\rightarrow} c_{Mo} c_{methanol} + k_{\leftarrow} c_{glycerol} c_{ME} \qquad \text{Eq. 5.3-10}$$

Lag times were observed before reaction started that varied between 3 and 10 minutes. After that period conversion changed while only two samples were withdrawn by 70 % indicating problems with experiment layout. The reaction at 30 °C could not be fitted by the proposed model. The reverse reaction rate constant $k_{\leftarrow}$ showed a negative activation energy. It was

concluded that the model did not reflect elementary steps and the reaction was carried out under the regime of mass transfer limitation.

Glycerol content is controlled by the solubility which was shown to be dependent upon the conversion in the ME layer. Therefore the conversion dependent glycerol content is fixed at a given temperature. At higher temperatures, glycerol content increases, but also methanol content is reduced and reaction rate constants change according to their activation energies.
Only the methanol content can be adjusted by a variation of pressure or by sweeping out methanol with help of a purge gas. In the case reduced pressure the methanol content is constant during reaction because the liquid phase and the gas phase are in equilibrium.

Therefore an independent variation of concentration could only be achieved by a variation of pressure. In this case only methanol concentration is changed. Methanol and glycerol content showed no cross correlation.

5.3.4 Selectivity

The influence of pressure on the reaction is shown in Fig. 5.3-10a. Conversions were previously shown in Fig. 5.2-6**.** For clarity selectivity S_{MO} is shown instead of the concentration of MO and DI.

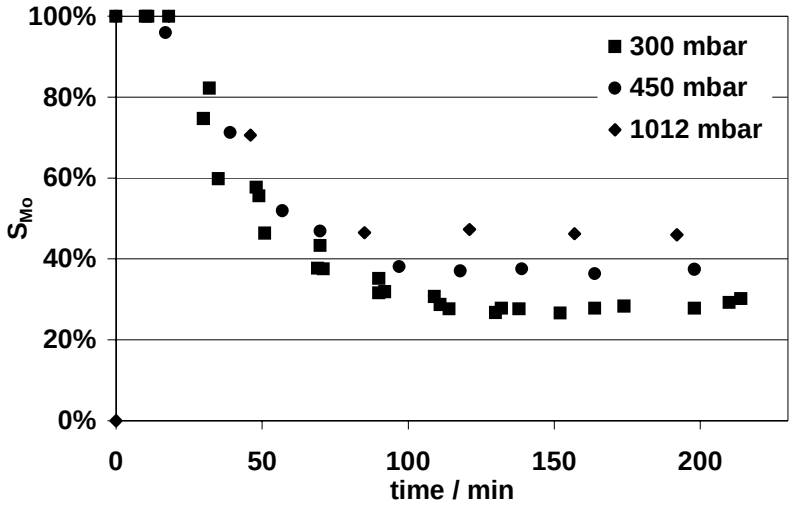

Fig. 5.3-10a: Selectivity towards monoglyceride S_{MO} vs. time at different pressures. Esters of oleic acid, 500 rpm, 130 °C, initial ME-glycerol-ratio 0.44, 1.09 % catalyst.

Selectivity is dependent on the pressure. At higher pressures, methanol content is increased. This alters the equilibrium conditions and leads to a lower maximum conversion, because methanol concentration takes part in both backward reactions steps. Differences between the runs are less pronounced when S_{MO} is plotted vs. conversion X, see Fig. 5.3-10b.

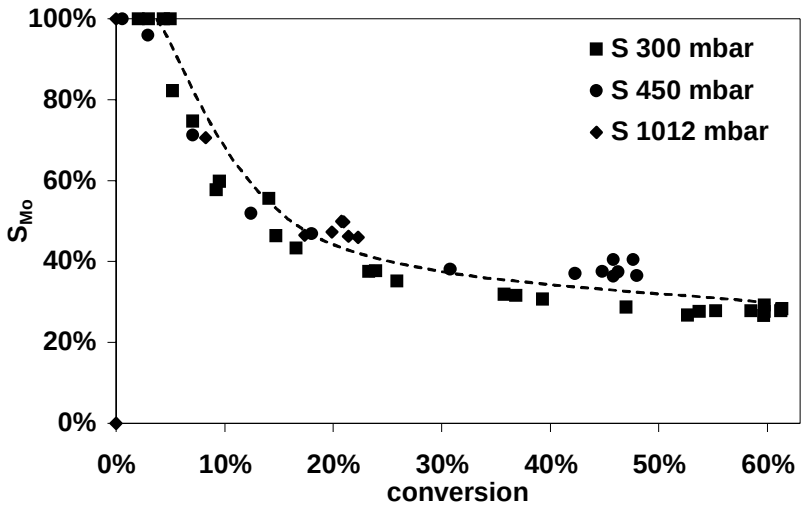

Fig. 5.3-10b: Selectivity towards monoglyceride S_{MO} vs. conversion at different pressures. Dashed line: overall trend.

This shows that S is not mainly a function of the pressure dependent methanol content but of conversion for a given temperature. This is a surprising result because methanol concentration should also affect the final selectivity at equilibrium conditions.

When temperature is increased methanol content is reduced. But major changes of the system are expected like a higher solubility of glycerol and contributions from individual activation energies of the reaction rate constants.

High Temperatures

In literature product compositions are given for the glycerolysis of ME. In this case the same reactions between MO, DI and TRI can take place as in the glycerolysis of ME. The difference is that ME as fourth fatty acid groups containing component is missing and no methanol is present.

Selectivity was calculated from data in literature [56], see Fig. 5.3-11. Selectivity for the products (61.2 ± 1.2) % is independent on temperature at high temperatures. First, this could indicate that the activation energies for the equilibrium reactions of MO and DI are not altered significantly. This is true if the reaction is modeled without phase separation.

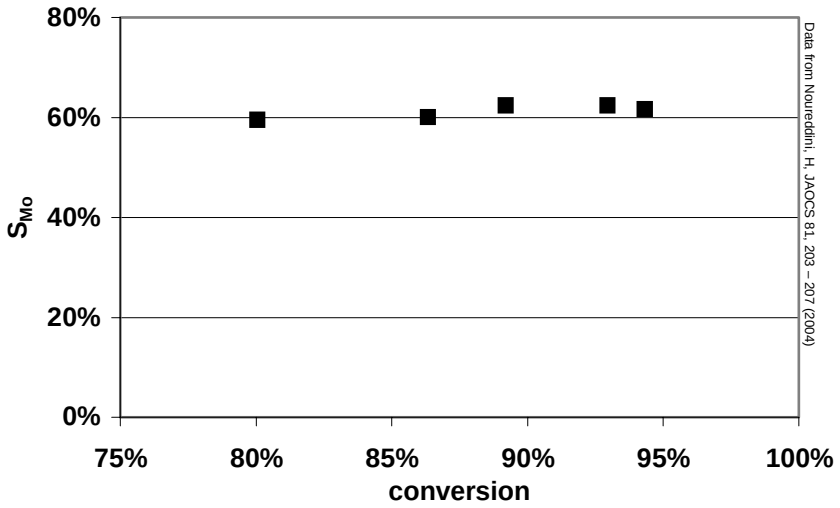

Fig. 5.3-11: Selectivity towards monoglyceride S_{MO} and conversion of fat glycerolysis between 200 – 240 °C. Conversion increases with temperature which was raised in steps of 10 °C. Initial molar ratio glycerol:soybean oil 5:2, 0.18 % sodium hydroxide as catalyst.

Secondly, it could be a result of a compensation of the enhanced solubility of glycerol which leads to a higher selectivity and an adverse effect of activation energies.

As own experiments were conducted at a lower temperature level and the selectivity found was lower than 62 %, this selectivity is regarded as maximum selectivity that can be obtained by the glycerolysis of ME for high conversions. At higher temperatures, it is expected that the products of fat glycerolysis resemble that of the glycerolysis of ME as methanol content is further reduced and the occurrence of triglycerides will be more pronounced. Own experiments at a temperature of 160 °C showed a final triglyceride content about 1 %.

In a second study [57] the final composition of the glycerolysis of ME were reported for different initial molar ratios of ME:glycerol between 0.25 and 1. Reaction was carried out under different conditions like reduced pressure, with purge gas, with pure glycerol or crude glycerol. Composition showed no clear dependency on the conditions changed in these runs. Conversion was high, 84 – 88 %, because reaction was carried out at an elevated temperature

of 200 – 210 °C. Selectivity S_{MO} was (53 ± 5) % which is a similar magnitude compared to fat glycerolysis.

This indicates that the equilibrium between MO and DI at elevated temperatures leads to a maximum selectivity of 50 – 60 %. It is neither affected by initial molar ratio nor by temperature or the presence of small amounts of methanol or ME.
Higher temperatures than 250 °C are not recommended for this reaction because color and smell of the products are affected and degradation occurs.

Low Temperatures

The effect of temperatures below 100 °C was examined using data from literature [58]. In this study a methanolysis reaction of soybean oil was carried out at temperature levels between 30 and 70 °C. As this study was not intended for the calculation of the intermediates MO and DI, selectivity was calculated using the given reaction rate constants and activation energies. This comparison was done to see if lower temperatures would be favorable to obtain higher selectivities. Methanolysis reaction leads to the same intermediates as the glycerolysis of ME. Especially at equilibrium conditions of both systems should reveal the ratios of reaction rate constants that determine equilibrium composition.

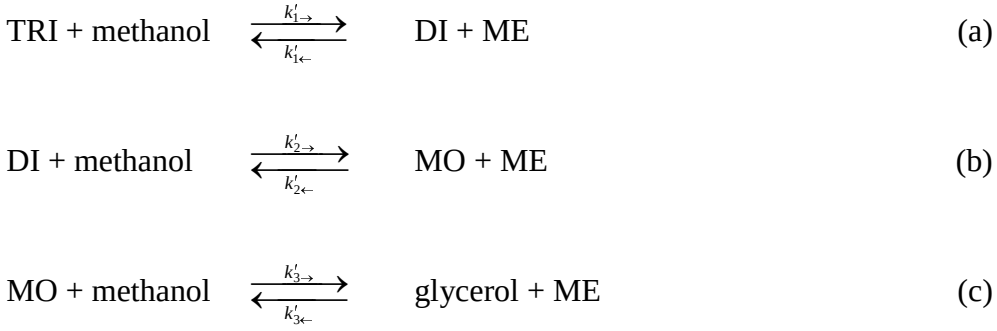

Scheme 5.3-1: Reaction steps of second order for the methanolysis of soybean oil (TRI) from literature [58]. E.g. the formation rate of the concentration of Monoglyceride (MO) in the third step is proportional to the reaction rate constant $k'_{3\leftarrow}$ giving $\delta c_{MO}/\delta t = k'_{1\rightarrow}\, c_{glycerol}\, c_{ME}$. ME is the methyl ester, DI the diglyceride of soybean oil.

Differing form Scheme 5.3-1 in literature [58] the backward reaction of step 1a was not calculated as $\delta c_{TRI}/\delta t = k'_{1\leftarrow}\, c_{DI}\, c_{ME}$, but as $\delta_{TRI}/\delta t = k'_{1\leftarrow}\, c_{DI}\, c_{methanol}$. All other reaction rates were in accordance with Scheme 5.3-1. Simulation is described in detail in the appendix.

Equilibrium conditions were simulated with the software Berkeley Madonna by using a final simulation time of 500 minutes. Rates and activation energies are given in Table 5.3-1.

Table 5.3-1: Activation energies *EA* and rate constants at 50 °C according to reaction Scheme 5.3-1 from literature [57].

	l/(mol s)	*EA* /(kJ/mol)		l/(mol s)	*EA* / (kJ/mol)		l/(mol s)	*EA* /(kJ/mol)
$k'_{1\rightarrow}$	0.050	55.0	$k'_{2\rightarrow}$	0.215	83.1	$k'_{3\rightarrow}$	0.242	26.9
$k'_{1\leftarrow}$	0.110	41.6	$k'_{2\leftarrow}$	1.228	61.3	$k'_{3\leftarrow}$	0.007	40.1

The values of the activation energies in Table 5.3-1 in a range between 27 and 83 kJ/mol were compared to a different study [59]. There a similar range between 34 and 83 kJ/mol of activation energies is reported for the acidic and basic catalysis of methanolysis, but no reaction rate constants were reported.
The simulated final selectivities are shown in Fig. 5.3-12.

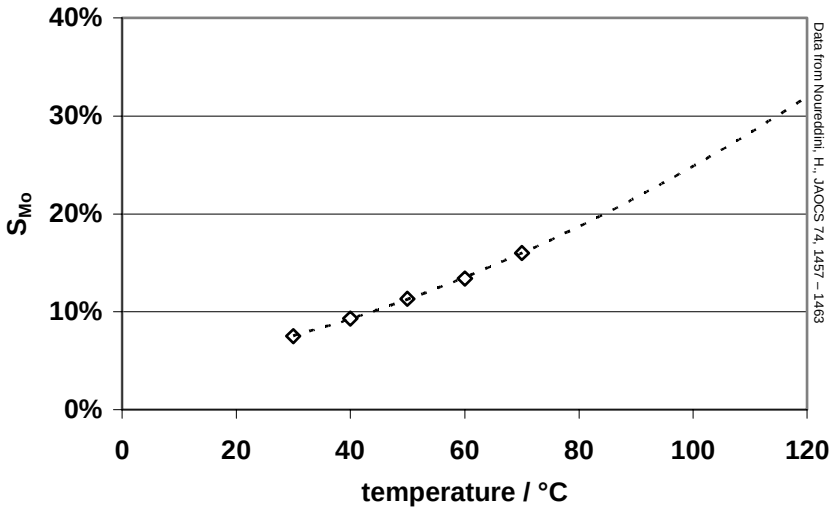

Fig. 5.3-12: Final selectivities towards monoglyceride S_{MO} vs. temperature for the methanolysis of soybean oil. Data calculated for equilibrium according to Scheme 5.3-1 and data in Table 5.3-1. Dashed line: extrapolation by a second order polynomial.

The reaction rate constants in literature [58] was determined at high conversions to ME because reaction took place at a high excess of methanol, the initial molar ratio of methanol:oil was 6:1. Phase separation due to glycerol settling was not taken into account. The selectivity shows an increase with temperature. If this trend is extrapolated using a polynomial of second order this leads to selectivities of 0.4 to 0.5 for a temperature range between 130 and 160 °C. This trend is qualitatively in accordance with the results of own experiments which showed final selectivities between 0.3 and 0.6 for this temperature range.

In literature [60] the final compositions of reaction mixtures that were carried out at the conditions of microemulsion are reported. Stearic acid methyl ester and glycerol or polyglycerol were used as raw materials with sodium hydroxide as catalyst together with surfactants. It was concluded that high temperatures lead to a loss of selectivity. Calculated selectivity towards MO vs. conversion is shown in Fig. 5.3-13.

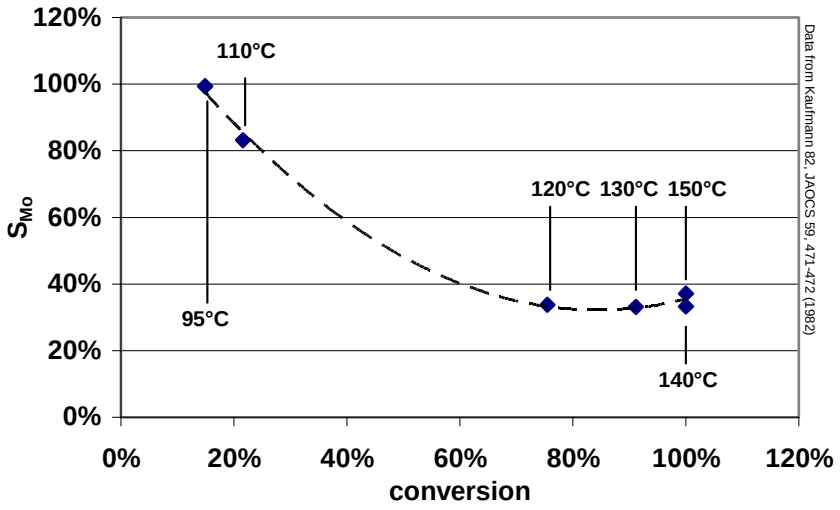

Fig. 5.3-13: Final selectivity towards monoglyceride S_{MO} for different temperatures vs. conversion. Data calculated from literature [60] for the glycerolysis of stearic acid methyl ester with sodium hydroxide as catalyst in microemulsion, dashed line: overall trend.

These results show both effects that were observed before. First we see a strong dependency of selectivity from conversion below 25 % conversion. At high conversion we observe no

pronounced influence of temperature or of conversion on selectivity between 120 and 150 °C. The final compositions reported were not obtained at defined conditions of equilibrium.

5.4 Modeling

The main problem that makes the kinetic examination and modeling of the reaction under investigation complex is the sigmoidal shape of the conversion plot.

Using reversible consecutive reaction schemes with power laws like the ones that will be introduced in the course of this chapter, generally a hyperbolic profile of conversion with time is to be expected. This is the case if all concentrations are either constant or the concentrations of the raw materials and products decrease or increase according only to the set of stoichiometric balances for one of the phases. An illustration of the problems to fit a model with a hyperbolic curvature to data with an S-shaped trend is given in Fig. 5.4-1.

The case that only the range of the final conversion is reproduced by the simulation is shown as simulation 1. The conversion before the final time will be overestimated by this approach and the maximum reaction rate will be underestimated. If a least square error method for the whole range of data is used, this will result in a fit similar to simulation 2. In order to minimize the maximum distance of data from the simulation curve, the hyperbolic curvature will become smaller and the simulation curve passes near the turning point of the S-shaped data. This divides the experimental data into two segments that form a positive and negative integral with the simulation curve of approximately the same absolute area. On top of the bad agreement of simulation and data this approach overestimates the reaction rate at the end of the simulation time, indicating a higher equilibrium conversion for a prolonged simulation time.

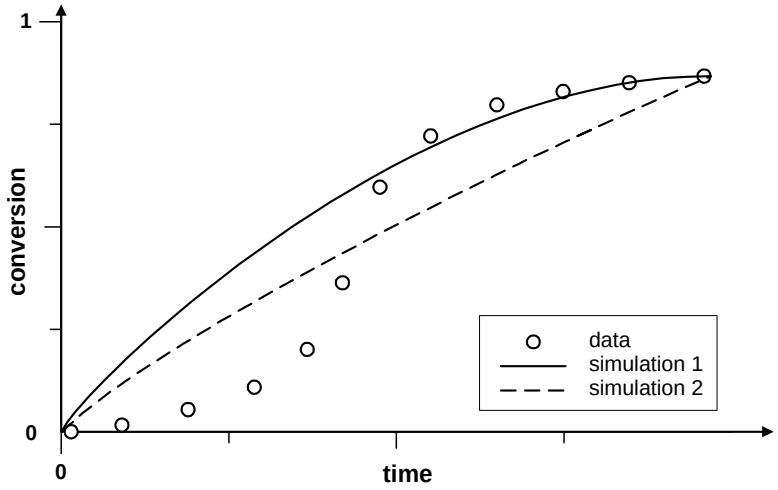

Fig. 5.4.1: Illustration of the general problems encountered if experimental data with an S-shaped trend are fitted with models that show a hyperbolic profile. Simulation 1 results if the final conversion is reproduced; simulation 2 if a least square minimization procedure is applied to the whole range of data.

A sigmoidal shape of the conversion plot cannot be described by this kind of differential equations if all concentrations are initially defined either as positive reservoirs or constants. Only if the reaction rate is additionally enhanced during reaction, a sigmoidal shape can be obtained. In this study the main parameter that is exclusively responsible for the sigmoidal shape of the conversion plot is the increasing glycerol concentration during reaction at a constant temperature. Results shown in chapter 4.3-2 show a linear dependency of the glycerol concentration in the ME layer on conversion. But is has to be kept in mind that the problems outlined in Fig. 5.4-1 will still be observable to some extent if the curvature of the S-shaped region will be underestimated by the model chosen.

In the previous chapter several influences of reaction conditions were shown that can be summarized by the assumption that reaction takes place in the methyl ester layer. The model is outlined in Fig. 5.4-2.

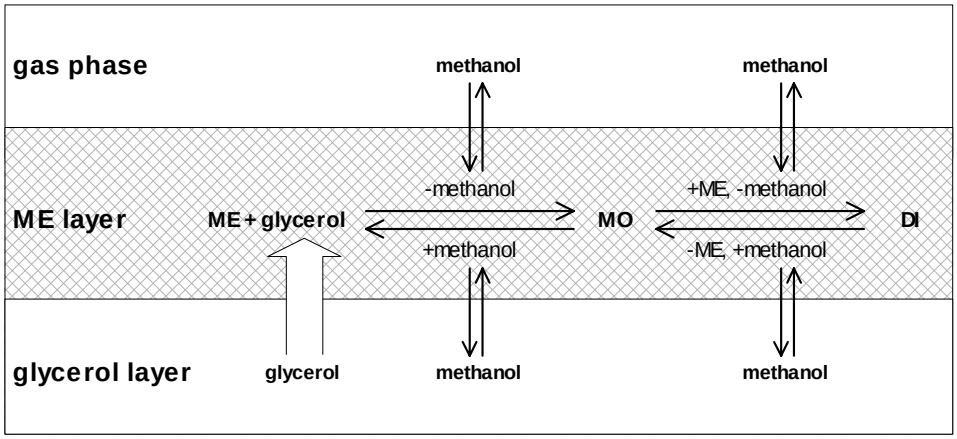

Fig. 5.4-2: Reaction takes place in the ME layer (hatched area). The glycerol layer is dispersed during reaction and acts as a reservoir for glycerol. Methanol concentration in the ME layer is constant because it is in equilibrium with the gas phase that consists of methanol and with the glycerol layer.

The glycerol layer acts only as a reservoir for glycerol. In the glycerol layer no glycerides were found, the concentration of methanol in this layer is constant during reaction. Glycerol concentration in the ME layer was shown to be dependent on conversion and temperature. The change of the glycerol concentration in the ME layer during reaction is caused by the occurrence of the products MO and DI which enhance the solubility of glycerol. Mass transfer of glycerol from the glycerol layer to the ME layer is fast with respect to reaction rate.
Methanol concentration is constant in the ME layer during reaction and is determined by the vapour pressure of methanol in the gas phase and the temperature.
In the following section, concentrations refer to the ME layer and are expressed in moles per kg. The ME layer takes the products MO and DI. The co-product methanol evaporates into the gas phase and is condensed. The amount of glycerol in the glycerol layer that is dispersed during reaction was not calculated because it was initially in excess compared to ME.

In literature several sets of second order reaction schemes are used for the description of the methanolysis or glycerolysis reaction. Usually Scheme 5.4-1 is the starting point for a kinetic description.

glycerol + ME $\rightleftharpoons$ MO + methanol (a)

MO + ME $\rightleftharpoons$ DI + methanol (b)

DI + ME $\rightleftharpoons$ TRI + methanol (c)

Scheme 5.4-1: System of second order reaction steps for the methanolysis of ME or glycerolysis of oils and fats. Fatty acid methyl esters (ME) are consecutively transformed in an equilibrium reaction to monoglyceride (MO), diglyceride (DI) and finally to Oils or fats which are triglycerides (TRI).

The number of key reactions needed in a reaction scheme to describe independently the change of the concentrations of all components can be calculated by subtracting the number of chemical elements from the number of components. In the case of a reaction system that contains six components (DI, glycerol, ME, methanol, MO and TRI) and three elements (C, O and H), three key reactions are sufficient to describe the reaction. If the system is simplified, e.g. because the concentration of TRI is neglected, the number of key reactions is reduced to two.

Additionally to the reaction network in literature a third order shunt reaction, see Equation 5.4-1, was proposed which did not improve the fit of the kinetic model in these studies.

TRI + 3 methanol $\rightleftharpoons$ glycerol + 3 ME Eq. 5.4-1

The use of third order systems which are from a physically point of view problematic indicate basic problems with simulation of data; e.g. in literature [58] the experimentally observed sigmoidal shape of the conversion curve could not be described by the model.
In study [61] the reaction of MO with methanol to ME was modeled using a second order model as well as a pseudo first order model with respect to methanol because reaction took place at a high excess of methanol.

TRI + glycerol $\rightleftharpoons$ MO + DI Eq. 5.4-2

DI + glycerol $\rightleftharpoons$ 2 MO Eq. 5.4-3

TRI + MO $\rightleftharpoons$ 2 DI Eq. 5.4-4

In literature [62] a set of reactions is discussed that are known to take place in the course of transesterification, see Equation 5.4-2 to 5.4.4. Each of these equations can be used to substitute single steps of different reaction schemes.

5.4.1 Model 1

In kinetic studies conversion and selectivity were fitted to a model according to Scheme 5.4-2. The third reaction path of 1.c in Scheme 5.4-1 was neglected, because triglyceride content in own experiments was only about 1 %.

glycerol + ME $\underset{k_{1\leftarrow}}{\overset{k_{1\rightarrow}}{\rightleftharpoons}}$ MO + methanol (a)

MO + ME $\underset{k_{2\leftarrow}}{\overset{k_{2\rightarrow}}{\rightleftharpoons}}$ DI + methanol (b)

Scheme 5.4-2: Second order reaction steps of Model 1.

This is small compared to the mass balance gap of about 5 %. The differential equations are given in Scheme 5.4-3. The results of a simulation for a reaction at 450 mbar are shown in Fig. 5.4-3.

$$\frac{dc_{ME}}{dt} = k_{1\leftarrow} c_{MO} c_{methanol} - k_{1\rightarrow} c_{ME} c_{glycerol} + k_{2\leftarrow} c_{DI} c_{methanol} - k_{2\rightarrow} c_{MO} c_{ME}$$

$$\frac{dc_{MO}}{dt} = k_{2\leftarrow} c_{DI} c_{methanol} - k_{2\rightarrow} c_{MO} c_{ME} + k_{1\rightarrow} c_{ME} c_{glycerol} - k_{1\leftarrow} c_{MO} c_{methanol}$$

$$\frac{dc_{DI}}{dt} = -k_{2\leftarrow} c_{DI} c_{methanol} + k_{2\rightarrow} c_{MO} c_{ME}$$

Scheme 5.4-3: Model 1: System of differential equations for the reaction rates of ME, MO and DI. Methanol concentration was constant and glycerol concentration dependent on conversion as described in the previous chapter.

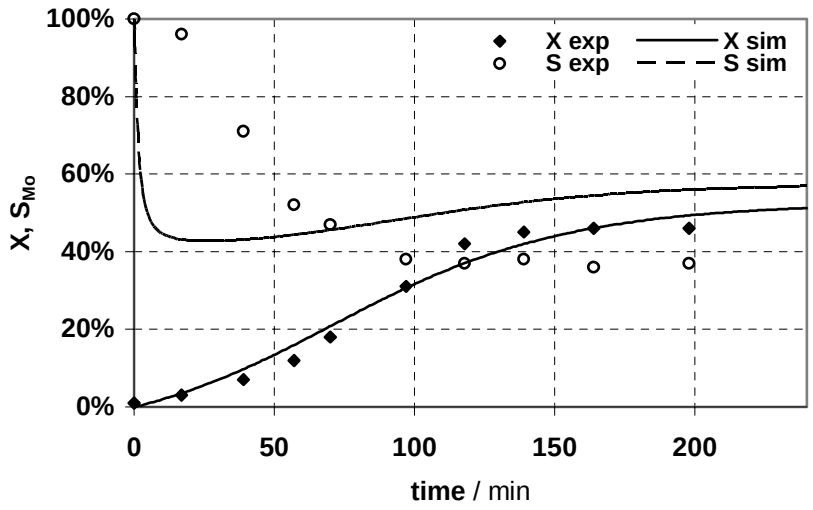

Fig. 5.4-3: Fit of Model 1 and experimental data of a run at 450 mbar. Methyl ester of oleic acid (ME), 500 rpm, 130 °C, initial ratio between ME and glycerol 0.44, 1.09 % catalyst. Conversion X and selectivity towards MO S_{MO} were determined by gas chromatography.

Conversion X and selectivity S_{MO} are fitted with help of the simulation software Berkeley Madonna. All plots with a dashed grid are derived from simulations with this software. The results show that a fitting criterion analogous to the least-squares method is used. In the documentation of the software neither the exact criterion nor the algorithm used to optimize the deviation from the fitting criterion for several parameters is given. In this study usually the value of the reaction rate constants were fitted. Results are given with three significant digits because the optimization tolerance was set to 0.1 %.

The fitted reaction rate constants used in Fig. 5.4-3 are shown in Table 5.4-1. The fitted forward reaction rate constants $k_{i\rightarrow}$ with i = 1 or 2 are called k_{if} according to the nomenclature in the simulation software Berkeley Madonna.

$$K_i \equiv \frac{k_{if}}{k_{ir}} \Leftrightarrow k_{ir} = \frac{k_{if}}{K_i} \qquad \text{Eq. 5.4-5}$$

The backward reaction rate constants $k_{i\leftarrow}$ are called k_{ir}. Instead of reporting directly the backward reaction rate constants, these constants are given in terms of equilibrium constants K_i which are defined according to Equation 5.4-5. These constants are related to the final equilibrium composition which is discussed in chapter 5.4.4. This approach simplifies the interpretation of the fitted data by a comparison to the final composition at the end of the reaction time.

The plot in Fig. 5.4-3 shows that the conversion is fitted well, but the trend of the selectivity shows a bad agreement. The slow decrease of S_{MO} between 0 and 90 minutes cannot be described by this set of differential equations. The same result was obtained for all other runs. In no case selectivity and conversion could be fitted successfully.

Table 5.4-1: Model 1, reaction rate constants fitted for runs at different pressures, T = 130 °C. All parameters were fitted simultaneously. Additionally mean and relative mean standard deviation (*SD*) are shown.

	300 mbar	450 mbar	600 mbar	1012 mbar	mean	rel. *SD*
k_{1f} /(kg/(mol min))	0.0240	0.0261	0.0365	0.0242	0.0277	19 %
k_{2f} /(kg/(mol min))	0.120	0.120	0.120	0.120	0.120	0 %
K_1	0.138	0.266	0.189	0.282	0.219	27 %
K_2	0.0413	0.0522	0.0499	0.0492	0.0481	9 %

The constants of different runs are of similar magnitude. The relative *SD* is between 0 and 27 %. The low *SD* of k_{2f} shows that this parameter is either the same for all runs or it is unaffected by the simulation algorithm. If it is changed manually it reveals a strong influence on the selectivity in the initial region. It was concluded that this parameter cannot be

simultaneously fitted because its main influence on selectivity is in a region in which the model has poor agreement with the experimental data. As the mean square error is minimized automatically it is trapped in a local minimum in which the integral between the fit and the experimental data for the selectivity before and after 60 min are of the same magnitude, but of opposite sign.

Therefore fitting procedure was repeated with different starting values of k_{2f} which was optimized separately from all other constants. This resulted in a better agreement of selectivity; see Fig. 5.4-4 and Table 5.4-2.

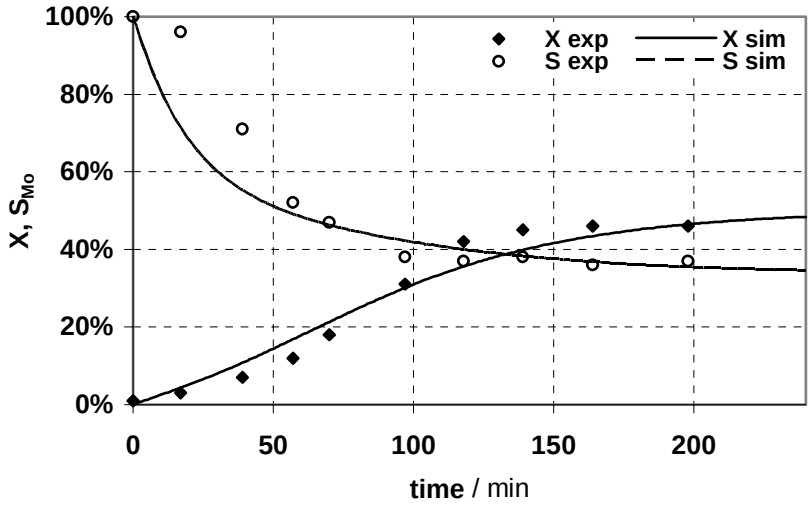

Fig. 5.4-4: Fit of Model 1 and experimental data. Run at 450 mbar. Initial value for k_{2f} optimized separately.

But this model does still not describe the initial selectivity and does qualitatively not show the same trend in the middle or at the end of the simulation time; experimental data of selectivity show no hyperbolic decrease as predicted by the model and at 120 minutes experimental data show only very slow reaction rates.

Table 5.4-2: Model 1, reaction rate constants fitted for runs at different pressures, $T = 130$ °C. Parameter k_{2f} was fitted separately. Additionally mean and relative mean standard deviation (*SD*) are shown, $K_i \equiv k_{if}/k_{ir}$.

	300 mbar	450 mbar	600 mbar	1012 mbar	mean	rel. *SD*
k_{1f} /(kg/(mol min))	0.0492	0.0531	0.0843	0.0368	0.0558	31 %
k_{2f} /(kg/(mol min))	0.00713	0.00705	0.00633	0.00332	0.00596	26 %
K_1	0.0740	0.110	0.143	0.229	0.139	41 %
K_2	0.212	0.0986	0.0899	0.103	0.126	40 %

5.4.2 Model 2

A second model was used in which the second order rate equation in Scheme 5.4-2 (b) is substituted by a second order term with respect to MO for the formation of DI, see Scheme 5.4-4.

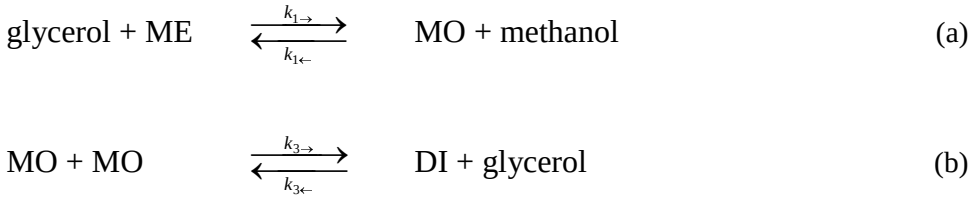

Scheme 5.4-4: Second order reaction steps of Model 2.

The differential equations are given in Scheme 5.4-5. The result for the run at 450 mbar is shown in Fig. 5.4-5. The agreement of conversion between fit and experimental data is similar to model 1. The main difference is the qualitative better agreement of the shape of selectivity. It shows a sigmoidal curve in the initial region that agrees better with the experimental data than a hyperbolic profile.

$$\frac{dc_{ME}}{dt} = k_{1\leftarrow} c_{MO} c_{methanol} - k_{1\rightarrow} c_{ME} c_{glycerol} \quad \text{(a)}$$

$$\frac{dc_{MO}}{dt} = 2k_{3\leftarrow} c_{DI} c_{glycerol} - 2k_{3\rightarrow} c_{MO}^2 + k_{1\rightarrow} c_{ME} c_{glycerol} - k_{1\leftarrow} c_{MO} c_{methanol} \quad \text{(b)}$$

$$\frac{dc_{DI}}{dt} = -k_{3\leftarrow} c_{DI} c_{glycerol} + k_{3\rightarrow} c_{MO}^2 \quad \text{(c)}$$

Scheme 5.4-5: Model 2: System of differential equations for the reaction rates of ME, MO and DI. Methanol concentration was constant and glycerol concentration dependent on conversion as described in the previous chapter.

Due to the square term with respect to MO for the formation of DI, decrease of selectivity is slower compared to the case when the rate of DI formation is proportional to MO.

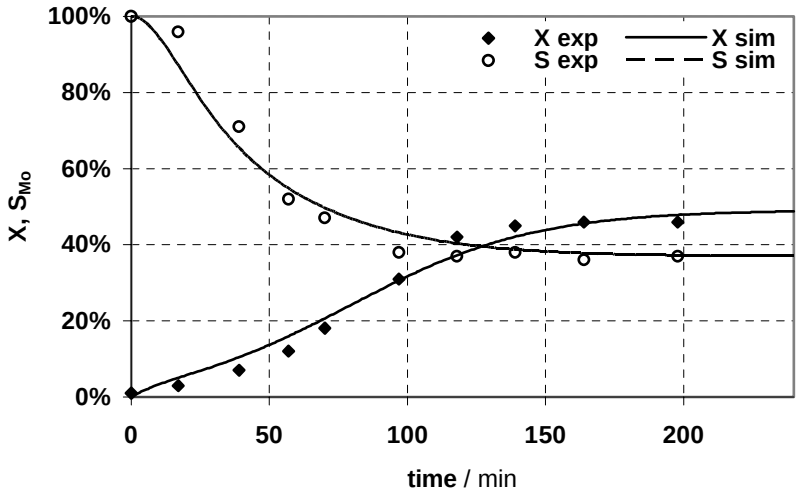

Fig. 5.4-5: Fit of Model 2 and experimental data. Run at 450 mbar.

The difference of selectivity between Model 2 and experimental data before 60 minutes is smaller compared to Model 1. After 60 minutes data show the same agreement. The small differences of Model 2 regarding the selectivity before 60 minutes could be explained by a small lag time due to the use of a solvent to add the catalyst. The solvent methanol slows the

initial reaction rate down because it is one of the products and has to be removed by distillation.

Table 5.4-3: Model 2, reaction rate constants fitted for runs at different pressures, T = 130 °C. Additionally mean and relative mean standard deviation (*SD*) are shown, $K_i \equiv k_{if}/k_{ir}$.

	300 mbar	450 mbar	600 mbar	1012 mbar	mean	rel. *SD*
k_{1f} /(kg/(mol min))	0.0734	0.0828	0.162	0.0606	0.0947	42 %
k_{2f} /(kg/(mol min))	0.0791	0.0732	0.0712	0.0843	0.0769	7 %
K_1	0.0783	0.118	0.136	0.215	0.137	36 %
K_2	1.65	0.713	0.681	0.425	0.867	54 %

The reaction rate constants are shown in Table 5.4-3; the deviation of K_1 from the mean is of the same magnitude compared to Model 1. Conversion trends show only small absolute differences between both models, but the trend in Model 2 shows a better agreement in the sigmoidal region. This is a result of the coupling of curvature of selectivity and conversion before 60 minutes; the main parameter that controls this curvature is the constant K_2.

5.4.3 Equilibrium Constants and Pre-Equilibrium

In Table 5.4-2, the fitted constants according to Model 1 are shown. The relative *SD* is between 26 and 41 %. Particularly the constant K_1 is responsible for the maximum conversion as it represents the ratio between the first product MO and the initial reactant ME at equilibrium. Agreement of model and experiment would be considerably improved if K_1 would be constant. K_2 is partly responsible for the final selectivity as it covers the ratio between DI and MO, see Equations 5.4-6 to 5.4-8. The formulation of K_2 is dependent on the model chosen.

Model 1 and 2: $$K_1 \equiv \frac{k_{1\rightarrow}}{k_{1\leftarrow}} = \frac{c_{methanol} c_{MO}}{c_{ME} c_{Gly}}$$ Eq. 5.4-6

Model 1: $$K_2 \equiv \frac{k_{2\rightarrow}}{k_{2\leftarrow}} = \frac{c_{DI}\, c_{methanol}}{c_{MO}\, c_{ME}}$$ Eq. 5.4-7

Model 2: $$K_2 \equiv \frac{k_{2\rightarrow}}{k_{2\leftarrow}} = \frac{c_{DI}\, c_{glycerol}}{c_{MO}^2}$$ Eq. 5.4-8

A third model, Model 3, was introduced which was expected to reduce the *SD* of K_1 by using the square of c_{ME}, see Equation 5.4-9. This was done as an analogy to the overall reaction rate formulation in Equation 5.4-1 that was used in literature [58, 59]. Because this equilibrium constant does not fulfill the stoichiometric balance and therefore has the unit kg/mol, this constant is marked by the superscript "#".

Model 3: $$K_1^{\#} \equiv \frac{k_{1\rightarrow}}{k_{1\leftarrow}} = \frac{c_{methanol}\, c_{MO}}{c_{glycerol}\, c_{ME}^2}$$ Eq. 5.4-9

Additionally the establishment of a pre-equilibrium between the alcoholates of methanol and glycerol was formulated, see Equation 5.4-10. This way was chosen because the concentration of the catalyst was of the same magnitude as the concentration of methanol. The catalyst is either present as sodium salt of glycerol or methanol which could not be analyzed separately by GC. The aim was to reduce the *SD* of K_1 by adding an additional parameter. This should show differences between the models. The equilibrium constant of that reaction is *K**.

$$R{-}OH + CH_3O^- \rightleftharpoons R{-}O^- + CH_3OH$$ Eq. 5.4-10

with R = $CH_2(OH)CH(OH)CH_2{-}$

$$K^* = \frac{c_{RO^-}\, c_{CH_3OH}}{c_{ROH}\, c_{CH_3O^-}}$$ Eq. 5.4-11

The concentrations c_{RO^-} and $c_{CH_3O^-}$ can be calculated using the constant total concentration of alcoholates present in the ME layer $c_{alc^-,0}$. The content of sodium as indicator for the overall

content of alcoholates in the ME layer was known from atomic absorption spectroscopy. The content of 25.2 mmol/kg Na^+ was constant during the reaction. $c_{alc^-,0}$ is related to the total balance of alcoholates.

$$c_{alc^-,0} = c_{RO^-} + c_{CH_3O^-} \qquad \text{Eq. 5.4-12}$$

The concentration of the neutral alcohols is calculated from the total concentration of the individual alcohols by gas chromatography $c_{ROH,0}$ and the component balance of each alcohol in Equation 5.4-13 with R = $CH_2(OH)CH(OH)CH_2-$ or R = CH_3-

$$c_{R\text{-}OH,0} = c_{RO^-} + c_{R\text{-}OH} \qquad \text{Eq. 5.4-13}$$

With help of Equation 5.4-14 the concentration of the alcoholate of methanol was calculated; the concentration of the alcoholate of glycerol was calculated subsequently from Equation 5.4-12.

$$c_{CH_3O^-} = \frac{\left(K^* c_{R0H,0} + c_{CH_3OH,0} + \left(1 - K^*\right) c_{alc^-,0}\right)}{2\left(K^* - 1\right)} \pm \sqrt{\frac{\left(K^* c_{R0H,0} + c_{CH_3OH,0} + \left(1 - K^*\right) c_{alc^-,0}\right)^2}{4\left(K^* - 1\right)^2} + \frac{c_{alc^-,0} c_{CH_3OH,0}}{\left(K^* - 1\right)}} \qquad \text{Eq. 5.4-14}$$

The interpretation of concentration terms of methanol and glycerol in Equations 5.4-6 to 5.4-9 changes. The concentrations of the alcohols have to be substituted by the concentration of the catalytic active species. The parameter *K** was used to minimize the *SD* of K_1 in Model 1 to 3. The equilibrium concentrations were approximated by using the composition of the reaction solutions at the end of the reaction when distillation of the co-product methanol came to an end, see Table 5.4-4.

Table 5.4-4: Concentrations used for the calculation of K_1 and K_2.

	1012 mbar	600 mbar	450 mbar	300 mbar
methanol /(mol/kg)	0.40	0.26	0.14	0.11
glycerol /(mol/kg)	0.27	0.40	0.34	0.67
ME /(mol/kg)	2.51	1.86	1.56	1.03
MO /(mol/kg)	0.33	0.50	0.55	0.78
DI /(mol/kg)	0.17	0.31	0.41	0.48

The results for K_1 and K_2 without the use of a pre-equilibrium are shown in Table 5.4-5. The constant K_1 is by definition the same for Model 1 and 2. K_2 shows a smaller *SD* of 10 % in Model 2 compared to Model 1. As the error of reproducibility is about 10 % for conversion, these differences are regarded as non significant. This calculation was repeated interpolating all trends observed in the sequence of the reactions at different pressures. So the scattering of the experimental values is reduced. This approach showed no advantage because the relative *SD* of K_2 in Model 2 was doubled while the relative *SD* of K_2 in Model 1 was increased by 2 %.

Table 5.4-5: Calculated equilibrium constants K_1 and K_2 for different models without pre-equilibrium, T = 130 °C. Mean and relative mean standard deviation (*SD*) for each constant are shown.

		1012 mbar	600 mbar	450 mbar	300 mbar	mean	rel. *SD*
Model 1,2	K_1	0.196	0.173	0.144	0.127	0.160	16 %
Model 1	K_2	0.0802	0.0859	0.0647	0.0677	0.075	12 %
Model 2	K_2	0.409	0.497	0.449	0.531	0.472	10 %

The calculation of K_1 and K_2 was repeated using a variable parameter K^* to minimize the relative *SD* of K_1 and K_2. Optimization was done with two initial guesses, one below 1 and one higher than 1, because Equation 5.4-14 is not defined at $K^* = 1$. The results are shown in Table 5.4-6. Additionally this procedure carried out for Model 3.
The relative *SD* as a criterion for the agreement of model and experimental data of the final products is not significantly decreased by the use of a pre-equilibrium. All relative *SD* are

between 14 and 16 %. These values are slightly higher than the values obtained without a pre-equilibrium of 10 to 16 %.

Table 5.4-6: Equilibrium constants K_1 and K_2 for different models with pre-equilibrium, T = 130 °C. Data from Table 5.4-4, K^* was optimized to minimize the relative mean standard deviation (*SD*).

	K^*		1012 mbar	600 mbar	450 mbar	300 mbar	mean	rel. *SD*
Model 1,2	1.10	K_1	0.179	0.158	0.132	0.116	0.146	16 %
Model 1	0.55	K_2 $*10^3$	3.66	4.46	4.95	3.49	4.14	14 %
Model 2	2.04	K_2	0.0219	0.0235	0.0278	0.0185	0.023	15 %
Model 3	$+\infty$	$K^{\#}_1$ $*10^7$ mol/kg	8.62	9.92	9.98	12.9	10.4	15 %

This result was verified by reducing the scattering of experimental data. All data were smoothed by a linear interpolation of the trends for conversion, selectivity, methanol and glycerol content in the experiments at different pressures. From these smoothed data the influence of K^* on the relative *SD* of K_1 and K_2 was calculated; results are shown in Fig. 5.4-6.

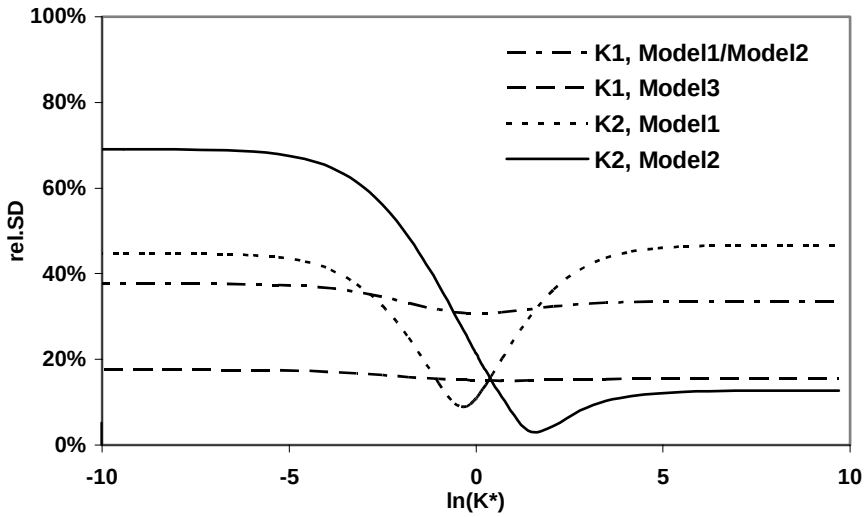

Fig. 5.4-6: Influence of the equilibrium constant of a pre-equilibrium (K*) on the relative standard deviation (*SD*) of the equilibrium constants (K) of Model 1 to 3. Experimental data used for the calculation were smoothed by an interpolation of the measured conversion and selectivity and final glycerol concentration at different pressures by linear trends.

For the constant K_2 in Models 1 and 2 a pronounced improvement is possible. The optimum for Model 1 is at $K^* = 0.70$ and for Model 1 at $K^* = 5.04$.
K_1 can be optimized too, but the improvement is poor. For K_1 in Model 1 and 2 the minimum is only 5 % below the linear overall trend. For Model 3 no optimum is noticeable.
As result the optimized K^* is not used for the kinetic model because it provides only an improved stability of K_2 for smoothed data. Apart from that K_2 has only a limited influence on the maximum conversion; the improved stability of K_2 does not grant an improvement of selectivity, because selectivity is dependent on both equilibrium constants. Additionally no reliable experimental data for K^* are available.

The differences of the calculated constants K_1 and K_2 are of the same magnitude whether a pre-equilibrium is used or not. As these differences are not significant, the calculation of the constants K_1 and K_2 gives no decisive factor for the choice of the model. An improvement of the agreement of data and simulation is expected if the liquid-liquid-equilibrium for the methyl ester layer is integrated into the model. The glycerol concentration plays a crucial rule, but could only be determined at the end of the reaction. For the simulation it was interpolated linearly with respect to conversion. But the formulation of this equilibrium was out of the scope of this work and is done in a separate study.

5.4.4 Activation Energy

The Arrhenius law accounts for the influence of temperature on the value of the reaction rate constants. It is formulated for a given temperature T in Kelvin relative to a reference temperature T_0, R is the gas constant.

$$k_i = k_{i,T=T_0} e^{\frac{E_A}{R}\frac{(T-T_0)}{TT_0}} \qquad \text{Eq. 5.4-15}$$

This law was not used in the classical formulation consisting of the product of a frequency factor and an exponential term containing the activation energy because in this form both Arrhenius parameters are correlated. Thus the value of k remains unchanged if activation energy and frequency factor are changed appropriately [63].

As a first guess of the activation energy, the apparent activation energy is calculated that does not use any information about the solubility of methanol and glycerol in the ME layer. This way is usually chosen if no detailed information about the reactive system and the individual composition of the phases is available as it is often the case when reactions between two liquids are carried out. It gives an impression of the acceleration of the reaction when the reaction is carried out at the same initial conditions like molar ratios and catalyst content if only the temperature is changed. In this case a simplified model is chosen that only accounts for the initial rate of the reaction before 25 minutes in Fig. 5.2-4. Solely the forward rate constant $k_{forward}$ for a second order reaction according to Equation 5.4-16 is considered.

$$\text{ME} + \text{glycerol} \xrightarrow{k_{forward}} \text{MO} + \text{methanol} \qquad \text{Eq. 5.4-16}$$

Formation of the consecutive products DI and TRI are neglected. Methanol and glycerol concentrations are assumed to be constant at a level of 1 and 2 %. The absolute values of methanol and glycerol concentration have no effect on the calculation of the activation energy because they are assumed to be the same for different temperatures. This is in accordance with the experimental conditions because the molar ratio of reactants was constant in the experiments. The result is an apparent activation energy of (100 ± 20) kJ/mol, with

$k_{forward}$ = 0.01 kg/(mol min). These values can be used as start values, when the complete reaction network will be fitted.

In a more detailed approach, the same data from Fig. 5.2-4 were fitted to Model 2. In this case the glycerol content was calculated according to Equation 5.3-7 and 5.3-8, methanol from Equation 5.3-2; these correlations were obtained in experiments with oleic acid esters. As selectivity was not recorded in the runs with palmitic acid methyl esters, the initial selectivity S_{MO} for the run at 130 °C was set to 0.30 %. This value was obtained in experiments with oleic acid methyl ester. This leads to reaction rate constants that are dependent upon temperature.
The activation energies for all steps in Model 2 were determined by an Arrhenius plot of the natural logarithm of the reaction rate constants k_i vs. the reciprocal of the absolute temperature T, see Fig. 5.4-7.

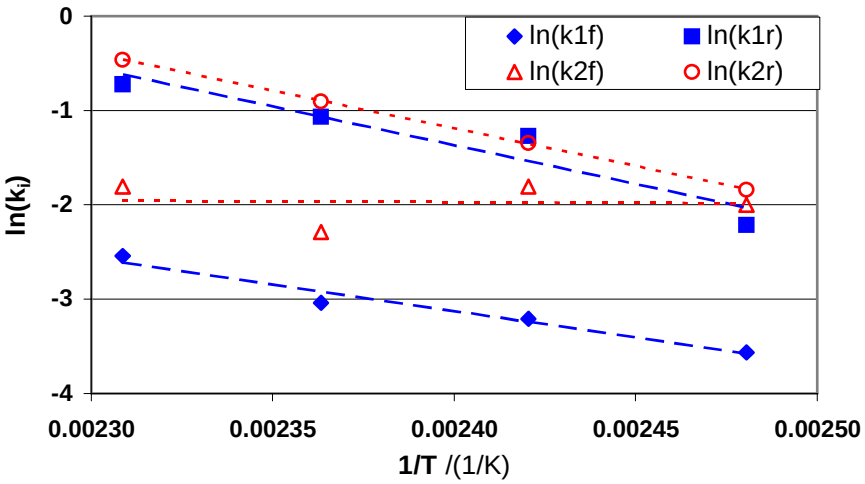

Fig. 5.4-7: Arrhenius plot of the natural logarithm of the reaction rate constants k_i vs. the reciprocal of the absolute temperature T. Dashed lines: linear trend.

The linear correlation for k_{1r} and k_{2r} is high, $R > 0.95$. The plots of k_{1f} and k_{1r} are nearly parallel which indicates only a small difference of activation energies which is in accordance with the assumption that transesterification reactions are about thermoneutral. The linearity of the correlation for k_{2f} is less pronounced; k_{2f} shows a very low linear correlation of $R = 0.29$. This can be caused by the small lag time observed when reaction is started. The influence of k_{2f} on the shape of the conversion curve is maximal at the initial region which shows a lag

time due to the addition and evaporation of the catalyst solution. Therefore this lag time interferes with fitting this parameter. A second reason could be that the occurrence of TRI was not taken into account.

Table 5.4-7: Reaction rate constants at 130 °C and activation energies determined in Fig. 5.4-7 for runs with palmitic acid methyl ester at different temperatures, Model 2, Equilibrium constants at T = 130 °C: K_1 = 0.213, K_2 = 0.858.

rate constant / (kg/(mol min))		***EA*** /(kJ/mol)
k_{1f}	0.0278	46.9
k_{1r}	0.131	68.2
k_{2f}	0.137	1.3
k_{2r}	0.160	66.5

The reaction rate constants and activation energies are summarized in Table 5.4-7. The reaction rate constants are smaller compared to the values obtained for the runs with esters of oleic acid esters. This can be caused by the higher acid value of palmitic acid which leads to a reduction of free catalyst sodium methoxide. The resulting simulation is shown in Fig. 5.4-8.

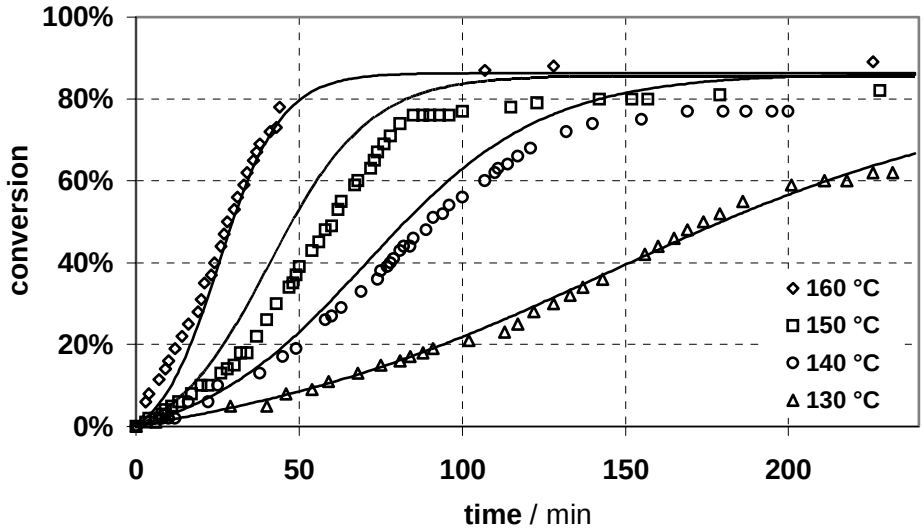

Fig. 5.4-8: Simulation (line) of conversion for different temperatures for palmitic acid methyl ester (ME) according to Model 2 and activation energy data in Table 5.4-7 derived from an Arrhenius plot. Reaction conditions: 300 mbar, initial ME-glycerol-ratio 0.46, 0.80 % catalyst, 500 rpm.

As conversion of the runs at 140 and 150 °C is overestimated by the simulation and all final conversions seem to approach the same final equilibrium conversion, it was tried to improve the simulation. Ignoring the results of the Arrhenius plot in Fig. 5.4-9, all four activation energies were fitted simultaneously by implementing the same reaction scheme four times into one simulation of the software Berkeley Madonna. Only the temperatures in each reaction scheme were different. The results for the activation energies are shown in Table 5.4-8.

Table 5.4-8: Simultaneously fitted activation energies *EA* for Model 2. Reaction rate constants and reaction conditions are shown in Table 5.4-7.

rate constant / (kg/(mol min))	***EA*** /(kJ/mol)
k_{1f}	48.6
k_{1r}	69.0
k_{2f}	57.7
k_{2r}	107.7

The differences between the simultaneously fitted activation energies of k_{1f} and k_{1r} and the values derived from the Arrhenius plot are negligible; absolute differences are smaller than 3 kJ/mol. For the second step differences are more pronounced. Particularly the activation energy of the reaction rate constant k_{2f} increased from about 0 up to 58 kJ/mol, a value of a similar magnitude compared to the activation energies for k_{1f} and k_{1r}. The activation energy for the backward reaction rate constant k_{2r} is increased accordingly. The difference of the activation energies ΔEA for the reaction rate constants of the second step in Model 2, k_{2f} and k_{2r}, shows only a small decrease compared to the results of the Arrhenius plot from –65.2 down to –50.0 kJ/mol.

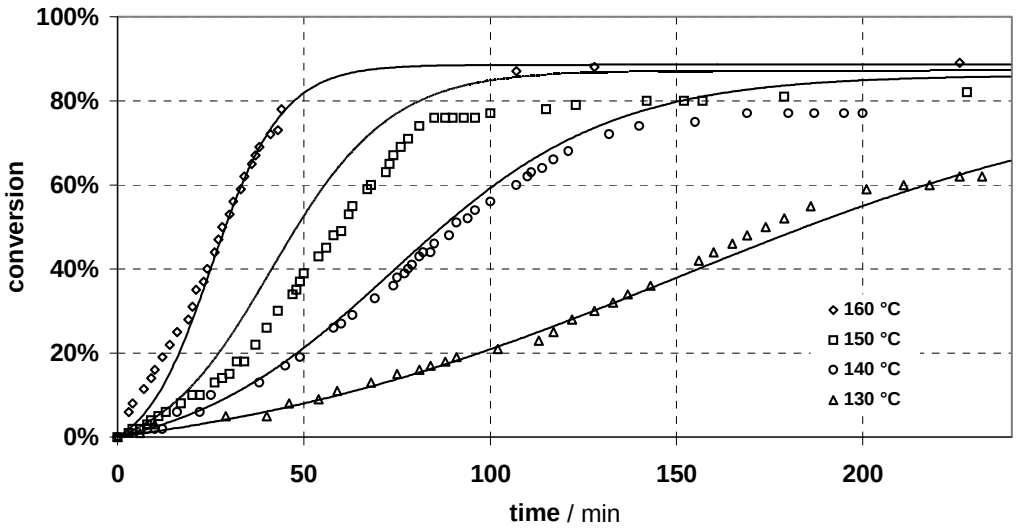

Fig. 5.4-9: Simulation (line) of conversion for different temperatures according to Model 2 and data in Table 5.4-8 derived by simultaneously fitting all activation energies. Same reaction conditions as in Fig. 5.4-8.

In Fig. 5.4-9 it can be observed that the fit for the temperature of 140 °C could be improved slightly. Additionally the spacing of the final conversions shows the expected order: the higher the temperature the higher is the final equilibrium conversion. Selectivities are in accord with the experiments with oleic acid methyl ester, for increasing temperatures the selectivities S_{MO} are 30.5, 41.7, 52.7 and 62.0 %.

Many reasons favor the use of the results in Table 5.4-8. The main difference to the activation energies in Table 5.4-7 are the values for the second step in Model 2. The Arrhenius plot

revealed problems with the determination of the activation energy of k_{2f}. The temperature dependency of this reaction rate constant had had the lowest linear correlation. A second clue is that activation energies of about 0 kJ/mol are not expected for this step, because the transesterification reaction of this step is basically not different from all other steps involved in the course of this reaction.

As a test for the plausibility of the activation energies, data of the autoclave experiments at different temperatures are interpreted according to the Van't Hoff Equation. It correlates the equilibrium constant K of a chemical reaction with the reaction enthalpy ΔH, Temperature T and the gas constant R.

$$\frac{d\ln(K)}{dT} = \frac{\Delta H}{RT^2} \qquad \text{Eq. 5.4-17}$$

In order to determine the reaction enthalpy ΔH, the natural logarithm of the equilibrium constants K_1 and K_2 is plotted vs. the reciprocal temperature according to Equation 5.4-18, shown in Fig. 5.4-10.

$$\frac{d\ln(K)}{d(1/T)} = \frac{\Delta H}{R} \qquad \text{Eq. 5.4-18}$$

The absolute values of the equilibrium constants derived from the experiments in the autoclave are not compared to the data in this section because during these experiments no reference standards for MO and DI for gas chromatography were available. Therefore only trends of the calculated values of the equilibrium constants can be interpreted and compared to the results obtained in other experiments.

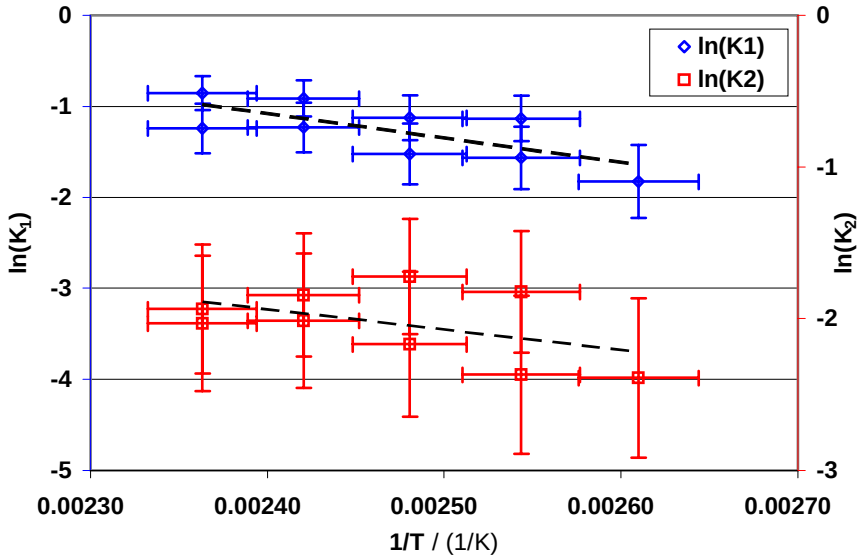

Fig. 5.4-10: Van't Hoff plot of the natural logarithm of the equilibrium constants K_1 and K_2 vs. the reciprocal temperature. Initial molar ratio between glycerol and oleic acid methyl ester 3:1, 0.5 % catalyst, error bars indicate the maximum errors, dashed lines are linear trends.

For the calculation of the errors of the equilibrium constants the maximum errors were used. When experiments were repeated at the same temperature, the calculated equilibrium constants showed deviances higher than expected by using a mean error propagation formula. The maximum error of K_1 and K_2 was determined by the assumption of an individual relative error for each concentration of 5 %. As an additional source of error, temperature was identified. The error of temperature was estimated by a control experiment with an additional thermometer which showed that turning off the stirrer leads to a temperature shift of approx. 5 °C. This is also the accuracy of the thermostat which showed graduations of 5 °C. The reason for the temperature shift is that during stirring the vortex reduces the contact between the liquid in the autoclave and the thermometer that was attached centrally to the lid. The temperature shift is caused by the collapse of the vortex, when stirring was stopped before sampling.

As a result a range for the reaction enthalpy $\Delta_1 H$ for the reactions of step 1 in Model 2 could be determined, for K_1 the range is between –20 and –65 kJ/mol. For K_2 the interval of $\Delta_2 H$ is +25 kJ to –65 kJ/mol.

If the Arrhenius Equation is introduced into the left side of Eq. 5.4-17 by substituting the equilibrium constant by the ratio of reaction rate constants, it follows that the reaction enthalpies are equivalent to differences of the activation energies ΔEA.

$$\Delta EA = \Sigma EA_{forward} - \Sigma EA_{backward} \qquad \text{Eq. 5.4-19}$$

The activation energy difference is defined by the activation energy of the reaction rate constants for the forward and backward steps of each equilibrium reaction. The differences of activation energies ΔEA are equivalent to the reaction enthalpy as shown in Equation 5.4-20.

$$\Delta H = +\Delta EA \qquad \text{Eq. 5.4-20}$$

The activation energy difference ΔEA between the forward and backward reaction steps calculated by simultaneously fitting the activation energies are −20 kJ/mol for step 1 and −50 kJ/mol for step 2. These differences are within the range calculated by the Van't Hoff plot.

In Table 5.4-9 the activation energies are compared with data from literature for the alcoholysis with butan-1-ol or methanol of soybean oil. These data were obtained at a different temperature level below 100 °C, whereas own experiments were conducted between 130 to 160 °C.

Table 5.4-9: Comparison of activation energies of the first step (a) of Model 2 with data from literature. Step (a) of Model 2: ME + glycerol $\underset{k_{1r}}{\overset{k_{1f}}{\rightleftharpoons}}$ MO + methanol, data in literature for the alcoholysis of soybean oil.

		literature[59]		literature[58]
rate constant	*EA* /(kJ/mol)	*EA* /(kJ/mol)	*EA* /(kJ/mol)	*EA* /(kJ/mol)
	base-catalyzed	base-catalyzed	acid-catalyzed	base-catalyzed
k_{1f} / *kg/(mol min)*	48.6	34.1	50.8	40.0
k_{1r} / *kg/(mol min)*	69.0	44.6	62.9	26.8

Only the first step of Model 2, the reaction of ME to MO can be compared with literature because the second step was formulated different from the approach in literature to account for the slow decrease of selectivity with time. The first value from literature[59] is for a base-catalyzed reaction, the second for an acid-catalyzed reaction. The value from literature[58] is for a base-catalyzed reaction. Compared to own data, data in literature show a similar magnitude of the range of activation energies between 27.8 to 62.9 kJ/mol. Values and trends of data in literature are not consistent. They give different answers to the question which step has the highest activation energy and they show different levels of activation energies. One reason can that the occurrence of a second phase was not taken into account. Therefore it can only be stated that the reports agree that the difference of forward and backward reaction steps is not very high. The relative difference of activation energies for k_{1f} and k_{1r} in literature is between 21 and 40 %. This is in agreement with the results of own experiments in which the difference is 37 %.

The results shows that the initial guess of the apparent activation energy for k_{1f} of (100 ± 20) kJ/mol derived from the initial rate was too high. The reason is that the dependency of the solubility of methanol and glycerol on temperature was neglected. Even with an activation energy of 0 kJ/mol the change of the solubility leads qualitatively to an increase of selectivity from 30 to 40 % with temperature. The main factor that accounts for these trends is the solubility of glycerol according to the law of mass action. The second factor is the reduced solubility of methanol at higher temperatures.
Activation energies were determined using Model 2 by an Arrhenius plot as well as by fitting all activation energies simultaneously. Both results are in accordance with the Van't Hoff plot, but the values which were obtained by simultaneously fitting the activation energies showed a better agreement with experimental data, see Table 5.4-8.

5.5 Mass Transfer

In this study no mass transfer limitation of the chemical reaction in the reactive layer was observed. But at higher temperatures and catalyst contents it is likely that mass transfer limitation will occur because an increase of temperature and catalyst concentration will accelerate chemical reaction rate more than mass transfer. The situation is shown in Fig. 5.5-1. The reaction under investigation takes place only in the continuous liquid ME phase. This phase is in contact with the gas phase in the reactor and with a second liquid phase, the dispersed glycerol layer.

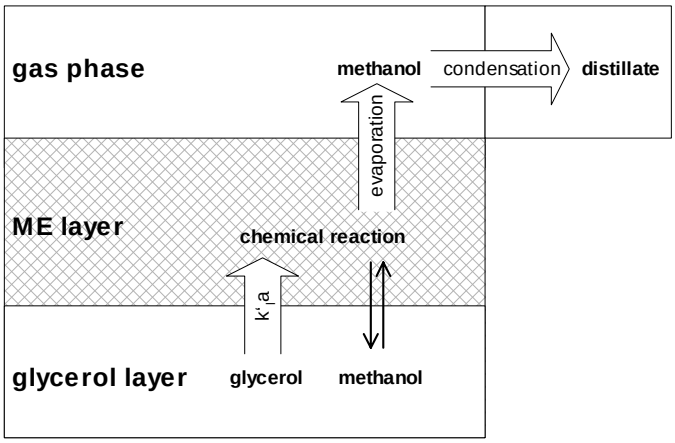

Fig. 5.5-1: Chemical reaction in the ME layer and mass transfer of methanol and glycerol between the adjacent phases. Mass transfer of glycerol is denoted by the mass transfer coefficient $k'_l a$. Methanol in the ME layer is in equilibrium with the glycerol layer. Excess methanol evaporates and is condensed. All other components like ME, MO and DI remain in the ME layer.

The products MO and DI are initially not present. They are formed by chemical reaction and accumulate in the ME layer because they show no solubility in the glycerol layer and have only a negligible vapour pressure. No ME, MO or DI were detected in the distillate. The couple product methanol is initially present in all phases because it is used as solvent for the catalyst. The main part of the methanol in the catalyst solution is removed quickly by distillation because it shows only a small solubility in both liquid phases. Because of this the glycerol layer and ME layer are supposed to be saturated initially with methanol and the gas phase is expected to consist mainly of methanol vapor. The analysis of both liquid phases shows a constant methanol content over the whole reaction time. This is equivalent to $dc_{methanol}/dt = 0$ for the ME layer. The methanol concentration of both liquid layers is in

equilibrium. The methanol formed by reaction that exceeds the solubility in the liquids is removed by distillation. The rate of methanol formation in Model 2 is shown in Equation 5.5-1. If the concentration of methanol in the ME layer, $c_{methanol}$, does not change, this means that the rate of a evaporation of methanol $\dot{n}_{evap.,methanol}$ divided by the volume of the ME layer $V_{ME\ layer}$ is of the same magnitude compared to the rate of the chemical reaction which is expressed in terms of concentrations c_i in the ME layer and the reaction rate constants k_j.

$$\frac{dc_{methanol}}{dt} = +k_{1\rightarrow}c_{ME}c_{glycerol} - k_{1\leftarrow}c_{MO}c_{methanol} - \frac{\dot{n}_{evap.,methanol}}{V_{MElayer}} \qquad \text{Eq. 5.5-1}$$

No accumulation in the gas phase can take place because it consists only of methanol and because pressure is held constant either by a controller for experiments at reduced pressure or by a connection to the environment for experiments at atmospheric pressure. Therefore gaseous methanol is removed by a fast convective gas flow from the surface of the liquid emulsion to the condenser. If temperature is maintained constant during the run, no mass transfer limitation is expected for the compound methanol, because evaporation is usually fast for vigorously stirred liquids. The main problem associated with this product is foaming which can interfere with stirring efficiency.

The glycerol concentration in the ME layer is not constant during reaction and was shown to cause the sigmoidal shape of the conversion curve. The initial solubility of glycerol in the ME layer is small, but enhanced during reaction. This means that $dc_{glycerol}/dt > 0$ for the ME layer. Glycerol has only a small vapor pressure and is consumed by reaction. The rate of glycerol consumption by chemical reaction without consideration of mass transfer according to Model 2 in the reactive layer is dependent upon the available glycerol in the ME layer $c_{glycerol}$.

$$\left[\frac{dc_{glycerol}}{dt}\right]_{chemical\_reaction} = -k_{1\rightarrow}c_{ME}c_{glycerol} - k_{3\leftarrow}c_{DI}c_{glycerol} + k_{1\leftarrow}c_{MO}c_{methanol} + k_{3\rightarrow}c_{MO}^2 \qquad \text{Eq. 5.5-2}$$

Reaction will show mass transfer limitation if the glycerol content in the ME layer $c_{glycerol}$ is smaller than the equilibrium concentration for the actual mixture of ME, MO, DI and methanol in the ME layer. As reaction time for e. g. 80 % of equilibrium conversion is about 100 minutes for 130 °C and 0.8 %wt catalyst, this change is slow. For the estimation of mass transfer limitation it is therefore appropriate to neglect the change of equilibrium concentration for small time intervals. In this case no mass transfer limitation will be observed if the rate of mass transfer from the glycerol layer to the reactive ME layer is at least equal to the consumption of glycerol by reaction.

The physical mass transfer rate $\dot{n}_{glycerol}/V_{ME\ layer}$ for the compound glycerol from the glycerol layer to the ME layer was estimated using Equation 5.5-3 [64]. The physical mass transfer rate is compared to the reaction rate which can be calculated using the simulation parameters that were derived in the the previous chapters. For this purpose magnitude of the reaction rate was extrapolated for elevated temperatures and higher catalyst contents.

$$\frac{\dot{n}_{glycerol}}{V_{MElayer}} = a k_l' \left(c_i - c_{glycerol} \right) \qquad \text{Eq. 5.5-3}$$

The mass transfer coefficient k'_l = 7.28 ·10^{-6} m/s was calculated in the theory section from Equation 2.2-10 for 130 °C. For this purpose a minimal power input of 0.16 J/(kg s) equivalent to 450 rpm was assumed, which was practically needed to form an emulsion. The concentration c_i of glycerol at the interphase was estimated by using experimental data for the dependency of glycerol concentration from conversion and temperature; see Equations 5.3-6 to 5.3-8. The concentration c_i is dependent on the conversion X and temperature T. $c_{glycerol}$ is the actual concentration of glycerol in the ME layer which will be for very fast reactions about zero, for a slow reaction it will be close to the equilibrium concentration in the ME-layer.

Mass transfer limitation will be observed if $\dot{n}_{glycerol}/V_{ME\ layer}$ is of the same magnitude as the reaction rate. Because of the sigmoidal shape of the conversion plot, reaction rate is maximal at a conversion of about 30–50 %. Therefore reaction rate and mass transfer were only calculated at this conversion interval.

The value of the interfacial area, a, per unit volume of the ME layer was varied from zero to the typical values obtained in own experiments [65] of a = 2·10^4 m²/m³.

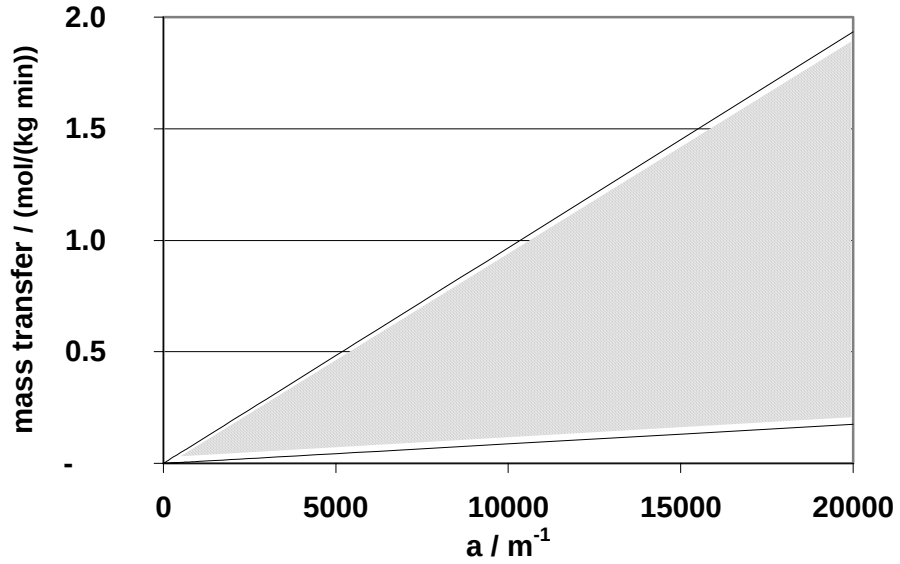

Fig. 5.5-2: Physical mass transfer estimated for glycerol in fatty acid methyl ester vs. specific interfacial area a at 130 °C. The upper limit is calculated for a maximal concentration difference ($c_i - c_{glycerol}$) in Equation 5.5.3 when $c_{glycerol}$ is zero in the reactive layer, the lower limit for a 10 % concentration difference. The mass transfer is calculated with respect to the mass of the ME layer.

The possible mass transfer rate of glycerol covers a huge range; see the hatched area in Fig. 5.5-2.
The reason for the width of this range is that the mass transfer rate $\dot{n}$ is linearly dependent on the concentration difference Δc and the specific interfacial area a. The effective concentration difference Δc is the difference between the equilibrium concentration at the phase boundary c_i and the bulk concentration $c_{glycerol}$ in the ME layer. The interval for Δc was calculated in two steps. First, the equilibrium concentration c_i was determined by the experimentally obtained solubility dependence on temperature and conversion. This is an extrapolation of the data obtained for temperatures between 130 and 160 °C for product mixtures. For 250 °C the extrapolated maximum solubility of glycerol is about 20 %. This is of the same magnitude compared to the solubility of glycerol in fats between 40 to 65 % at 250 °C reported in literature [66]. Secondly, it is assumed that the concentration $c_{glycerol}$ is zero, this leads to the maximal physical mass transfer rate. The minimum physical mass transfer rate was calculated from a difference that was only 10 % of Δc. This is also the minimum difference that can be analyzed by the chosen sampling procedure and gas chromatography.

The maximum reaction rates were calculated according to the activation energies that were determined in the previous chapter. Glycerol and methanol solubility were extrapolated from experimental data. A possible increase of catalyst amount up to 5 % was included as a linear

factor increasing from 1 (equivalent to 0.8 % catalyst used in this study) to a maximum of 8 (equivalent to 5 %). The resulting range for the reaction rate is given in Fig. 5.5-3.
It is of a smaller or of the same magnitude compared to Fig. 5.5-2, when no rate enhancement by adding more catalyst is proposed and temperature is below 180 °C.

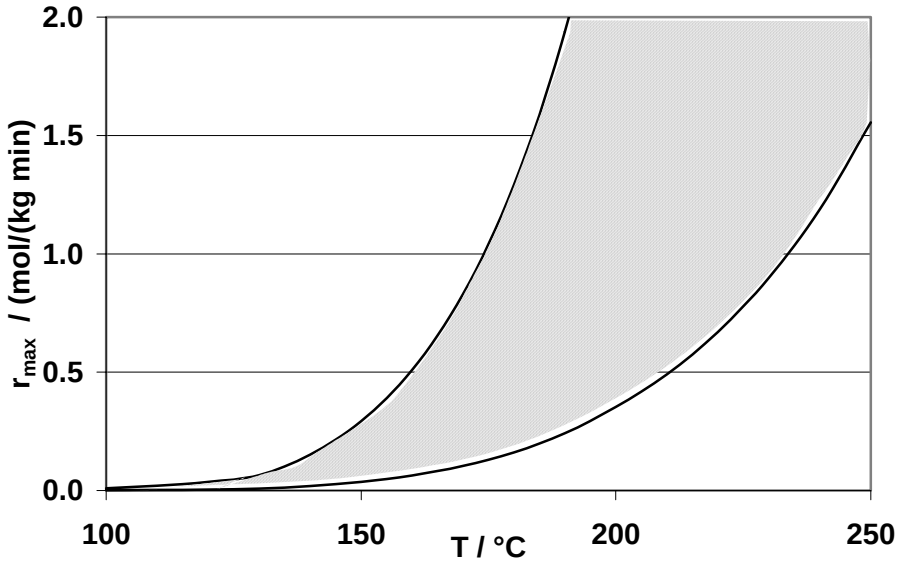

Fig. 5.5-3: Maximum reaction rate estimated by simulation. The lower limit is calculated for a standard catalyst concentration of 0.8 %, the upper limit for 5 % catalyst sodium methoxide.

Mass transfer limitation is only expected when both parameters, temperature and catalyst concentrations, are increased to values higher than those in this study. But is has to be kept in mind that this comparison was derived for the physical mass transfer of glycerol in pure ME. In practice the presence of catalyst and product will give rise to changes of the systems that will affect transfer properties. The use of activity coefficients and the mixing properties of the ME layer will improve this predictions, but the best improvement would be the measurement of transport properties during reactive conditions. The reason is that physical mass transfer can be enhanced in a reactive environment by consumption of the transfer species in the stagnant film between both phases.

The prediction is in agreement with a report of the glycerolysis of soybean oil at high temperatures, but with lower catalyst content in literature [66]. Temperature was between 200 and 220 °C and 0.18 % of the less active sodium hydroxide was used as catalyst. Only a limited influence of stirring rate on reaction was reported between 360 to 3600 rpm. A difference of about 10 % of the final composition at a fixed reaction time was observed.

6 Summary and Conclusion

When this study was started, the first hypothesis [67] was that the increase of the size of the interfacial area during reaction accelerates the reaction rate by enhancing the mass transfer rate of the starting materials into the reactive region. The reason that led to this hypothesis was the sigmoidal shape of the conversion plot. Using common kinetic formulations for this kind of reaction, an S-shaped plot could only be reproduced if a factor is identified which is able to accelerate the reaction rate. At this time the composition of the individual phases during reaction could not be determined separately. The only parameter that could be observed during reaction and which increased apart from the concentrations determined by the stoichiometric balances was the size of the interfacial area. This was the reason, why it was expected that this parameter accounts for the S-shaped region of the conversion plots. The calculated high initial activation energy of 60 kJ/mol that is not typical for mass transfer limited reactions was explained by the assumption that the reaction takes place mainly at the interphase. A supporting argument for this hypothesis was the expectation that the catalyst should be exclusively soluble in the glycerol layer and the observation that the starting material ME was only sparingly soluble in the glycerol layer. In this case the location where all components and the catalyst meet would be the interfacial area.

But this argumentation could be refuted step by step. First it was shown that the size of the interfacial area had no influence on reaction rate which was proved by changing the volume fraction and the stirring speed. The concentration of catalyst could be determined by atomic absorption spectroscopy. The only concentration that changed independently from the initial concentrations that were connected by the stoichiometric balances was the glycerol concentration. The glycerol concentration in the reactive ME layer was increased during reaction because its solubility was enhanced due to the accumulated reaction products. The glycerol was supplied by the glycerol layer. The increase of the glycerol concentration as one of the starting materials explains the enhancement of the reaction rate during the course of the reaction and the sigmoidal shape of the conversion curve. This approach is in accord with a mainly theoretical study [68], in which the consideration of the liquid-liquid equilibrium between the glycerol and methyl ester layer was suggested in order to model the kinetics of this reaction.

Following the course of the investigation, first the results for the drop size measurement and the optimization of analytical methods and procedures are summarized. It is followed by a more detailed compilation of the arguments that led to the refutation of the hypothesis of a

reaction that is dependent on the size of the interfacial area. The model discrimination and the results of the kinetic simulations with different models are summarized. Conclusions are drawn from the comparison of extrapolated chemical kinetic rates and the estimated physical mass transfer rates for carrying out the reaction at a technical scale.

An endoscopic micro photographic set up was chosen for the determination of the drop sizes in the reactive liquid-liquid emulsion. Photography was the only method suitable for this system. Under reactive conditions many parameters of the dispersion change like color, phase fraction and contrast. Each parameter affects the measurement with alternative methods which use e.g. light transmission or scattering. The method was improved by the use of a metal mirror attached to the endoscope that enhanced contrast and the range of drop sizes that could be determined. The ability to record drop sizes was improved from initially a maximal stirring rate of 600 to more that 900 min^{-1}. Additionally the period after catalyst addition in which drop size determination was not possible was continuously shortened.

The drop sizes show a distribution of Gaussian type. Drop size recording was shown to be independent of the location of the endoscope. The mean size decreases monotonously with reaction time. The influence of stirring rate was correlated according to the Weber number at similar conversions. The dependency was more pronounced than usually stated in literature for non reactive systems. This behavior can be explained by the presence of surface active components, occurrence of mass transfer and the decrease of the phase fraction of dispersed phase. Mean drop size without catalyst is about 300 – 200 µm, with catalyst about 150 – 50 µm.

Sampling and temperature program for gas chromatography (GC) were optimized. The sampling procedure was extended to the analysis of the single phases at the end of the reaction at reduced pressure. This was only possible by using an air lock and a preheated syringe for sampling. By this procedure temperature constancy in the reactor was enhanced.

The procedure for sample quenching that was used in preliminary studies revealed problems with pyridine as solvent. Samples in pyridine show further reaction. The main product of the reaction in pyridine is monoglyceride with a high selectivity. Whether this is caused by a selective effect of pyridine alone or of the competitive reaction of the components in the samples with the silylating agent used for GC analysis could not be differentiated. This could be done only by the use of a different analytical method like high pressure liquid chromatography. As this problem was severe, the influence of sampling procedure was

studied in detail by the use of “Dummies”, that are test solutions of the pure products with catalyst and solvent that resemble the quenched samples. Only if these preparations showed no change in composition it was concluded that no further reaction was to be expected. Dioxane with 1 % acetic acid was chosen as solvent for the determination of the composition of reactive mixtures; it did not alter the composition of samples significantly during preparation and analysis, and it neutralizes the catalyst which is corrosive to the GC column.

GC analysis of the glycerides, glycerol and the simultaneous determination of methanol was optimized. The main problem was to separate the methanol peak from the quenching solvent. Separation could be achieved by an initial period of 20 minutes at room temperature before starting the temperature program of the GC. Peak shape and resolution of the compounds with a higher boiling point were not affected by this operation. The calibration of methanol showed a linear trend with a high correlation similar to that for all other components.

The reactive system does not offer many possibilities to vary the initial chemical concentration of glycerol, methanol and methyl ester. Only the methanol content could be controlled by the use of different levels of reduced pressure. Both phases show the presence of methanol. The concentration decreases if pressure is reduced or temperature increased. Methanol content was constant throughout reaction. Catalyst concentration was measured in both phases by atomic absorption spectroscopy. The main part of the catalyst is solved in the glycerol layer. The concentration in both phases shows no trend during reaction. Therefore catalyst concentration is believed not to cause the sigmoidal shape of the conversion curve.

The influence of mass transfer on reaction rate could not be confirmed. A variation of the stirring rate between 500 and 900 rpm showed no significant trend of reaction rate. This was verified by removing ½ of the dispersed phase glycerol during reaction which resulted in no significant change of reaction rate. When the two phases of the emulsion were separated at the end of the reaction, no glycerides or methyl esters could be detected in the glycerol layer. A change of the initial molar ratio between glycerol and methyl ester in experiments conducted in an autoclave showed no influence on reaction rate. Therefore the glycerol layer is regarded only as a reservoir for glycerol. Reaction takes place in the methyl ester layer. The glycerol concentration in the methyl ester layer shows a pronounced dependency on conversion. As this concentration is proportional to the reaction rate of the first step of the consecutive reaction, it was successfully used to describe the sigmoidal shape of the conversion curve.

Consequently the hypothesis of a mass transfer limited reaction was not confirmed, because an influence of stirring rate on reaction rate could not be stated and the sigmoidal shape of the conversion curve could be explained instead by the trend of the glycerol concentration in the reactive phase. This conclusion is only valid for the conditions under investigation: pressure 1012 to 300 mbar, temperature 130 and 160 °C, catalyst concentration 0.8 % sodium methoxide.

The observation of preliminary studies that indicated a pronounced optimum of the selectivity towards monoglyceride during the reaction could not be repeated. This difference is attributed to the problems of the former used quenching method. Only a monotonous decrease of selectivity with conversion could be observed. Influence of temperature on selectivity was investigated by a comparison of own experiments and data in literature. The final selectivity of reaction products at a high conversion level increases with temperature in the range between 30 and 240 °C. The maximum selectivity is about 60 %. Therefore the optimum temperature regarding selectivity at high conversions is the maximum temperature of 240 °C. At higher temperatures products show degradation.

After the methyl ester (ME) layer was identified to be the location were reaction takes place, a model discrimination was carried out with respect to the measured concentration of the species in this phase. Two models were compared which formulate the reaction rate by a set of two reversible consecutive steps for the formation of monoglyceride (MO) and diglyceride (DI), each being of second order. A third consecutive step for the formation of triglyceride (TRI) could be neglected; the maximum content of 1 % TRI was always smaller than the mass balance deficit of 5 %. The two models differ in the formulation of the second consecutive step which describes the formation of DI. The first model was frequently used in literature and describes the formation of DI proportional to the product of the concentrations of MO and methyl ester. The second model describes the formation of DI proportional to the square of the concentration of MO. Simulations show that the main difference between both models is the shape of the selectivity plot at low conversion levels. The second model shows a better fit of this initial region.

The simulation of the conversion at different pressures shows for the equilibrium constant K_1 in both models a high relative standard deviation of 27 to 41 % for the first step of the reaction. It was tried to improve the agreement of experimental data by introducing an additional parameter, the equilibrium constant of a pre-equilibrium of the catalytic active

alcoholates. This approach was chosen because the concentration of the catalyst sodium methoxide was of similar magnitude compared to the concentration of methanol. The methanol concentration has a strong influence on the value of K_1, but both species could not be separated by GC analysis. The equilibrium constant of the pre-equilibrium was used to minimize the mean standard deviation of K_1. But this approach showed no advantage.

It is concluded that an improvement of the model can be obtained only by modeling the liquid-liquid equilibrium, because a second parameter that affects the value of K_1 is the glycerol concentration that is difficult to measure. Its trend was based only on few data that were assumed to be linear with respect to the conversion. But the formulation of the liquid-liquid equilibrium was not within the scope of this study; it is modeled in a parallel project in our working team.

With increasing temperature a higher selectivity S_{MO} towards MO is observed. Both models are able to describe qualitatively this trend even when no temperature dependency of the reaction rates is assumed. The reason is the enhanced solubility of glycerol in the ME layer with increasing temperature. This explains why the activations energies for both models are significantly smaller than the apparent activation energy of 100 ± 10 kJ/mol that was calculated without the consideration of the solubility of methanol and glycerol in the ME layer. The increase of selectivity of the final products from 30 to 60 % was simulated according to the second Model using activation energies determined by using the Arrhenius law.

The occurrence of mass transfer limitation at different reaction conditions was estimated by an extrapolation of the reaction rates derived from the model parameters and the estimation of the physical mass transfer of the limiting component glycerol. A comparison of both rates indicates that mass transfer limitation is likely to occur only if temperature and catalyst concentration are simultaneously increased at temperatures above 180 °C. On the other hand the observation that the mass transfer of glycerol is fast compared to the rates of the chemical reaction simplifies the scale up of this type of reaction. Therefore mixing is identified as a non critical process because this reaction is usually carried out at a lower level of catalyst compared to the runs conducted in this study. Reaction is not expected to show a high reaction enthalpy because transesterification reactions usually show a behavior similar to thermoneutral reactions. The reaction enthalpies determined by the Van't Hoff plot show a value of about -70 kJ/mol which is lowered by the energy demand for the evaporation of methanol of about 25 kJ/mol. These data indicate an exothermic reaction, but enthalpy data

should be verified by calorimetric experiments. If calorimetric data are not available, precautions for a sufficient cooling of the reactor should be taken.

As selectivity and final composition resembles that of the glycerolysis of fats, know-how of this field can be used which is described in a recent study [7]. A special problem of the glycerolysis of fatty acid methyl esters is the occurrence of methanol gas. It has to be removed in order to shift the equilibrium to high conversions. This can be done simply by condensation at normal pressure in a separate tank.

For this kind of reaction even a reactor type like a reactive rectification column comes into consideration in which mixing is mainly a result of the gas stream of the evaporating methanol. As a standard reactor type, a continuously stirred tank reactor can be used that should contain internals which reduce foaming, foaming is discussed in detail in literature [68]. In this study foaming was only critical when reaction was started at high temperatures and the methanol containing catalyst solution was added. This was done in order to obtain an even level of temperature for kinetic studies. This is not necessary at a technical scale, but precaution should be taken in order to control reaction rate by temperature and the nature and amount of catalyst to prevent foaming. Apart from that, catalyst can be added as solid matter or at a lower temperature. Moisture in the starting material should be minimized because this will lead to the formation of soaps. In order to obtain a short reaction time for a reactive column it will be favorable to use reduced pressure or an additional gas stream to remove the methanol. But this will increase the costs for this process. The final products are of the quality level of “mono-diglycerides” with a weight ratio of MO to DI of approx. 1:1. A higher quality level like that of “distilled monoglycerides” can not be reached only by the choice of the reaction conditions. If this quality level is desired, monoglycerides have to be separated by additional downstream processes like molecular distillation.

7 Symbols and Abbreviations

- Latin Symbols

- Greek Symbols

- Abbreviations

- Subscripts and Superscripts

Latin Symbols

a	1/m	interfacial area per unit volume of methyl ester layer in m^2/m^3
$Å$	m	angstroem: 10^{-10} m
c	mol/m³	bulk concentration in the Film model
Δc	mol/m³	effective concentration difference in the Film model
c_i	mol/kg	concentration of component *i* in own experiments, *i* = alc^-, DI, glycerol, ME, methanol, MO
c_i	mol/m³	inner concentration in the Film Model
c_i	mol/m³	concentration of component *i* in literature, *i* = DI, glycerol, ME, methanol, MO, TRI
d	m	impeller diameter
d	m	impeller diameter
d_{32}	m	Sauter mean diameter
$<d>$	m	arithmetic mean diameter
D	m^2/s	diffusion coefficient
$D°_{AB}$	m^2/s	mutual diffusivity at infinite dilution of A in B
E	1	exponent
EA	J/mol	activation energy according to the Arrhenius law
ΔEA	J/mol	activation energy difference
H	Pa	Henry coefficient
ΔH	J/mol	enthalpy of reaction
$\Delta_i H$	J/mol	enthalpy of reaction for reaction step number *i*
$\Delta_S H$	J/mol	enthalpy of solution
k_i	$l^n/(mol^n\ s)$	reaction rate constant used in literature and modeling, for a reaction with number i either forward (→) or backward (←). The unit depends on the order (n-1) of the reaction.
k'_l	m/s	liquid-phase mass transfer coefficient
$k_{ir/f}$	$kg^n/(mol^n\ s)$	reaction rate constant according to the nomenclature of

Latin Symbols

		the simulation software Berkeley Madonna for reaction number *i* either forward k_{if} or backward k_{ir}. The unit depends on the order (*n*-1) of the reaction.
$\boldsymbol{K}$	1	equilibrium constant
$\boldsymbol{K_i}$	1	equilibrium constant for reaction i, for a second order reaction step forward and backward: $K_i \equiv k_{if}/k_{ir}$
$\boldsymbol{K^{\#}_i}$	kg/mol	modified equilibrium constant K_i for Model 3
$\boldsymbol{K^*}$	1	pre-equilibrium constant for alcoholates
$\boldsymbol{kt}$	kg	kiloton = 10^6 kg
$\boldsymbol{\dot{n}}$	mol/s	interphase rate of mass transfer
$\boldsymbol{M_i}$	g/mol	molecular weight of species i
$\boldsymbol{n}$	1	number of data
$\boldsymbol{n}$	1/s	stirring rate
$\boldsymbol{n_i}$	mol	amount of component i
$\boldsymbol{n^d_{20}}$	1	refractive index
$\boldsymbol{N_A}$	mol/(s m²)	interphase mass-transfer rate of solute A per interfacial area
$\boldsymbol{N_{Re}}$	1	Reynolds number for mixing operation in vessels $nd^2\rho/\mu$
$\boldsymbol{N_{Sc}}$	1	Schmidt number $\mu/(D\rho)$
$\boldsymbol{p}$	Pa	pressure
pdf	1	probability density function
$\boldsymbol{P_V}$	J/(s m³)	power dissipated by agitator per unit volume
$\boldsymbol{R}$	1	square of the Pearson correlation coefficients
$\boldsymbol{R}$	J/(mol K)	gas constant = 8.314 J/(mol K)
rpm	1/min	revolutions per minute
RT	s	retention time
$\boldsymbol{S_i}$	1	selectivity towards component *i*
$\boldsymbol{S}$	s	relative separation of peaks in gas chromatography

Latin Symbols

SD	…	mean standard deviation, unit dependent on variate
T	K	temperature
V_i	m³/mol	molar volume of liquid *i* at its normal boiling point
w	1	weight fraction
We	1	Weber number
WP	s	waiting period
x		variate, unit dependent on variate
X	1	conversion
Y	1	yield

Greek Symbols

δ	m	film model: thickness of film
ϑ	°C	temperature
μ		mean, unit dependent on variate
μ	kg/(s m), Pas	viscosity, kg/(s m) = Pas
ν	1	stoichiometric coefficient
ϕ	1	association factor for Wilke-Chang equation
φ	1	volumetric phase fraction of dispersed phase
ρ	kg/m³	density
σ	J/m²	interfacial tension

Abbreviations

DI	diglyceride containing a spectrum of fatty acids obtained from ME or pure diolein
FA	fatty acid
FAME	fatty acid methyl ester
ME	75 % oleic acid methyl ester

Abbreviations

MO	monoglyceride containing a spectrum of fatty acids obtained from ME or pure monoolein
R	alkyl group
TRI	triglyceride

Subscripts

(for missing subscripts see “Abbreviations”)

0	initial value
alc^{-}	alcoholate ion
f	forward
i	species or number
g	glycerol
k	stoichiometrically limiting species
m	methanol
r	backward

Superscripts

(for missing subscripts see “Abbreviations”)

´	kinetic constants: *k´* different from *k*
´	film model: phase I
´´	film model: phase II
*****	equilibrium of alcoholates

8 Appendix

8.1 Chemicals

Chemicals used in this study are listed below. Purity is reported as stated by the supplier in % weight. Own analytical results are given for water content, composition and acid number. Water content was analyzed by Karl-Fischer titration (KF), composition of methyl esters by gas chromatography (GC) was calculated relative to the total area of methyl ester peaks, free acids were titrated with potassium hydroxide (acid number, see appendix 8.2). The acid number was converted into SI units as moles of free acids (FA) per kg of methyl ester.

Fatty Acid Containing Compounds

Abbrev.	Chemical	Purity	Supplier
DI	diolein	>99 %	Sigma-Aldrich
ME	oleic acid methyl ester	75 %	Lancaster
	oleic acid methyl ester	85 % (GC)	
	water	< 0.01 % (KF)	
	acid number	0.2 (=4.2 mmol FA/kg)	
	palmitic acid methyl ester	> 95 %	Henkel
	palmitic acid methyl ester	92 % (GC)	
	water	<0.05 % (KF)	
	acid number	1.4 (=26 mmol FA/kg)	
MO	monoolein	>99 %	Sigma-Aldrich

Solvents and Alcohols

Abbrev.	Chemical	Purity	Supplier
	dioxane	99.5 %	Riedel-de Haen, Roth
	ethanol	99 %	Roth
	glycerol	99.8 %	Fluka
	water	< 0.03 % (KF)	
	hexadecane	98 %	Fluka
MeOH	methanol	99.8 %	Roth
	2-propanol	99 %	Roth
	pyridine	> 99.8 %	Fluka
	triacontane	≥ 99.5 %	Fluka

Salts and Silylating Agents

Abbrev.	Chemical	Purity	Supplier
	cesium acetate	95 %	Fluka
BSTFA	(N.O-Bis(trimethylsilyl)-trifluoroacetamide)	> 97 %	Merck, ABCR
	sodium acetate	98.5 %	Fluka
catalyst	sodium methoxide	30 % in methanol	Fluka
TMCS	trimethylchlorosilane	99 %	Fluka

8.2 Acid Number

The acid number is defined as the amount of potassium hydroxide needed to neutralize the free acids in a sample of 1 kg oil or fat. It is determined by titration with 0.01 N potassium hydroxide in 2-propanol against phenolphthalein. The titration of the fatty acid methyl esters was carried out in analogy to the determination of the acid number in fats and oils. To enhance resolution the common concentration for the determination of the acid number of 0.1 N was reduced by 1/10. A sample of 5 g of methyl ester was dissolved in 50 ml of a 1:1 volume ratio mixture of toluene and 2-propanol. A blank titration of the solvent was carried out and used to correct titration values. KOH content was determined by titration against aqueous HCl. Titration had to be done fast because of the occurrence of saponification. To validate the titration procedure a calibration was carried out. Samples of oleic acid methyl ester containing approx. 0.05 to 0.50 % of palmitic acid were titrated. Calibration is shown in Fig. 2A1.

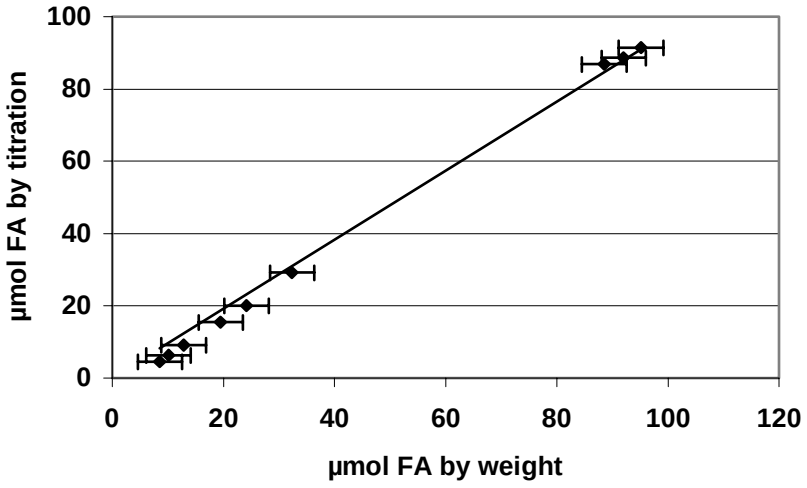

Fig. 2A1: Calibration for the determination of the acid number. FA is the amount of palmitic acid.

8.3 Simulation: Kinetic Modeling of Methanolysis

The methanolysis of soybean oil was modeled according to literature [58]. The set of differential equations is derived from Scheme 5.3-1 with second order reversible reaction steps. The scheme is repeatedly shown below.

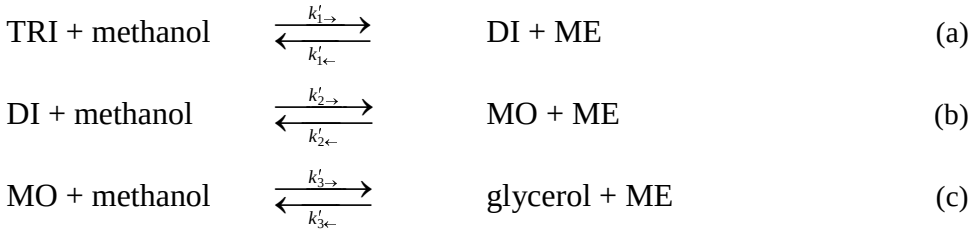

The set of differential equation used to simulate this system was cited in the reference and showed an unusual formulation of step (a). It was given as

$$\frac{dc_{TRI}}{dt} = k'_{1\leftarrow} c_{DI} c_{methanol} - k'_{1\rightarrow} c_{TRI} c_{methanol}$$

The complete set of differential equation is shown below which was introduced into the software Berkeley Madonna.

$$\frac{dc_{TRI}}{dt} = k'_{1\leftarrow} c_{DI} c_{methanol} - k'_{1\rightarrow} c_{TRI} c_{methanol}$$

$$\frac{dc_{DI}}{dt} = k'_{2\leftarrow} c_{MO} c_{ME} - k'_{2\rightarrow} c_{DI} c_{methanol} - k'_{1\leftarrow} c_{DI} c_{ME} + k'_{1\rightarrow} c_{TRI} c_{methanol}$$

$$\frac{dc_{MO}}{dt} = k'_{2\rightarrow} c_{DI} c_{methanol} - k'_{2\leftarrow} c_{MO} c_{ME} + k'_{3\leftarrow} c_{ME} c_{glycerol} - k'_{3\rightarrow} c_{MO} c_{methanol}$$

$$\frac{dc_{ME}}{dt} = k'_{1\rightarrow} c_{TRI} c_{methanol} - k'_{1\leftarrow} c_{DI} c_{ME} + k'_{2\rightarrow} c_{DI} c_{methanol} - k'_{2\leftarrow} c_{MO} c_{ME} + k'_{3\rightarrow} c_{MO} c_{methanol} - k'_{3\leftarrow} c_{ME} c_{glycerol}$$

The results of the simulation were graphically compared to experimental data shown in literature (Fig. 5 in literature) showing agreement.

For the purpose of repeatability of the calculations the complete script in the equation window in the software Berkeley Madonna, version 8.0.1, is given below. The script is more complex

than needed for the modeling of the methanolysis because it was

also used to model different sets of own experimental data. Additionally the setting for the slider is shown as well as the resulting plot that was compared with the plot in literature (not shown).

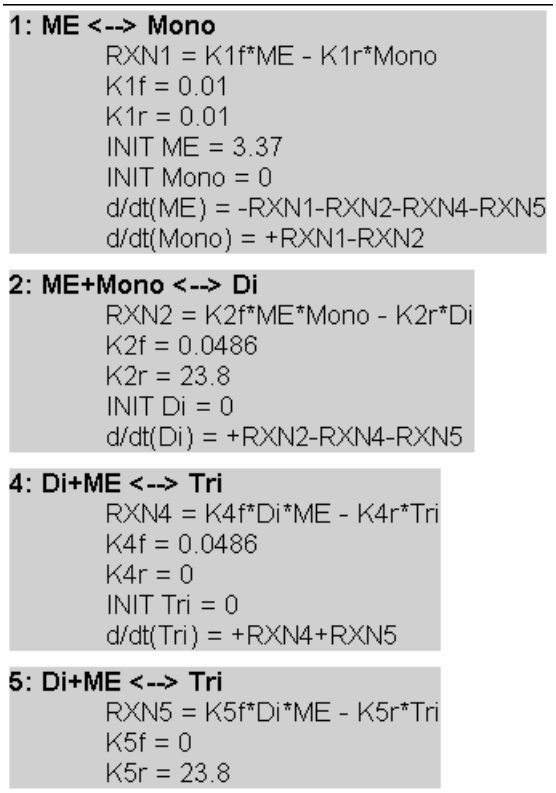

Fig. 3A1: Chemical reaction boxes in Berkeley Madonna.

(Scrip in equation window)

```
Original = 0; Flag, das regelt, ob eigene Daten
            ; bei =0 oder Daten aus der Literatur
            ; =1 simuliert werden
INIT Mono = 0.00000001
INIT DI   = 0.00000001
; initial value for TRI 0.8
; read from graph in literature in Fig. 1
Tri0 = 0.8

INIT TRI = IF (Original=1) THEN Tri0 ELSE 0
INIT ME  = IF (Original=1) THEN 0 ELSE 1000/296.49

Temp0 = IF (Original=1) THEN 50 ELSE 130; °C
Temp  = IF (Original=1) THEN 50 ELSE 130; °C

K5r = 0.050
K5f = 0
K4r = 0
K4f = 0.110
K2r = 0.215
K2f = 1.228
K1r = 0.242
K1f = 0.007

EA5r = 13145 *4.186 ;cal/mol converted to j/mol
EA4f = 9932  *4.186
EA2r = 19860 *4.186
EA2f = 14639 *4.186
EA1r = 6421  *4.186
EA1f = 9588  *4.186

wenig_Kat = 0
Faktor_Druckversuch = 1.38; for this run catalyst
                   ;concentration was higher, modeld
                   ; as linear factor to all k.
Drucklevel = 3    ; 1: 1013, 2: 600, 3: 300 mbar
```

(Scrip in equation window, continued)

```
Druck_[1]=1013     ; not in use
Druck_[2]= 600
Druck_[3]= 300

Druck = IF (Drucklevel <1.5) THEN Druck_[1]
            ELSE IF (Drucklevel <2.5)
            THEN  Druck_[2] ELSE Druck_[3]
T_Kelv   = Temp + 273.15
T0_Kelv  = Temp0 + 273.15
R        = 8.314

; Definitions
ME_0 = 3.37
X    = 1-ME/ME_0
S    = IF ((Mono + DI)<=0) THEN 1
       ELSE (Mono / (Mono + DI))
       ; yield without “IF” a “floating point error”

Gly1     = IF (Temp<135) THEN 0.058 ELSE IF (Temp<145)
           THEN 0.046
           ELSE IF (Temp<155) THEN 0.11 ELSE 0.14

Gly0     = 0.0000886*Temp - 0.00700096
Endumsatz= 0.00566821969234513*Temp-0.113303453810959;
           ; fitted from experimental data
Gly      = IF (Original=1) THEN (Tri0-Mono-DI-TRI)
           ELSE (Gly0
                +(Gly1-Gly0)*X/Endumsatz)*1000/92

MeOH_[3] = IF (Temp<135) THEN 0.00388*1000/32
           ELSE IF (Temp<145) THEN 0.00264*1000/32
           ELSE IF (Temp<155) THEN 0.00255*1000/32
           ELSE 0.00221*1000/32
MeOH_[2] = 0.0083*1000/32
MeOH_[1] = 0.0128*1000/32
```

(Scrip in equation window, continued)

```
MeOH     = IF (Original=1) THEN (6*Tri0-ME)
           ELSE IF (Drucklevel <1.5) THEN MeOH_[1]
           ELSE IF (Drucklevel <2.5) THEN  MeOH_[2]
           ELSE MeOH_[3]

; temperature dependency of reaction rate constants
; as a separate factor Tv

Tv5r=exp(EA5r/R*(T_Kelv-T0_Kelv)/(T_Kelv*T0_Kelv))
Tv4f=exp(EA4f/R*(T_Kelv-T0_Kelv)/(T_Kelv*T0_Kelv))
Tv2r=exp(EA2r/R*(T_Kelv-T0_Kelv)/(T_Kelv*T0_Kelv))
Tv2f=exp(EA2f/R*(T_Kelv-T0_Kelv)/(T_Kelv*T0_Kelv))
Tv1r=exp(EA1r/R*(T_Kelv-T0_Kelv)/(T_Kelv*T0_Kelv))
Tv1f=exp(EA1f/R*(T_Kelv-T0_Kelv)/(T_Kelv*T0_Kelv))

v=1 ; no volume correction


RXN1 = IF (Druck<>1013)
       THEN Tv1f*v*K1f*Gly*ME-Tv1r*v*K1r*Mono*MeOH
       ELSE Faktor_Druckversuch
            *(Tv1f*v*K1f*Gly*ME-Tv1r*v*K1r*Mono*MeOH)
RXN2 = IF  (Druck<>1013)
       THEN Tv2f*v*K2f*ME*Mono-Tv2r*v*K2r*DI*MeOH
       ELSE Faktor_Druckversuch
            *(Tv2f*v*K2f*ME*Mono-Tv2r*v*K2r*DI*MeOH)

;modeling the unusual reaction rate equation
RXN4 = IF (Druck<>1013) THEN Tv4f*v*K4f*DI*MeOH
       ELSE Faktor_Druckversuch*(Tv4f*v*K4f*DI*MeOH)
RXN5 = IF (Druck<>1013) THEN -Tv5r*K5r*TRI*MeOH
       ELSE Faktor_Druckversuch*(-Tv5r*K5r*TRI*MeOH)

Bilanz = ME + Mono + 2*DI+3*TRI
```

```
(Scrip in equation window, continued)

METHOD Auto ; only autostep ("Auto")
            ; or Stiff can be used,
            ; else a “floating point error” occurs,
            ; may be also a problem of settings
            ; in graphic display

LIMIT X    <= 1.1
LIMIT ME   >= -0.1
LIMIT Mono >= 0
LIMIT DI   >= 0

STARTTIME = 0
STOPTIME  = 240
DT        = 0.02
DTOUT     = 0.1

(Scrip in equation window, end)
```

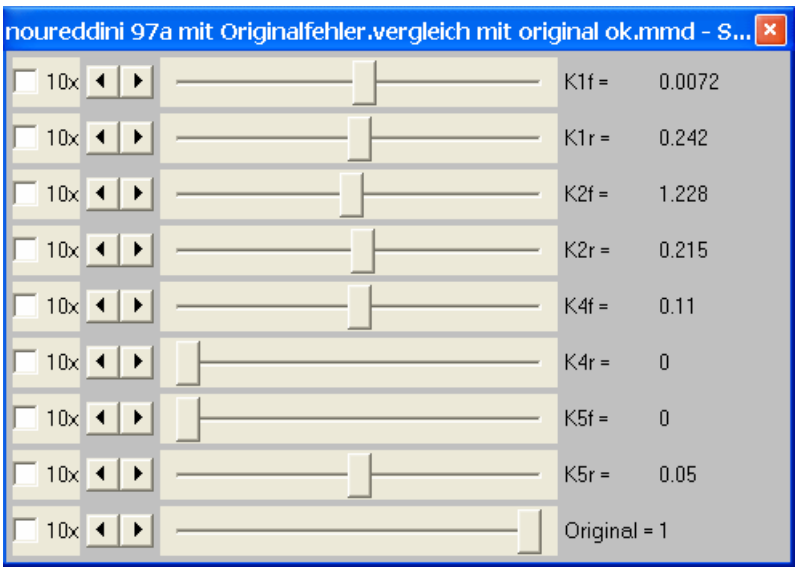

Fig. 3A1: Sliders in Berkeley Madonna

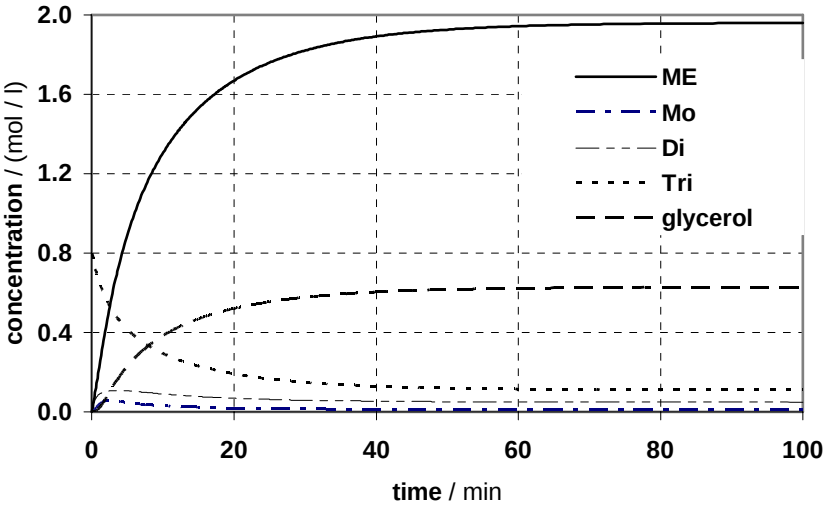

Fig. 3A3: Simulated Methanolysis of Soybean Oil According to Literature [51]. Plot for the Verification of the Correct Implementation of Differential Equations by Comparison with Fig. 5 in Literature [51] (not shown). Concentrations of soybean methyl ester (ME), monoglyceride (MO), diglyceride (DI), triglyceride (TRI) and glycerol in mol/l. The plot of methanol is not shown because it was not given in literature. Run at 50 °C, 0.20 % catalyst sodium hydroxide, initial molar ratio between methanol and soybean oil 6:1.

8.4 Software Control of Image Recording

Images of drops in an emulsion were recorded using a cooled endoscopic lens system attached to a CCD-Camera (JAI CV-M10BX) with a frame grabber card (IMNA PX 610-10) and a separate flash light (Drello 250). The endoscopic lens system was shown in chapter 4.3. Synchronization of all parts was achieved using a software program written in visual basic. A standard image software is usually not able to record drop size because of the special light and contrast situation in an emulsion. A small interval of contrast levels has to be expanded in order to make the drop boundaries visible. This can be done by setting gain and offset. Both have to be adjusted for each reactive environment separately and change with time due to darkening of the solution and drop size decrease.
Drop size is recorded by first opening the electronic shutter and then sending a delayed trigger signal to the flash light. After a few µs the shutter is closed. The imaged is transferred from the camera into the buffer of the frame grabber and finally displayed with help of the visual basic software by reading this buffer.
The program was written with support of the supplier. The basis of this program was a program written in C+ that was part of frame grabber package. The main task was to read the image in non-interlaced mode because only in this mode an undistorted image could be recorded at a short shutter time. Additionally the software was able to record the temperature of the reactor using a serial interface to the thermostat (Haake B5, Controller Haake F6). The part of the software that was used for temperature recording (“Ueberwachung”) is based upon a routine written by Nora Weitbrecht.

The complete source code of the visual basic program for image recording and the structure of the visual basic project is shown below. The program was operating on a 400 MHz Athlon computer with 300 MB RAM, operating system was Windows NT. The visual basic project consists of frames (“Formulare”) for displaying and control and of modules (“Module”) which contain only source code. A routine for displaying a histogram of the viewed image was not in use because the image processing in visual basic was too slow. The library wpx5_NT.dll was provided by the supplier of the frame grabber. The name of the visual basic project is PXZOOMNT_NEU.

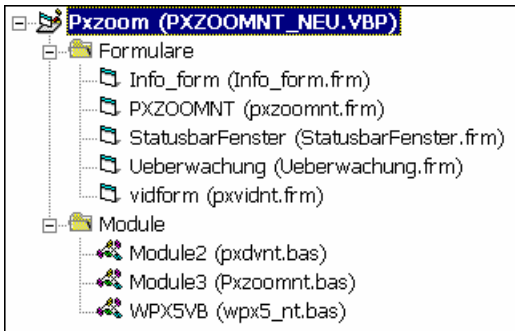

Fig. 4A1: Structure of the Visual Basic project.

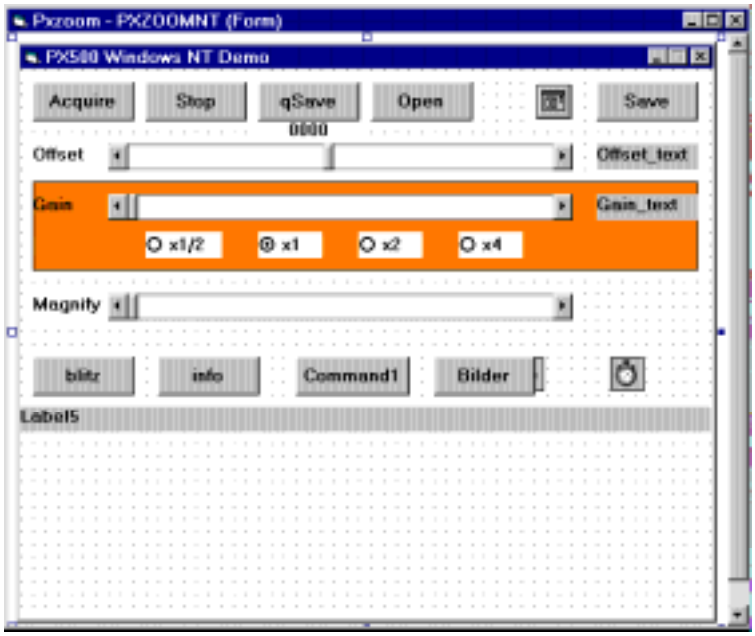
Pxzoom - PXZOOMNT (Form)
PX580 Windows NT Demo
Acquire
Stop
qSave
Open
Save
Offset
Offset_text
Gain
Gain_text
x1/2
x1
x2
x4
Magnify
blitz
info
Command1
Bilder
Label5

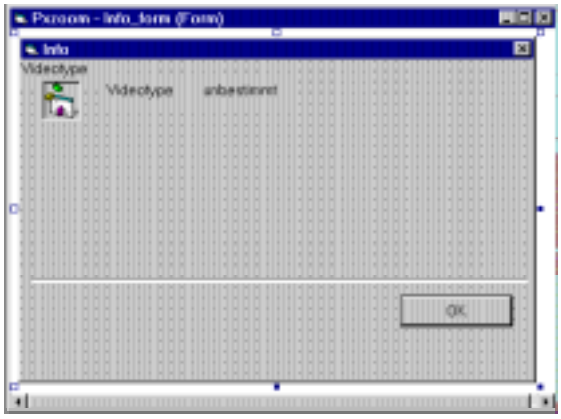
Pxzoom - Info_form (Form)
Info
Videotype
Videotype
unbestimmt
OK

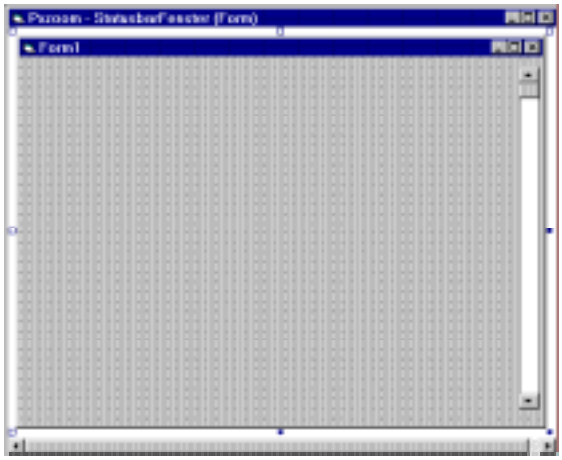
Pxzoom - StatusbarFenster (Form)
Form1


Pxzoom - Ueberwachung (Form)
Ueberwachung
WertName1
Text2
WertEinh
WertName2
Text1
WertEinhe
tempInt
comLesen
protokollBack

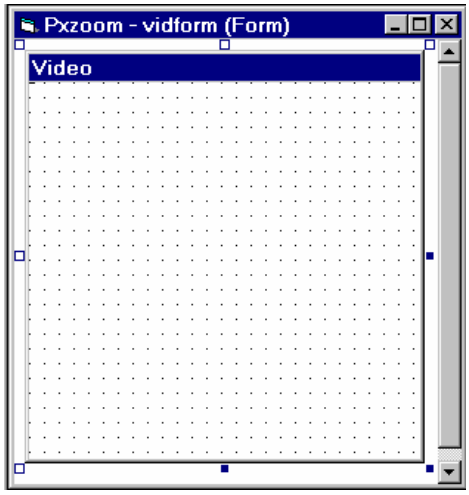
Pxzoom - vidform (Form)
Video

Fig. 4A2: Frames of the Visual Basic project. The name of the frame is displayed in the top left corner of the frame.

When the software is started, temperature recoding begins immediately. Temperatures are backed up in a file called "`c:\protokoll_Ueberwachung.log"`". The image of the camera is displayed as continuous video. For image recording first the button "Stop" has to be selected. Image recording is started using the button "blitz". Usually the conditions for contrast have to be adjusted step by step using the zoom of the camera system and the sliders "offset" and "gain". When an image is obtained that should be preserved, the button "qsave" has to be selected. First the directory for image recording has to be selected. Images are saved in a file called "bildNNNN.bmp". NNNN is a number beginning with 0000 which is increased by one each time the button is pressed. A direct image recording and saving is not possible because usually only 1 of 3 pictures is useful. The button "save" will ask each time for a name of the picture. The buttons "acquire", "open", "command1", "info" and "bilder" were not used.

The visual basic source code for the five frames and two of modules is given below with their filenames (bold). The third module WPX5VB.bas is not listed because it was part of the frame grabber software. Two components have to be included into the visual basic environment: Microsoft Comm Control 6.0 and Microsoft Common Dialog Control 6.0 (SP3).

```
'Microsoft Visual Basic
'Version 8176
```

Info_form.frm (Code)

```
Private Sub cmdOK_Click()
  Unload Info_form
End Sub

Private Sub Form_Load()
Debug.Print "Sub Form_Load aufgerufen"
End Sub

Private Sub lblTitle_Click()
End Sub

Private Sub Label2_Click()
End Sub
```

PXZOOMNT (Code)

```
'Form wird nicht mehr sauber entladen!!!
'd.h. das ganze Projekt muss zum
'Neustart geschlossen werden.

Dim t1 As Long
Dim gainRangeParameter As Integer
Dim fineGain As Integer
Dim BildNummer As String
Dim BildNummerInt As String
Dim BildPfad As String

'Dim Status As String

'Dim x, y As Integer

Private Sub BlitzEinstellungen()

rueckgabe0 = SetStrobeType(fgh, STROBE_NORMAL)

'Zeit ist ein Vielfaches von 64 (CCIR) bzw 63.5
'Mikrosekunden
Strobewert_Einheit = 0.000064

Strobezeit_Kamera = 0.0015  'Sekunden
Strobewert_Pause  = 0.0015  'Sekunden
Strobezeit_Blitz  = 0.0015  'Sekunden

Strobewert_Kamera = Strobezeit_Kamera / Strobewert_Einheit
Strobewert_Pause  = Strobezeit_Pause / Strobewert_Einheit
Strobewert_Blitz  = Strobezeit_Blitz / Strobewert_Einheit

Debug.Print Strobewert '20 war für Blitz ok

rueckgabe2 = SetStrobePeriods(fgh
             , Strobewert_Kamera, Strobewert_Pause, Strobewert_Blitz)
End Sub

Private Sub Bilder_Click()
If (Bilder <> Null) Then
    If (Bilder.Visible = True) Then Bilder.Visible = False
Else: Bilder.Show
End If
```

```
End Sub

Private Sub blitz_Click()
BlitzEinstellungen
’ganze Strobesequenz feuern: STROBE_0
rueckgabe1 = FireStrobe(fgh, STROBE_0)

’Bild auslesen und anzeigen
tmp = Grab(fgh, frh, SINGLE_FLD)
    If (tmp = 0) Then
        Debug.Print "Grab failed"
    End If
    Call displayit

’Debug-info
Debug.Print fgh
Debug.Print STROBE_0

If CheckError(fgh) = ERR_NONE Then
        Debug.Print "kein Fehler"
        Else:   Debug.Print "Fehler"
        End If

        If ((rueckgabe0 <> 0) And (rueckgabe1 <> 0)) Then
                Debug.Print "Strobe_0 jefeuert"
        Else:   Debug.Print "Strobe_0 kaputt"
        End If

'Zählt die AutoBilder automatisch hoch
counter_Timer3 = counter_Timer3 + 1
If (counter_Timer3 > AutoBilderMax) Then counter_Timer3 = 1
End Sub

Private Sub Command1_Click()
    counter_Timer3 = 0
    AutoBilderMax = 5
    AutoBildIntervall = 400
    PXZOOMNT.Timer3.Interval = AutoBildIntervall
    t3 = Timer
End Sub

Private Sub Command2_Click()
End Sub
```

```
Private Sub Form_Load()
'Module3.StatusAlt = Array(Module3.StatusZaehlerMax)
Module3.StatusZaehler = 0

  TimerStatusbar.Interval = 200
  Module3.Status = "Form wird geladen"

  BildNummerInt = -1

  Dim vblank As Integer
  Dim ImageMaxX As Integer
  Dim ImageMaxY As Integer

  'CCIR style noninterlace
  ImageMaxX = 768
  ImageMaxY = 576
  vblank = 39

  'NTSC style noninterlace
  'ImageMaxX = 640
  'ImageMaxY = 486
  'vblank = 49

  Module3.Status = "Frame grabber wird initalisiert"
    If (InitLibrary() = 0) Then
        Debug.Print "init fail"
        End
    End If

    fgh = AllocateFG(-1)
    If (fgh = 0) Then
        ExitLibrary
        Debug.Print "frame grabber fail"
        End
    End If

    frh = AllocateBuffer(ImageMaxX, ImageMaxY, 8)
    If (frh = 0) Then
        FreeFG (fgh)
        ExitLibrary
        Debug.Print "buffer fail"
        End
    End If
```

```
    'tmp = SetImageSize(fgh, 640, 256, 0, 4, 640, 480, 8)
    tmp = SetVideoFormat(fgh, 2000, vblank, USER_SYNC)
    tmp = SetFieldSize(fgh, ImageMaxX, 256, 0, 0, ImageMaxX, ImageMaxY, 8)
    If (tmp = 0) Then Debug.Print "SetImageSize failed"
    End If

    'Bilder.Show
    Module3.Main

    Module3.Status = "Vieofenster wird geöffnet"
    vidform.Show
    Module3.Status = "Prozessüberwachungsfenster wird geöffnet"
    Ueberwachung.Show
    Module3.Status = "Form laden beendet."
End Sub

Private Sub Form_Unload(Cancel As Integer)
    vidform.Timer1.Interval = 0
    Unload vidform
    Unload Bilder

    FreeFrame (frh)
    FreeFG (fgh)
    ExitLibrary
End Sub

Private Sub grange_Click(Index As Integer)
    gainRangeParameter = Index
    GainAendern
    tmp = SetGainRange(fgh, gainRangeParameter, 0)
End Sub
Private Sub GainAendern()
    totalGain = 256 / (512 - fineGain) * 2 ^ (gainRangeParameter)
    totalGain = CInt(totalGain * 100) / 100
    Gain_text.Caption = totalGain
End Sub

Private Sub gslide_Change()
    fineGain = gslide.Value
    tmp = SetFineGain(fgh, fineGain, 0)
    GainAendern
End Sub

Private Sub HScroll1_Change()
```

```
    Call displayit
End Sub

Private Sub info_Click()
    Rueckgabewert = Videotype(fgh)
    Select Case Rueckgabewert
        Case 0
            Videotyp = "No Video"
        Case 1
            Videotyp = "NTSC Video"
        Case 2
            Videotyp = "CCIR/PAL Video"
        Case 3
            Videotyp = "Unknown Video"
    End Select
    Videotype_text = Videotyp
    Load Info_form
    Info_form.Show

End Sub

Private Sub offslide_Change()
    tmp = SetOffset(fgh, offslide.Value, 0)
    Offset_text.Caption = offslide.Value
End Sub

Private Sub Open_Click()
    stop_click
    CMDialog1.FileName = ""
    CMDialog1.Action = 1
    If (CMDialog1.FileName <> "") Then
        Screen.MousePointer = 11
        If ReadBMP(frh, CMDialog1.FileName) Then
            Screen.MousePointer = 0
            MsgBox "Could Not Read File", 48, "PX500 Demo"
        End If
        Screen.MousePointer = 0
    End If
    vidform.Refresh
End Sub

Private Sub play_Click()
    vidform.Timer1.Interval = 10
    counter = 0
```

```
    t1 = Timer
End Sub

Private Sub qSave_Click()

    stop_click

    If (BildNummerInt <> -1) Then
        FileName = "bild" & BildNummer & ".bmp"
        FileName = BildPfad & FileName
        If WriteBMP(frh, FileName, 1) Then
           MsgBox "Could Not Write File", 48, "PX500 Demo"
        Else:
            Module3.Status = FileName & "wurde gespeichert"

            Call BildNummerHochzaehlen
            Label4.Caption = BildNummer

        End If
    Else:
            Call BildNummerHochzaehlen

            FileName = "bild" & BildNummer & ".bmp"
            CMDialog1.FileName = FileName
            CMDialog1.Action = 2

            If (CMDialog1.FileName <> "") Then
                Screen.MousePointer = 11
                If WriteBMP(frh, CMDialog1.FileName, 1) Then
                    Screen.MousePointer = 0
                    MsgBox "Could Not Write File", 48, "PX500 Demo"
                    BildNummerInt = -1
                End If
                Screen.MousePointer = 0

                i = 0
                Beenden = False
                gefunden = False
                While ((gefunden <> True) And (Beenden <> True))
                    i = i + 1
                    If (Mid$(CMDialog1.FileName, i, 4) = "bild")
                       Then gefunden = True
                    If ((i + 4) > Len(CMDialog1.FileName))
                       Then Beenden = True
```

```
                Wend

                If (gefunden = True) Then
                    BildPfad = Left$(CMDialog1.FileName, i - 1)
                    MsgBox ("BildPfad: " & BildPfad)
                Else: MsgBox ("Pfad für Bilder unbestimmt")
                End If
            End If
    End If
End Sub

Private Sub BildNummerHochzaehlen()

    BildNummerInt = BildNummerInt + 1
    BildNummer = CStr(BildNummerInt)

    While Len(BildNummer) < 4
        BildNummer = "0" + BildNummer
    Wend

End Sub
Private Sub save_Click()
    stop_click
    CMDialog1.FileName = "bild.bmp"
    CMDialog1.Action = 2
    If (CMDialog1.FileName <> "") Then
        Screen.MousePointer = 11
        If WriteBMP(frh, CMDialog1.FileName, 1) Then
            Screen.MousePointer = 0
            MsgBox "Could Not Write File", 48, "PX500 Demo"
        End If
        Screen.MousePointer = 0
    End If
End Sub

Private Sub Statusbar_Click()
Load StatusbarFenster
End Sub

Private Sub stop_click()
    vidform.Timer1.Interval = 0
    PXZOOMNT.Timer3.Interval = 0
End Sub
```

```
Private Sub TimerStatusbar_Timer()
If (Statusbar.Caption = Module3.Status) Then

    If (toggleStatus = True) Then
        toggleStatus = False
        Zusatzzeichen = "."
    Else:
        toggleStatus = True
        Zusatzzeichen = ".."
    End If
End If

If (Module3.Status <> "")
   Then Statusbar.Caption = Module3.Status & Zusatzzeichen

'alte Meldungen speichern
Module3.StatusZaehler = Module3.StatusZaehler + 1
If (Module3.StatusZaehler >= Module3.StatusZaehlerMax) Then
Module3.StatusZaehler = 0
Module3.StatusAlt(Module3.StatusZaehler) = Module3.Status
Module3.Status = ""
```

Info_form (Code)

```
End Sub

Private Sub Timer3_Timer()
    blitz_Click

    FileName = "AutoBild" + CStr(counter_Timer3) + ".bmp"
    If WriteBMP(frh, FileName, 1) Then
       MsgBox "Could Not Write File", 48, "PX500 Demo"
    End If
    If (FlagBilderbogen = True) Then
        Bilder.Image1(i) = LoadPicture(FileName)
        Bilder.BildNr1(i).Caption = counter_Timer3
    End If
End Sub
```

Ueberwachung.frm (Code)

```
'MSComm1.InputLen = 1
Dim initcom1 As Boolean
Dim TempAbfrageExtern As Boolean
```

```
Dim TempAbfrageIntern As Boolean
Dim TempExtern As String
Dim TempIntern As String
’Dim toggleTemp As Boolean
Dim toggleTimer1 As Boolean
Dim toggleTemp2a As Boolean
Dim toggleTemp2b As Boolean
’Dim NachInternExtern As Boolean
Dim StatusAlt As String
Dim ProtokollkanalOffen  As Boolean
Dim Protokolldatei As String
Dim ProtokolldateiBackup As String
Dim ProtokollNummerInt As Integer
Dim ProtokollNummer  As String
Dim TimerZaehler As Integer
Dim antwort As String
Const debugComm As Boolean = False

Private Sub Data1_Validate(Action As Integer, save As Integer)

End Sub
Private Sub ComportInit()
Ueberwachung.MSComm1.CommPort = 1
Ueberwachung.MSComm1.Settings = "4800,N,8,1"
Ueberwachung.MSComm1.PortOpen = True
Ueberwachung.MSComm1.RThreshold = 14 'für temp ok
Ueberwachung.MSComm1.InputLen = 1
initcom1 = True

End Sub

Private Sub Ueberwachung_Unload()
   Ueberwachung.MSComm1.PortOpen = False
   End
End Sub

Public Sub ComPortAuslesen()
    TimeBegin = Timer
    TimeMax = Timer + 10
    Fertig = False
    Schleifen = 0
    SchleifenMax = 20
    LaengeTemp = 8
    instring = ""
```

```
Schleifen = Schleifen + 1
instring = Ueberwachung.MSComm1.Input

 If (instring <> "") Then

     If (Asc(instring) <> 10) Then
            antwort = antwort & instring

            If (debugComm = True) Then Out (instring)

     ElseIf (TempAbfrageIntern = True) Then
     If (debugComm = True) Then Out ("<-")

                  'MsgBox ("Len(antwort) = " & Len(antwort))
                  TempIntern = Left$(antwort, LaengeTemp)

                          If (toggleTemp2a = True) Then
                                toggleTemp2a = False
                                Zusatzzeichen = "<"
                          Else:
                                toggleTemp2a = True
                                Zusatzzeichen = ">"
                          End If

                       Ueberwachung.Wert1 = TempIntern & Zusatzzeichen
                       TempAbfrageIntern = False
                       If (debugComm = True)
                           Then Out ("anwort: " & antwort)
                       antwort = ""
                       Fertig = True

     ElseIf (TempAbfrageExtern = True) Then
     If (debugComm = True) Then Out ("<-")

                     TempExtern = Left$(antwort, LaengeTemp)

                       If (toggleTemp2b = True) Then
                               toggleTemp2b = False
                               Zusatzzeichen = "<"
                       Else:
                               toggleTemp2b = True
                               Zusatzzeichen = ">"
                       End If
```

```
                            TempAbfrageExtern = False
                            Ueberwachung.Wert2 = TempExtern & Zusatzzeichen
                            If (debugComm = True)
                               Then Out ("anwort: " & antwort)
                            antwort = ""
                            Fertig = True
                            'MsgBox ("extern")

        Else: Module3.Status = ("Fehler: unaufgeforderte
                                 Rückmeldung vom Gerät")
        End If

    Else: Module3.Status = ("Fehler: leerer Rückmeldungsteil")
    End If
'Wend

'Fehlerauswertung
If (Fertig <> True) Then
    Module3.Status = ("Schleifenabbruch bei onComm durch ")
    If (Time >= TimeMax)
        Then Module3.Status = Module3.Status & "Zeitüberlauf"
    If (Schleifen >= SchleifenMax)
        Then Module3.Status = Module3.Status & "zu viele Schleifen"
End If

End Sub
Private Sub TemperaturAnfrageIntern()
'intern
Ueberwachung.MSComm1.Output = "F1" & Chr$(13)
TempAbfrageIntern = True
If (debugComm = True) Then Out ("intern")
End Sub
Private Sub TemperaturAnfrageExtern()
'extern
Ueberwachung.MSComm1.Output = "F2" & Chr$(13)
TempAbfrageExtern = True
If (debugComm = True) Then Out ("extern")
End Sub
Private Sub Command1_Click()
Call TemperaturAnfrageIntern
End Sub

Private Sub Command2_Click()
```

```
Call ComPortAuslesen
End Sub

Private Sub Command3_Click()
Call Protokoll
Call ProtokollBackup
End Sub

Private Sub MSComm1_OnComm()
Call ComPortAuslesen
End Sub

Private Sub Timer1_Timer()

TimerZaehler = TimerZaehler + 1

If (TimerZaehler > 5) Then
    Call ProtokollBackup
    TimerZaehler = 0
End If

Call Protokoll

If (toggleTimer1 = True) Then
    toggleTimer1 = False
    Call TemperaturAnfrageIntern
Else:
    toggleTimer1 = True
    Call TemperaturAnfrageExtern
End If

End Sub
Private Sub Form_Load()
'NachInternExtern = False

Protokolldatei = "c:\protokoll_Ueberwachung.log"
ProtokolldateiBackup = "c:\protokoll_Ueberwachung_log.bak"
ProtokollkanalOffen = False
toggleTemp2a = True
toggleTemp2b = True

TempIntern = "falsch"
TempExtern = "falsch"
```

```
’ initalisierung des commPortes
initcom1 = False
Call ComportInit
If initcom1 = False Then MsgBox ("Fehler bei Comport Initalisierung!")

Timer1.Interval = 5000

’ Initaliserung der Formularfelder
Ueberwachung.WertName1.Caption = "T (intern)"
Ueberwachung.WertName2.Caption = "T (extern)"
Ueberwachung.WertEinheit1.Caption = "°C"
Ueberwachung.WertEinheit2.Caption = "°C"
End Sub
Private Sub Protokoll()
If (ProtokollkanalOffen = False) Then Call ProtokollInit
Print #2, Date, Time, TempIntern, TempExtern
End Sub
Private Sub ProtokollInit()
If (Dir(Protokolldatei) <> "") Then
        DateiWarSchonDa = True
Else:   DateiWarSchonDa = False
End If

Open Protokolldatei For Append As #2

ProtokollkanalOffen = True

'erste Zeile der Protokolldatei
If (DateiWarSchonDa = False) Then
    Print #2, "Date", "Time", "TempIntern", "TempExtern"
End If

End Sub
Private Sub ProtokollBeenden()
Close #2
ProtokollkanalOffen = False
End Sub

Private Sub ProtokollBackup()
'erstellt Backups der Kontrolldatei, erstellt
'jedoch auch neue Protokolldateien, falls
'diese zu gross (siehe ProtokollMax) geworden sind

ProtokollMax = 100000 ' maximale Länge in Bytes
```

```
Call ProtokollBeenden

’Backup
FileCopy Protokolldatei, ProtokolldateiBackup

’Test, ob Datei zu gross
If (FileLen(Protokolldatei) > ProtokollMax) Then

    ProtokollNummerInt = -1
    ProtokollNummerHochzaehlen

    Ueberlauf = False

    While ((Dir(Left$(Protokolldatei, Len(Protokolldatei) - 4)
           & ProtokollNummer & Right$(Protokolldatei, 4)) <> "")
           And (Ueberlauf = False))
        Call ProtokollNummerHochzaehlen
        If (ProtokollNummerInt > 99) Then Ueberlauf = True
    Wend

    If (Ueberlauf = True) Then
            MsgBox ("Überlauf bei der Anzahl der Protokolldateien!")
    Else    'dann umbenennen der alten Datei
            Name Protokolldatei As
                 Left$(Protokolldatei, Len(Protokolldatei) - 4)
                 & ProtokollNummer & Right$(Protokolldatei, 4)
            'und neue Datei beginnen
    End If

End If

Call ProtokollInit

End Sub
Private Sub ProtokollNummerHochzaehlen()

    ProtokollNummerInt = ProtokollNummerInt + 1
    ProtokollNummer = CStr(ProtokollNummerInt)

    While Len(ProtokollNummer) < 4
        ProtokollNummer = "0" + ProtokollNummer
    Wend
```

```
End Sub
Private Sub Out(Text)
Debug.Print (Text)
End Sub
```

vidform pxvidnt.frm (Code)

```
Private Sub Form_Load()
    Dim x As Integer
    Dim y As Integer

    'There are two ways of making the image the same size
    'as the window: fixing the image size and setting
    'the window size to match, or vice versa.  The two
    'methods are listed below, with one commented out.

    '**Fixed Image Size**
    'The screen resolution set by the user can change
    'the size of the form in pixels, so this size must
    'be calculated at run time to avoid making the image
    'the wrong size.

    'x = vidform.ScaleWidth - vscroll1.Width
    'y = vidform.ScaleHeight - hscroll1.Height
    'Call cxSetWindowSize(0, 0, x, y)

    '**Fixed Window Size**
    'This requires moving the scrollbars.

    vidform.ScaleMode = 3
    VScroll1.Top = 0
    VScroll1.Left = 640
    VScroll1.Height = 512
    HScroll1.Top = 512
    HScroll1.Left = 0
    HScroll1.Width = 640
    Call pxSetWindowSize(0, 0, 640, 512)
    'We calculate the new window size in twips because
    'screen coordinates are in twips.
    vidform.ScaleMode = 1
    x = VScroll1.Left + VScroll1.Width
    y = HScroll1.Top + HScroll1.Height
    'account for the window border size
    x = x + (vidform.Width - vidform.ScaleWidth)
```

```
    y = y + (vidform.Height - vidform.ScaleHeight)
    vidform.Width = x
    vidform.Height = y

    vidform.Timer1.Interval = 10
End Sub

Private Sub Form_Paint()
    Call displayit
End Sub

Private Sub HScroll1_Change()
    Call displayit

End Sub

Private Sub Timer1_Timer()
    counter = counter + 1
    tmp = Grab(fgh, frh, SINGLE_FLD)
    If (tmp = 0) Then
        Debug.Print "Grab failed"
    End If
    Call displayit
End Sub

Private Sub VScroll1_Change()
    Call displayit
End Sub
```

Pxzoom - Module2 (Code)
pxdvnt.bas

```
'Declarations for the PXDVNT.DLL library.

Declare Sub pxPaintDisplay Lib "pxdvnt.dll" (ByVal hDC As Long, ByVal frm
As Long, ByVal x As Long, ByVal y As Long, ByVal dx As Long, ByVal dy As
Long)
Declare Sub pxSetWindowSize Lib "pxdvnt.dll" (ByVal x As Long, ByVal y As
Long, ByVal dx As Long, ByVal dy As Long)
```

Pxzoom - Module3 (Code)
Pxzoomnt.bas

```
Global fgh As Long
```

```
Global frh As Long
Global counter As Long
Global x, y As Integer

Global Status
Global StatusAlt(100) As String
Global StatusZaehler As Integer
Global Const StatusZaehlerMax As Integer = 100


'für AutoBild
Global FlagBilderbogen As Boolean
Global counter_Timer3 As Integer
Global AutoBilderMax As Integer
Global AutoBildIntervall As Integer
Global FileName As String
Global FileNr As String
Global FilePath As String

'für Histogramm
Global H(1000, 2) As Long
Global HistogrammInit As Boolean


Sub Main()
'StatusAlt = Array(StatusZaehlerMax)

Debug.Print ("Module3 gestartet")
FlagBilderbogen = False
HistogrammInit = False

x = 768
y = 577

End Sub

Sub displayit()
    Dim x As Integer, y As Integer
    Dim dx As Integer, dy As Integer
    dx = (640& * PXZOOMNT.HScroll1.Value) / 100&
    dy = (486& * PXZOOMNT.HScroll1.Value) / 100&
    x = (640& - dx) * vidform.HScroll1.Value / 100&
    y = (486& - dy) * vidform.VScroll1.Value / 100&
```

```
    Call pxPaintDisplay(vidform.hDC, frh, x, y, dx, dy)

End Sub
```

8.5 Impeller Design

The design is based on literature [69]. The impeller was manufactured in the workshop of the institute. Connections are soldered. Two different sizes were manufactured; the one that was most frequently used is referred to as “normal”, the other one as “broad”. They differ in the ratio between the inner reactor diameter D_T and the diameter of the impeller D_l.

	D_l/D_T
Normal	0.33
Broad	0.50

Design of a six blade disc stirrer

normal: $D_I/D_T = 0.33$

Reactor (Tank)

inner diameter	$\mathbf{D_T}$	100.0	mm
fill height	H_L	100.0	mm

Impeller

flat six blade turbine stirrer

total diameter	$\mathbf{D_I}$	33.3	mm

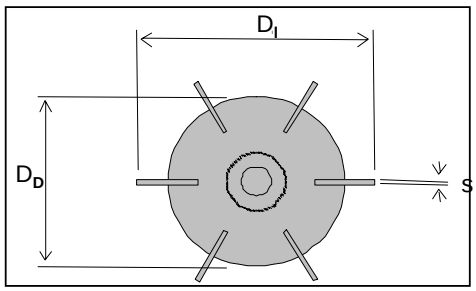

Single blades

height	$\mathbf{W_I}$	6.7	mm
length	$\mathbf{L_I}$	8.3	mm
thickness	**s**	0.7	mm

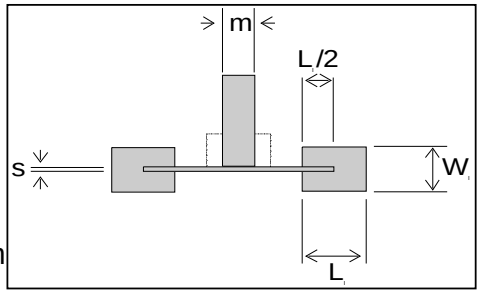

Turbine

disc diameter	$\mathbf{D_D}$	33.3	mm
shaft diameter	**m**	4.3	mm

Baffles

width	$\mathbf{W_B}$	10.0	mm

Design of a six blade disc stirrer

broad: $D_I/D_T = 0.50$

Reactor (Tank)

inner diameter	$\mathbf{D_T}$	100.0	mm
fill height	H_L	100.0	mm

Impeller

flat six blade turbine stirrer

total diameter	$\mathbf{D_I}$	50.0	mm

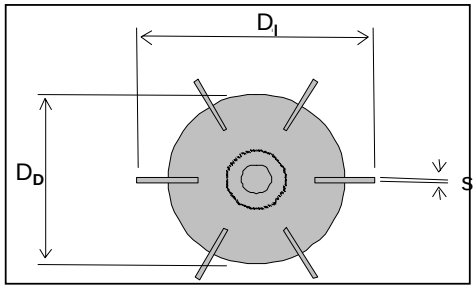

Single blades

height	$\mathbf{W_I}$	10.0	mm
length	$\mathbf{L_I}$	12.5	mm
thickness	**s**	0.7	mm

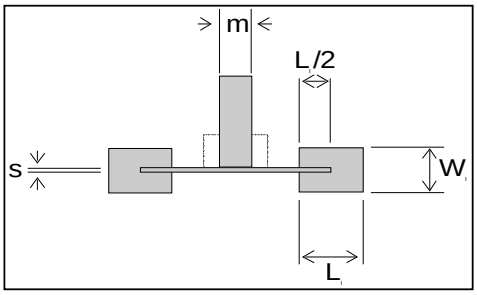

Turbine

disc diameter	$\mathbf{D_D}$	50.0	mm
shaft diameter	**m**	4.3	mm

Baffles

width	$\mathbf{W_B}$	10.0	mm

9 Literature

This is a collection of all articles cited in this work. Some articles are cited repeatedly because each chapter has a separate bibliography.

1 Onken, U., Behr, A., *Chemische Prozesskunde – Lehrbuch der Technischen Chemie*, Band 3, p. 277, G. Thieme-Verlag, New York: 1996

2 Fangrui, M. A., Milford, A., Hanna, A., Biodiesel Production: a Review, *Biosource Technology* 70, 1–15, (1999)

3 Ondruschka, D., Dittmar, T., Dimmig., T., et al., Herstellung von Fettsäuremethylestern aus Rapsöl und Altfetten im kontinuierlichen Betrieb, *Chem. Ing. Tech.* 75, 595-601 (2003)

4 Jeong, G.-T., Park, D.-H., Kang, C.-H, et al., Production of Biodiesel Fuel by Transesterification of Rapeseed Oil, *Appl. Biochem. Biotechnol.* 113–116, 747–758, (2004)

5 Freedman, B., Butterfield, R. O., Pryde, E. H., Transesterification Kinetics of Soybean Oil, *J. Am. Oil Chem. Soc.* 63, 1375–1380 (1986)

6 Noureddini, H., Zhu, D., Kinetics of Transesterification of Soybean Oil, *J. Am. Oil Chem. Soc.* 74, 1457–1463 (1997)

7 Karmee, S. K., Mahesh, P., Ravi, R., Chadha, A., Kinetic Study of the Base-Catalyzed Transesterification of Monoglycerides from Pongamia Oil, *J. Am. Oil Chem. Soc.* 81, 425–430 (2004)

8 Boyle, Elizabeth, Monoglycerides in Food Systems: Current and Future Uses, *Food Technology* 51, 52–59 (1997)

9 Sonntag, Norman O. V., Glycerolysis of Fats and Methyl Esters – Status, Review and Critique, *J. Am. Oil Chem. Soc.* 59 (1982), 795A–802A

10 Noureddini, H., Medikonduru, V., Glycerolysis of Fats and Methyl Esters, *J. Am. Oil Chem. Soc.* 74, 419–425 (1997)

11 Noureddini, H., Harkey, D. W., Gutsman, M. R., A Continuous Process for the Glycerolysis of Soybean Oil, *J. Am. Oil Chem. Soc.* 81, 203–207 (2004)

12 Bornscheuer, U., Lipase-Catalysed Synthesis of Monoglycerides, *Fat Science Technology* 97, 241–249 (1995)

13 Gunstone, F. D., Enzymes as Biocatalysts in the Modification of Natural Lipids, *J. Sci. Food Agric*. 79, 1535–1549 (1999)

14 Stokes, Robert J., Evans, D. Fennell, *Fundamentals of Interfacial Engineering*, Wiley-VCH, New York: 1997

15 Dahlstrom, Donald A., et al., "Phase Contacting and Liquid-Solid Processing" in *Perry's Chemical Engineers' Handbook*, Perry, R. H., (ed.), 7 ed., section 18–21, McGraw-Hill, New York: 1997

16 Hewitt, G. F., "Measurement of Drop and Bubble Size" in *Handbook of Multiphase Systems*, Hetsroni, Gad (ed.), section 10.2.2.6, McGraw-Hill, New York: 1982

17 Azzopardi, B. J., Measurement of Drop Sizes, *International Journal of Heat and Mass Transfer* 22, 1245–1279 (1979)

18 Hastings, N. A. J., Peacock, J. B., *Statistical Distributions. A Handbook for Students and Practitioners*, Butterworth & Co, London: 1975

19 Cooper, B. E., *Statistic for Experimentalists*, Pergamon Press, London: 1969

20 Knudsen, James G., Wankat, Phillip C., Knaebel, Kent S., "Heat and Mass Transfer" in *Perry's Chemical Engineers' Handbook*, Perry, R. H., (ed.), 7 ed., section 5–51, McGraw-Hill, New York: 1997

21 Daubert, T. E., Danner, R. P., *Physical and Thermodynamic Properties of Pure Chemicals*, Hemisphere Publishing Corp., New York: 1989

22 Knudsen, James G., Wankat, Phillip C., Knaebel, Kent S., "Heat and Mass Transfer" in *Perry's Chemical Engineers' Handbook*, Perry, R. H., (ed.), 7 ed., section 5–70, McGraw-Hill, New York: 1997

23 Bates, R. L., Fondy, P. L., Corpstein, R. R, An Examination of some Geometric Parameters of Impeller Power, *Ind. Eng. Chem. Process Design Develop.* 2, 310 (1963)

24 Pereira, W., Close, V., Patton W., et al., Transesterification with an Anion-Exchange Resign, *J. Org. Chem.* 34, 2032–2034 (1969)

25 Hatch, G. B., Adkins, H., Replacement Series of Alkyl Groups Determined by Alcoholysis of Esters, *J. Am. Chem. Soc.* 59, 1694 (1937)

26 Schuchardt, U., Sercheli, R., Vargas, R. M., Transesterification of Vegetable Oils: a Review, *Journal of the Brazilian Chemical Society* 9, 199–210 (1998)

27 Sonntag, Norman O. V., Glycerolysis of Fats and Methyl Esters – Status, Review and Critique, *J. Am. Oil Chem. Soc.* 59, 795A–802A (1982)

28 Knothe, G, Analytical Methods Used in the Production and Fuel Quality Assessment of Biodiesel, *T. ASAE* 44, 193–200 (2001)

29 Darnoko, D., Cheryan, M., Perkins, E., Analysis of Vegetable Oil Transesterification Products by Gel Permeation Chromatography, *J. Liq. Chromatogr. R. T.* 23, 2327–2335 (2000)

30 Freedman, B., Pryde, E. H., Mounts, T. L., Variables Affecting the Yields of Fatty Esters from Transesterified Vegetable Oils, *J. Am. Oil Chem. Soc.* 61, 1638–1643 (1984)

31 Plank, C., Lorbeer, E., Quality Control of Vegetable Oil Methyl Esters Used as Diesel Fuel Substitutes: Quantitative Determination of Mono-, Di- and Triglycerides by Capillary GC, *J. High Res. Chrom.* 15, 609–612 (1992)

32 Sonntag, Norman O. V., Glycerolysis of Fats and Methyl Esters – Status, Review and Critique, *J. Am. Oil Chem. Soc.* 59, 10, 795A–802A (1982)

33 Mittelbach, M., Roth, G., Bergmann, A., Simultaneous Gas Chromatographic Determination of Methanol and Free Glycerol in Biodiesel, *Chromatographia* 42, 7–8, 431–434 (1996)

34 Mittelbach, M., Roth, G., Bergmann, A., Simultaneous Gas Chromatographic Determination of Methanol and Free Glycerol in Biodiesel, *Chromatographia* 42, 7–8, 431–434 (1996)

35 Danielson, N. D., Gallagher, P. A., Bao, J. J., “Chemical Reagents and Derivatization Procedures in Drug analysis” in *Encyclopedia of Analytical Chemistry*, Meyers, R. A., (ed.), 7042–7076, John Wiley & Sons Ltd., Chichester: 2000

36 Sonntag, Norman O. V., Glycerolysis of Fats and Methyl Esters - Status, Review and Critique, *J. Am. Oil Chem. Soc.* 59, 795A–802A (1982)

37 Plank, C., Lorbeer, E., Quality Control of Vegetable Oil Methyl Esters used as Diesel Fuel substitutes: Quantitative Determination of Mono-, Di- and Triglycerides by Capillary GC, *J. High Res. Chrom.* 15, 609–612 (1992)

38 Vermeulen, Theodore, Williams, Gael M., Langlois, Interfacial Area in Liquid-Liquid and Gas-Liquid Agitation, *Chem. Eng. Prog.* 51, 85F–94F (1955)

39 Rodger, W. A., Trice, Jr. V. G., Rushton, J. H., Effect of Fluid Motion on the Interfacial Area of Dispersions, *Chem. Eng. Prog.* 52, 515–520 (1956),

40 Coulaloglou, C. A., Tavlarides, L. L., Drop Size Distributions and Coalescence Frequencies of Liquid-Liquid Dispersions of Flow Vessels, *AIChE* 22, 289–297 (1976)

41 Zerfa, M., Brooks, B. W., Vinyl Chloride Dispersion with Relation to Suspension Polymerisation, *Chem. Eng. Sci.* 5, 3591–3611 (1996)

42 Zaldivar, J. M., Molga, E., Alós, M. A., Hernández, H., Westerterp, K. R., Aromatic Nitrations by Mixed Acid. Slow Liquid-Liquid Reaction Regime, *Chem. Eng. Process.* 34, 543–559 (1995)

43 Zaldivar, J. M., Molga, E., Alós, M. A., Hernández, H., Westerterp, K. R., Aromatic Nitrations by Mixed Acid. Fast Liquid-Liquid Reaction Regime, *Chem. Eng. Process.* 35, 91–105 (1996)

44 Ritter, J., Kraume, M., Inline-Messtechnik zur Tropfengrößenbestimmung in flüssigen Zweiphasensystemen bei hohen Dispersphasenanteilen, *Chem. Ing. Tech.* 71, 717–720 (1999)

45 Kaufman, V. R., Garti, N., Organic Reactions in Emulsions – Preparation of Glycerol and Polyglycerol Esters of Fatty Acids by Transesterification Reaction, *J. Am. Oil Chem. Soc.* 59, 471–474 (1982)

46 Hong, Paul O., Lee, James M., Changes of the Average Drop Sizes During the Initial Period of Liquid-Liquid Dispersions in Agitated Vessels, *Ind. Eng. Chem. Process Dev.* 24 , 868–872 (1985)

47 Hetsroni, Gad (ed.), *Handbook of Multiphase Systems*, McGraw-Hill, section 4.10–4.13, New York: 1982

48 Sprow, F. B., Drop Size Distribution in Strongly Coalescing Agitated Liquid-Liquid Systems, *AIChE* 13, 995–998 (1967)

49 Chen, Hsiao Tsung, Middleman, Stanley, Drop Size Distribution in Agitated Liquid-Liquid Systems, *AIChE* 13, 992–995 (1967)

50 Desnoyer, C., Masbernat, O., Gourdon, C., Experimental Study of Drop Size Distributions at High Phase Ratio in Liquid-Liquid Dispersions, *Chem. Eng. Sci.* 58, 1353–1363 (2003)

51 Ban, T., Kawaizumi, F., Nii, S., Takahashi, K., Effects of Surface Activities of Extractants on Drop Coalescence and Breakage in a Mixer-Settler, *Ind. Eng. Chem. Res.* 41, 5477–5482 (2002)

52 Fogg, P. G. T, Gerrard, W., *Solubility of Gases in Liquids*, John Wiley & Sons, section 4.2, New York: 1991

53 Gmehling, J, Brehm, A., *Grundoperationen, Lehrbuch der Technischen Chemie*, volume 2, Georg Thieme Verlag, section 3.4, Stuttgart: 1996

54 Fogg, P. G. T, Gerrard, W., *Solubility of Gases in Liquids*, John Wiley & Sons, section 3.2, New York: 1991

55 Karmee, S. K., Mahesh, P., Ravi, R., Chadha, A., Kinetic Study of the Base-Catalyzed Transesterification of Monoglycerides from Pongamia Oil, *J. Am. Oil Chem. Soc.* 81, 425–430 (2004)

56 Noureddini, H., Harkey, D. W., Gutsman, M. R., A Continuous Process for the Glycerolysis of Soybean Oil, *J. Am. Oil Chem. Soc.* 81, 203–207 (2004)

57 Noureddini, H., Medikonduru, V., Glycerolysis of Fats and Methyl Esters, *J. Am. Oil Chem. Soc.* 74, 419–425 (1997)

58 Noureddini, H., Zhu, D., Kinetics of Transesterification of Soybean Oil, *J. Am. Oil Chem. Soc.* 74, 1457–1463 (1997)

59 Freedman, B., Butterfield, R. O., Pryde, E. H., Transesterification Kinetics of Soybean Oil, *J. Am. Oil Chem. Soc.* 63, 1375–1380 (1986)

60 Kaufman, V. R., Garti, N., Organic Reactions in Emulsions – Preparation of Glycerol and Polyglycerol Esters of Fatty Acids by Transesterification Reaction, *J. Am. Oil Chem. Soc.* 59, 471–474 (1982)

61 Karmee, S. K., Mahesh, P., Ravi, R., Chadha, A., Kinetic Study of the Base-Catalyzed Transesterification of Monoglycerides from Pongamia Oil, *J. Am. Oil Chem. Soc.* 81, 425–430 (2004)

62 Noureddini, H., Harkey, D. W., Gutsman, M. R., A Continuous Process for the Glycerolysis of Soybean Oil, *J. Am. Oil Chem. Soc.* 81, 203–207 (2004)

63 Verenich, S., Laari, A., Kalla, J., Parameter Estimation and Sensitivity Analysis of Lumped Kinetic Models for Wet Oxidation of Concentrated Wastewaters, *Ind. Eng. Chem. Res.* 42, 5091–5098 (2003)

64 Knudsen, James G., Wankat, Phillip C., Knaebel, Kent S., “Heat and Mass Transfer” in *Perry’s Chemical Engineers’ Handbook*, Perry, R. H., (ed.), 7 ed., section 5–54, McGraw-Hill, New York: 1997

65 Kimmel, T., Smita, Schomäcker, R., Reactive Liquid-Liquid-System Characterization - Transesterification of Fatty Acid Methyl Esters with Glycerol, 2nd International Berlin Workshop – IBW2 on Transport Phenomena with Moving Boundaries, F.-P. Schindler (Ed.), *Fortschritt-Berichte VDI*, VDI Verlag, Düsseldorf: 2004

66 Noureddini, H., Harkey, D. W., Gutsman, M. R., A Continuous Process for the Glycerolysis of Soybean Oil, *J. Am. Oil Chem. Soc.* 81, 203–207 (2004)

67 Kimmel, T., *Beiträge zur Umesterung von Fettsäuremethylestern mit Glyzerin durch Reaktivrektifikation*, unpublished diploma work, Technische Universität Berlin, Berlin: 1998

68 Jeromin, L., Wollmann, G., Gutsche, B., Peukert, E., Glyzerinolyse – Modellierung und Auslegung einer Reaktion mit Mischungslücke, *Fat Sci. Technol.* 90, 507-510 (1988)

69 Okufi, S., Perez de Ortiz, E. S., Sawistowski, H., Scale-up of Liquid-Liquid Dispersions in Stirred Tanks, *Can. J. Chem. Eng.* 68, 400–406 (1990)